Time-Delayed Models of Genetic Regulatory Networks

Kiresh Parmar

A thesis submitted for the degree of Doctor of Philosophy

School of Mathematical and Physical Sciences

University of Sussex

March 2017

Declaration

I hereby declare that this thesis has not been, and will not be, submitted in whole or in part to another University for any other academic award. I also declare that this thesis was composed by myself and that the work contained therein is my own, except where explicitly stated otherwise.

Signature .....

Kiresh Parmar

Acknowledgements

First and foremost I would like to thank my incredible supervisors, Dr Yuliya Kyrychko and Dr Konstantin Blyuss, whose encouragement during my undergraduate degree gave me the confidence to pursue a PhD. I am grateful for their guidance and support throughout this research and I am so happy to have chosen them as my MMath project supervisors back in 2012.

I would also like to thank Dr Stephen John Hogan whom I collaborated with, alongside my supervisors, on my paper.

A special thanks goes to the University of Sussex Mathematics department for funding my PhD. The staff and faculty have made my 8 years at Sussex a memorable experience.

I am eternally grateful to have such an amazing wife, who keeps me calm and focussed. I am blessed to have my Mum, Dad, and brother, who have all helped me along this journey.

My thanks also extends to my in-laws and all of my family and friends, who have encouraged and inspired me. In particular, I would like to thank Charlie, whose support has been invaluable throughout my time at Sussex.

Abstract

In this thesis I have analysed several mathematical models, which represent the dynamics of genetic regulatory networks. Methods of bifurcation analysis and direct numerical simulations were employed to study the biological phenomena that can occur due to the presence of time delays, such as stable periodic oscillations induced by Hopf bifurcations. To highlight the biological implications of time-delayed systems, different models of genetic regulatory networks as relevant to the onset and development of cancer were studied in detail, as well as genetic regulatory networks which describe the effects of transcription factors in the immune system. A network of an oscillator coupled with a switch was explored, as systems such as these are prevalent in genetic regulatory networks. The effects of time delays on its oscillatory and bistable behaviour were then investigated, the results of which were compared with available results from the literature.

Contents

List of Figures

Preface

Genetic regulatory networks (GRNs) are often modelled mathematically to gain information about a vast array of life processes within an organism. The ability to derive simple models which capture the important dynamical behaviours in a biological system, such as a GRN, allows one to understand the impact of specific system parameters on the network dynamics. The level of control that can be achieved through parameter tuning can yield valuable results and help make crucial predictions on biological phenomena outside of an experimental environment. One such parameter type that can be more easily represented mathematically, but are more difficult to measure accurately experimentally, are the time delays associated to transcriptional and translational processes in GRNs. Mathematical models of GRNs which consider these time delays are essential in obtaining a better understanding of the processes in their representative biological environment.

In the first part of the thesis I investigate the role of transcriptional and translational time delays in GRN models, and show how such delays can be introduced in a paradigmatic two-gene activator-inhibitor GRN. Depending on a particular biological regime in which a given GRN is operating, it is often possible to encounter a situation where there is a significant separation of time scales due to, for instance, very fast mRNA dynamics compared to other characteristic time scales. In such a case it is possible to perform dimensional reduction and concentrate on the dynamics of a smaller number of variables. A reduced model of this type is analysed and conditions are derived that lead to a transition from a stable steady state to stable periodic oscillations that are impossible in the model without the time delays. This result highlights the importance that time delays have on the dynamical behaviour of GRNs, revealing information that would have otherwise been inaccessible. Analysis is then extended to the full nonlinear system to illustrate differences in stability conditions, and it is shown how critical values of the parameters at the Hopf boundary change when the time delay increases from zero.

In order to better understand the role of time delays in genetic regulatory networks, in the next part of the thesis I derive a delayed model based on the so-called *Repressilator*. The model incorporates auto-activation, which is a process present in many gene networks in the immune system. After proving that the model is well posed, the model is analysed and conditions are derived for the existence of a Hopf bifurcation leading to stable periodic oscillations. This result was not possible for the earlier models of the symmetric *Repressilator* without a large Hill coefficient. Numerical simulations are performed and they fully support theoretical findings.

Many GRNs are known to be composed of interconnected sub-networks of oscillators and switches. To investigate the role of transcriptional and translational time delays on networks such as these I introduce discrete delays to a five-gene network, which extends the work in the earlier literature, of the *Repressilator* coupled with a *Toggle switch*. I focus on analysing analytically and numerically the dynamics of the delayed model, and show the existence of new behaviours, which were not present in the model system without the time delays.

Chapter 1

Introduction

The networks of interactions between DNA, RNA, proteins and molecules, are defined as *gene regulatory networks* (GRNs). GRNs play a major role in a large number of normal life processes, including cell differentiation, metabolism, the cell cycle and signal transduction, hence, significant efforts have been made to develop mathematical techniques for their analysis [1–3].

The process of protein synthesis by a gene is known as gene expression. In this process a promoter, which is a regulatory region that precedes the gene in its DNA sequence, determines the rate at which the RNA polymerase (RNAp) transcribes encoded information into mRNA. mRNA are then translated into proteins, which accumulate and perform a certain task in the organism. The rate of transcription can be affected by special types of proteins called transcription factors, which are themselves encoded by genes. External signals influence whether a transcription factor is in the active state. When active, the transcription factor binds to the promoter and influences the probability of the RNAp producing an mRNA [1]. Thus, transcription factors can either activate or repress the transcription of its target gene. Multiple connections of gene products that regulate transcription of other genes then give rise to GRNs, which are usually formalised as networks (undirected or directed) where the nodes represent individual genes, proteins etc, and the edges correspond to some form of regulation between the nodes.

An important consideration to be made is the separation of timescales within each process of gene expression. The influence of external signals on the transcription factor typically takes less than a second, binding of transcription factors to its target DNA

sites takes seconds, whereas transcriptional and translational processes take minutes and accumulation of protein products can take minutes to hours [1]. It is therefore vital to account for these timescales within mathematical models of GRNs to enable a more complete picture of the underlying behaviours within the biological environment.

1.1 Literature Review

1.1.1 Mathematical Models of Gene Regulatory Networks

In the analysis of gene regulatory networks and their dynamics, the first step is the identification of key modules or components and possible relations between them, which is often done by interrogating available expression data. Once the topology of the GRN has been fixed, the next step in modelling the dynamics is making realistic assumptions about specific rules that govern the expression of particular genes. Depending on the level of understanding of underlying processes, the complexity of the GRN under investigation, and the specific questions to be addressed, there are several methodologically different approaches that can be employed. Endy & Brent [4] and Hasty et al. [5] discuss biological underpinnings for studying and modelling GRNs, while excellent reviews by de Jong [2], Bernot et al. [3], Tušek & Kurtanjek [6], and Hecker et al. [7] give an overview of mathematical and statistical techniques that have been successfully used to model GRNs, and some of these methods are discussed below.

Boolean Networks

Some of the first models developed for modelling GRNs were the so-called *Boolean networks* [8–10], where the states of all genes participating in the interactions are represented by binary variables having the values of ON and OFF, or 1 and 0, with the possibility of either synchronous or asynchronous update rules for the nodes. Boolean logic rules are then used to approximate regulatory control of gene expression [11], with updates of binary states of all genes taking place simultaneously [12]. Boolean networks approach has been extended in several directions to provide a better approximation of real GRNs. Shmulevich et al. [13] have proposed a probabilistic analogue of Boolean networks to account for stochastic nature of many processes involved in gene expression. Silvescu and Honavar [14] have proposed temporal Boolean networks, where the next state of genes in

the networks is determined not only by their current state, but also by a fixed number of their previous states, which effectively allows one to take into account some history of transitions in a GRN. Recently, Boolean network models of GRNs have been compared to models based on ordinary differential equations (ODEs), and, in fact, it has been shown that some Boolean models can be rigorously derived as coarse-grained analogues of some ODE models [15].

Significant advantage of using Boolean networks to model GRNs lies in the fact that they allow one to consider networks with a very large number of nodes. At the same time, there are several deficiencies in this approach. The first one concerns the fact that since the gene states only admit the values of ON or OFF, this formalism does not take into account intermediate stages of gene expression [16]. Another issue is that GRNs modelled by Boolean networks can exhibit behaviour not observed in real life, hence, special care has to be taken when choosing the class of admissible Boolean functions [17].

Fuzzy Methods

Due to intrinsic imprecision and uncertainty associated with gene expression data, it may be appropriate to move away from precise rules of Boolean logic in favour of machine learning techniques based on fuzzy logic. The basic idea is that rather than trying to reconstruct some assumed fixed gene network topology, one considers the whole family of possible networks with all possible distributions of links between nodes. The problem lies in using actual data to assign appropriate probabilities to each of these configurations, so that for a given input the fuzzy network would provide an output that most resembles actual data. A significant advantage of fuzzy logic for inferring the structure of GRNs lies in their ability to rely on already available knowledge of biological relations between different nodes in the network, and, at the same time, being able to recover important previously unknown connections. On the other hand, fuzzy methods for GRN inference are characterised by a high level of computational complexity.

To give a few examples, fuzzy approach has been used to analyse microarray data from the yeast cell cycle and to recover a set of GRNs, with k-nearest-neighbour algorithm being used to replace missing data [18]. Woolf and Wang [19] have used a k-means clustering algorithm to reconstruct and evaluate GRNs for *Saccharomyces cerevisiae*. In this approach, groups of co-regulated genes are considered as clusters, and the clustering

algorithm is then used to detect cluster centres. Volkert and Mahlis [20] have used a smooth response surface algorithm to recover GRNs from gene expression data for *Saccharomyces cerevisiae*. Approaches based on an artificial bee colony search algorithm have allowed the reconstruction of a GRN in *Escherichia coli* [21]. A very recent review by Al Qazlan et al. [22] gives an overview of different fuzzy methods, as well as their combinations with other approaches, such as ordinary differential equations, with the purpose of optimising data mining of gene expression and microarray datasets to recover GRNs.

Ordinary and Delay Differential Equation Models

A very powerful and mathematically insightful methodology for analysis of GRNs is based on nonlinear ordinary or delay differential equations (ODEs or DDEs). In this approach, a gene regulatory network is represented by concentrations of different mRNAs and proteins, and the dynamics can be written as a system of ODEs or DDEs using the law of mass action for individual reactions [1]. Some of the earliest results on ODE models of gene regulation go back to Goodwin [23, 24], who introduced and studied a negative feedback loop involving the concentrations of mRNA, an enzyme and a metabolite. It has been later shown that a negative feedback loop is absolutely essential to ensure the existence of stable periodic solutions, while positive feedback is required for multi-stationarity [25, 26]. This approach was subsequently generalised and expanded [27–30]; reviews by Smolen et al. [12], de Jong [2] and Hecker et al. [7] discuss some of these models based on systems of nonlinear ODEs. A very important aspect of all these models is a *regulation function* that controls the rates of gene expression. In light of experimental evidence suggesting monotonic sigmoidal shape of regulation functions [31], a conventional choice for this function is given by the Hill function [32–34]. Weiss [35] has discussed various chemical mechanisms associated with the Hill function, including different kinds of ligand binding, and a more recent review of the uses of the Hill function in GRN models can be found in [36].

In order to more accurately represent a switch-like behaviour of the gene expression, several authors have developed models of GRNs using piecewise-linear differential equations, in which the continuous Hill function is replaced by a discontinuous step function [37–42]. Besides regular steady states, the piecewise-linear models also allow for singular steady states, which although important for representing homeostasis in GRNs, are

complex to analyse due to discontinuities at the thresholds [43,44]. Polynikis et al. [32] discuss various features of piecewise-linear ODE models and different dynamical regimes that can be exhibited in these models, including possible periodic solutions, sharp-threshold dynamics, and the comparison with models based on continuous regulation function.

In terms of applications to cancer, ODE models have explained aberrant dynamics of the NF-κB transcription factor linked to oncogenesis, tumour progression and resistance to therapy, as well as the dynamics of IκB-NF-κB [45,46]. Another example is the analysis of the feedback loop between the tumour suppressor p53 and the oncogene Mdm2 [47], and the single-cell response of p53 to radiation-induced DNA damage [48]. Clinical evidence suggests that different components of the PI3K/AKT pathway can lead to aberrant cell growth, metastatic competence and therapy resistance, and some progress has been made in modelling this pathway and identifying inhibitors responsible for the regulation of PI3K/AKT signalling [49]. Cheng *et al.* [50] and Edelman *et al.* [51] give a number of examples of the uses of differential equation based models for the analysis of GRNs in cancer.

Another aspect that has to be properly accounted for in dynamical models is the fact that transcription and translation during gene expression often take place over non-negligible time periods. Monk [52] has shown how time delays can cause oscillatory gene expression and provide insights into the dynamics of interactions between p53 and Mdm2 proteins associated with cancer suppression. Subsequent research has focused on the role of time delays in GRN dynamics [53–57]. Xiao and Cao [58] have analysed a Hopf bifurcation in a gene network with two transcriptional delays, which occurs when the sum of the delays passes through a critical value, and shown how the amplitude and period of oscillations of gene expression change with the time delays. Due to the fact that it may not be practically possible to identify discrete transcription/translation time delays, a better alternative would be to use models with distributed delay [59]. Models with time delays have been used to understand the regulation of feedback loops involving transcription factors E2F and Myc, known oncogenes and possible tumour suppressors [60,61]. Ribeiro et al. [62] have developed a delayed stochastic simulation algorithm for analysis of the p53-Mdm2 feedback loop whose malfunction is associated with 50% of cancers. Sequences of multiple reactions with unknown intermediate kinetics can also be successfully analysed using time-delayed models [63,64].

Stochastic Models

Experimental evidence suggests that significant stochastic fluctuations are observed during gene expression and regulation, hence, in many cases it is paramount to use stochastic models for studying GRN dynamics [65, 66]. Even in the absence of extrinsic noise associated with variability in different environmental factors, there are several fundamental processes responsible for intrinsic stochasticity of gene expression [67, 68]. One of these is the process of initiation of transcription, which starts by first forming an *elongation complex* by binding RNA polymerase (RNAp) to the promoter region of the gene, and there is a significant variation in the duration of elongation processes between different transcription events [69–72]. Binding of RNAp to the promoter regions of different genes results in switching of these genes on and off, thus either blocking or facilitating further transcription, which gives another major source of noise in GRNs. Stochasticity in expression of individual gene results in stochastic behaviour of larger genetic circuits and GRNs [65, 73]. Some of the early work on stochastic gene expression emerged from experiments in synthetic biology [74, 75] that demonstrated how stochasticity can result in sustained oscillations, and significant amount of research has been subsequently done both theoretically and experimentally on the analysis of stochastic (and delayed) oscillations in gene regulatory networks [68, 76–78]. Zavala and Marquez-Lago have recently considered delay-induced oscillations in deterministic and stochastic models of single-cell gene expression, highlighting important differences between these two types of models and associated behaviours [79].

Besides being an intrinsic feature of biological dynamics, stochasticity has proved to be important in the context of engineered genetic switches [74, 80]. de Jong [2] and El Samad et al. [81] discuss various methods for modelling stochastic GRN models, including stochastic master equation and various stochastic simulation algorithms. Bratsun et al. [78] have developed an algorithm for analysis of non-Markovian dynamics in GRNs with time delays and showed that these delays are able to induce oscillatory dynamics in the case where deterministic models do not exhibit oscillations. This methodology was later improved, and several exact stochastic simulation algorithms have been developed for simulations of time-delayed models [82, 83]. A review by Ribeiro [72] discusses various techniques for simulating stochastic time-delayed dynamics of gene expression, and very

recently Jansen et al. [84] have reviewed the role of delay distribution in the stochastic dynamics during gene expression.

Another way to approach stochasticity in the analysis and reconstruction of GRNs is by using so-called *Bayesian networks* [85], where gene expression values are represented as random variables, and relations between them are probabilistic. Learning techniques for Bayesian networks [86,87] allow one to combine expression data with an *a priori* knowledge to deduce the structure of GRN that best matches the available expression data. Friedman et al. [85] have developed an algorithm for deriving Bayesian networks that circumvents a dimensionality problem, and this method has been used to analyse the cell cycle data for *S. cerevisiae* containing numerous measurements of mRNA expression levels [88]. Out of 800 genes it was possible to identify a few genes controlling the regulation of cell cycle processes.

1.1.2 Delay Differential Equations

Mathematical investigation into the behaviour caused as a result of the elapsed time between the initiation and completion of mRNA transcription, and likewise protein translation, has received great interest [52–58]. Types of models that best capture such information are those of delay differential equations. A general delay differential equation with a single time delay can be written in the form

$$\frac{dx(t)}{dt} = f(t, x(t), x(t-\tau); \mu), \tag{1.1}$$

where $x(t) \in \mathbb{R}^n$ is the state variable, $\tau \in \mathbb{R}$ is the time delay, function f is a nonlinear smooth function and $\mu \in \mathbb{R}^m$ are time-independent parameters. Since the derivative $\dot{x}(t)$ depends on the solution at past times, the initial condition for DDEs is defined as a function over the interval $[-\tau, 0]$. If $x_t = x_0(\sigma)$, where $-\tau < \sigma < 0$ denotes the solution on the interval $[-\tau, 0]$, then for a fixed parameter μ and given the initial solution $x_0(t)$ on $[-\tau, 0]$, there is a unique solution $x(t)$ for $t \in [0, \infty)$. Time delays themselves can be constant or time/state-dependent.

In the case of multiple constant discrete time delays, a general delay differential equa-

tion (1.1) can be modified as follows

$$\frac{dx(t)}{dt} = f(t, x(t), x(t-\tau_1), x(t-\tau_2), ..., x(t-\tau_n); \mu), \tag{1.2}$$

where $\tau_1 \geq 0$, $\tau_2 \geq 0$, ..., $\tau_n \geq 0$ are the time delays. In this case, the derivative of x depends on the solution at some fixed time in the past, represented by the time delays $\tau_1, \tau_2, ..., \tau_n$ and the initial conditions must take the form of an initial function established over the interval $[-\tilde{\tau}, 0]$ where $\tilde{\tau} = \max\{\tau_i\}$, $i = 1, ..., n$.

The solutions of some delay differential equations can be obtained using the method of steps [89]. The idea of this method is to compute the solution over a small time interval using a given initial condition. The solution over that interval is then used as a history function to calculate the solution over the next interval. This process is continued indefinitely. As an example of this method, consider the following simple delay differential equation:

$$\frac{dx(t)}{dt} = -x(t-2), \quad x(s) = 1 \quad \text{for} \quad -2 \leq s \leq 0. \tag{1.3}$$

The solution over a particular time interval must use known initial data, thus the time step must be chosen accordingly. For a DDE of the form (1.2), the time interval cannot exceed the size of $T = \min(\tau_i)$, $i = 1, ..., n$. This way all values of $x(t - \tau_i)$ are known in the interval $0 \leq t \leq T$. For the case of DDE (1.3) this simply means looking for the solution in the interval $0 \leq t \leq 2$ as the first step, which is given by:

$$x(t) = \int_0^t -x(v-2)dv + x(0) = 1 - t.$$

Next, using this result as a history function, the solution in the interval $2 \leq t \leq 4$ can be solved, and is given by:

$$x(t) = \int_2^t -x(v-2)dv + x(2) = \frac{t^2}{2} - 2t + 1.$$

The solution in the interval $4 \leq t \leq 6$ can then be found, and so on. This method, however, becomes tedious in finding solutions over a large time scale, and can be troublesome with DDE equations that are more difficult to integrate.

A linear discrete delay differential equation with n delays takes the form:

$$\frac{dx(t)}{dt} = A_0 x(t) + \sum_{i=1}^{n} A_i x(t-\tau_i), \tag{1.4}$$

where $x \in \mathbb{R}^n$ and $A_i \in \mathbb{R}^{n\times n}$, $i = 0, 1, ..., n$. The characteristic equation for (1.4) can be found in a similar way to ordinary differential equations, by supposing that linear delay differential equations have exponential solutions. By substituting the solution $x(t) = Be^{\lambda t}$ into (1.4) and using basic linear algebraic theory, the characteristic equation is expressed as

$$\det\Delta(\lambda) = 0, \tag{1.5}$$

where

$$\Delta(\lambda) = \left(A_0 + \sum_{i=1}^{n} A_i e^{-\lambda\tau_i} \right) - \lambda I$$

is the characteristic matrix, I is the $n \times n$ identity matrix, and λ denotes the eigenvalue. Due to the exponential terms, there are infinitely many eigenvalues that solve equation (1.5). There is, however, only a finite number of eigenvalues that can lie on and to the right of the imaginary axis [90]. When a pair of complex conjugate eigenvalues crosses the imaginary axis into the right half plane, a Hopf bifurcation is induced, generating a periodic solution in the neighbourhood of a steady state whose stability changes [91].

To highlight the appearance of periodic solutions that can arise as a result of time delays, first consider the following linear ordinary differential equation:

$$\frac{dx(t)}{dt} = ax(t), \quad x(0) = 1, \tag{1.6}$$

where $a \in \mathbb{R}$ is a non-zero constant. This can be easily solved using the method of separation of variables which yields

$$x(t) = e^{at}.$$

It can be deduced that the steady state, $\bar{x} = 0$, of ODE (1.6) is stable for $a < 0$ and unstable for $a > 0$. To introduce a time delay, consider the following delay differential equation:

$$\frac{dx(t)}{dt} = ax(t-\tau), \qquad x(s) = 1, \quad s \in [-\tau, 0). \tag{1.7}$$

By seeking a particular solution, $x_p(t) = Be^{\lambda t}$, where $B \in \mathbb{R}^*$, and its derivative, $\dot{x}_p(t) = B\lambda e^{\lambda t}$, a solution can be obtained by substituting these into (1.7):

$$\begin{aligned} B\lambda e^{\lambda t} &= aBe^{\lambda(t-\tau)} \\ &= aBe^{\lambda t}e^{-\lambda\tau}. \end{aligned}$$

Dividing both sides of this equation by $Be^{\lambda t}$ gives

$$\lambda = ae^{-\lambda\tau}.$$

Thus, the solution of the delay differential equation (1.7) is

$$x(t) = Be^{\lambda t}, \quad \text{where} \quad \lambda = ae^{-\lambda\tau}.$$

In the limit $\tau = 0$, it follows that $\lambda = a$. As one would expect, the DDE (1.7) behaves in the same way as the corresponding ODE (1.6) when $\tau = 0$, that is, in the absence of the time delay. The steady state $\bar{x} = 0$ is unstable when $a > 0$ and stable when $a < 0$. It can be shown that a periodic solution is possible for $\tau > 0$ by alternatively looking for a particular solution of the form $x_p(t) = C\sin(\omega t)$, its derivative $\dot{x}_p(t) = C\omega\cos(\omega t)$, where $C \in \mathbb{R}^*$, and substituting into (1.7), which gives

$$\begin{aligned} C\omega\cos(\omega t) &= aC\sin(\omega t - \omega\tau) \\ &= aC\left[\sin(\omega t)\cos(\omega\tau) - \cos(\omega t)\sin(\omega\tau)\right]. \end{aligned}$$

Equating coefficients of $\cos(\omega t)$ and $\sin(\omega t)$, the following conditions are found:

$$\cos(\omega\tau) = 0 \quad \text{and} \quad \sin(\omega\tau) = -\frac{\omega}{a}.$$

Since the period of the cosine function is 2π, the two values of $\omega\tau$ in the range $[0, 2\pi]$ that will satisfy the first condition are $\omega\tau = \pi/2$ or $\omega\tau = 3\pi/2$. Combining this with the

second condition leads to the following possibilities:

$$\begin{aligned} &\text{(i)} \quad \omega\tau = \frac{\pi}{2} \quad \text{and} \quad a\tau = -\frac{\pi}{2}, \\ &\text{(ii)} \quad \omega\tau = \frac{3\pi}{2} \quad \text{and} \quad a\tau = \frac{3\pi}{2}. \end{aligned}$$

It then follows that for the particular values of a and τ that satisfy one of these conditions, the DDE (1.7) admits the harmonic solution, $x(t) = C\sin(\omega t)$ [91].

1.1.3 Autoinhibition Model with Transcriptional Delay

To motivate the work in this thesis we first look at an existing model of a genetic regulatory network studied by J. Lewis [92]. Delay differential equations have been used to describe a self inhibiting gene, giving rise to oscillations which describe the dynamics of the somite segmentation clock in Zebrafish, see Figure 1.1. To investigate the behaviour of the model we perform a stability analysis of the steady states of the model analytically. To gain a better insight into the dynamics, we numerically compute the eigenvalues using the TraceDDE suite in Matlab, and use direct numerical simulations to illustrate the behaviour under different parameter schemes and confirm analytical findings.

We consider a single-cell GRN consisting of a single gene which is assumed to inhibit the production of its own mRNA. Denoting the concentration of proteins as p and concentrations of transcribed mRNAs as m, the rate of change of p and m are described by the following pair of ordinary differential equations:

$$\begin{aligned} \frac{dp(t)}{dt} &= am(t) - bp(t), \\ \frac{dm(t)}{dt} &= f(p(t)) - cm(t), \end{aligned} \tag{1.8}$$

where $p(t)$ is the number of protein molecules per cell at time t, $m(t)$ is the number of mRNA molecules per cell at time t, a is the protein synthesis initiation rate, $f(p)$ is the mRNA synthesis initiation rate as a function of p, b is the protein degradation rate, and c is the mRNA degradation rate. Assume that transcription is inhibited by the protein p, so that

$$f(p) = \frac{k}{1 + p^2/p_0^2},$$

where k and p_0 are constants. However, with more careful consideration of the transcrip-

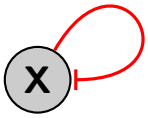

Figure 1.1: Network motif for the auto-inhibitory gene, X, of the Zebrafish somite segmentation clock. The node is gene X and the loop represents regulation of mRNA production by self-inhibition.

tion and translation processes, one should note that the concentration of protein determines the production of mRNA molecules and likewise the amount of mRNA molecules influence the rate of protein production. There is a significant amount of time that passes between the initiation of transcription and the arrival of a mature mRNA cell. This is also the case with the production of a protein molecule after the initiation of translation. Accounting for these delays, model (1.8) can be modified, giving the following pair of delay differential equations:

$$\begin{aligned} \frac{dp(t)}{dt} &= am(t - T_p) - bp(t), \\ \frac{dm(t)}{dt} &= f(p(t - T_m)) - cm(t), \end{aligned} \tag{1.9}$$

where T_p is the delay during translation of proteins and T_m is the delay during transcription of mRNAs. To reduce the number of free parameters in the model, we define a phase-shifted protein concentration by introducing a new variable:

$$p_{advanced}(t) = p(t + T_p), \tag{1.10}$$

where we shall denote $p_{advanced}(t)$ by $p_{adv}(t)$. The first equation of system (1.9) evaluated at $t + T_p$ then has the form:

$$\dot{p}(t + T_p) = am(t) - bp(t + T_p),$$

and in terms of the new variable (1.10) this can be rewritten as

$$\dot{p}_{adv}(t) = am(t) - bp_{adv}(t).$$

The second equation of system (1.9) transforms into

$$\dot{m}(t) = f(p_{adv}(t - T_m - T_p)) - cm(t).$$

Thus, omitting the 'adv', system (1.9) takes the form:

$$\begin{aligned} \frac{dp(t)}{dt} &= am(t) - bp(t), \\ \frac{dm(t)}{dt} &= f(p(t-\tau)) - cm(t), \end{aligned} \tag{1.11}$$

where $\tau = T_m + T_p$ is the new combined time delay [92].

Before continuing with any analysis of system (1.11) we first must establish that the solutions are nonnegative for all time to ensure their biological feasibility. The initial conditions for model (1.11) are given by:

$$\begin{aligned} p(s) &= \phi_1(s), \quad s \in [-\tau, 0], \\ m(s) &= \phi_2(s), \quad s \in [-\tau, 0], \end{aligned} \tag{1.12}$$

where $\phi_i(s) \in C([-\tau, 0], \mathbb{R})$ with $\phi_i(s) \geq 0$ ($-\tau \leq s \leq 0$, $i = 1, 2$). Here, $C([-\tau, 0], \mathbb{R})$ is the Banach space of continuous mappings of the interval $[-\tau, 0]$ into $\mathbb{R}$. It is also assumed that $m(0) > 0$, as this ensures that at least some amount of proteins will be produced.

We now prove that the solution $(p(t), m(t))$ of DDE (1.11) with the initial condition (1.12) is positive for all $t > 0$. This result can be proved by contradiction, following the methodology used in [93]. We begin by showing that $m(t) \geq 0$ for all $t > 0$. Let $t_1 > 0$ be the first time when $p(t_1)m(t_1) = 0$; assuming that $m(t_1) = 0$ implies $p(t) \geq 0$ for all $t \in [0; t_1]$, and since t_1 is the first time when $m(t_1) = 0$, this also means $dm(t_1)/dt \leq 0$, that is, the function $m(t)$ is decreasing at $t = t_1$. However, evaluating the second equation of the system (1.11) at $t = t_1$ yields

$$\frac{dm(t_1)}{dt} = \frac{k}{1 + p(t-\tau)^2/p_0^2} > 0,$$

which gives a contradiction. Since $m(0) > 0$, this implies $m(t) > 0$ for all $t > 0$. Now that the positivity of $m(t)$ has been established, let $t_2 > 0$ be the first time when $p(t_2) = 0$. For this to happen, one must have $dp(t_2)/dt \leq 0$, that is, the function $p(t)$ should be

decreasing at $t = t_2$. At the same time, evaluating the first equation of the system (1.11) at $t = t_2$ yields

$$\frac{dp(t_2)}{dt} = am(t_2) > 0,$$

which gives a contradiction, therefore, $p_b(t) > 0$ for all $t > 0$. Hence, solutions $p(t)$ and $m(t)$ of the model (1.11) are positive for all $t > 0$.

The steady states $\bar{p}$ and $\bar{m}$ of system (1.11) can be found as the roots of the following system of algebraic equations:

$$\begin{aligned} a\bar{m} - b\bar{p} &= 0, \\ \frac{k}{1 + \bar{p}^2/p_0^2} - c\bar{m} &= 0. \end{aligned} \tag{1.13}$$

From the first equation of (1.13) we find that $\bar{m} = \dfrac{b}{a}\bar{p}$. Substituting this into the second equation of (1.13) leads to the following polynomial equation for $\bar{p}$:

$$\bar{p}^3 + p_0^2\bar{p} - \frac{akp_0^2}{bc} = 0,$$

where a, b, c, p_0, $k > 0$. Replacing $\bar{p}$ with $u - \frac{p_0^2}{3u}$, some algebraic manipulation yields

$$u^6 - \frac{akp_0^2}{bc}u^3 - \frac{p_0^6}{27} = 0.$$

This can be easily solved for u^3 as

$$u^3 = \frac{akp_0^2}{2bc} \pm \frac{1}{2}\sqrt{\frac{a^2k^2p_0^4}{b^2c^2} + \frac{4p_0^6}{27}}.$$

There are six solutions for u, namely

$$\begin{aligned} u_{1,2,3} &= \sqrt[3]{\frac{akp_0^2}{2bc} + \frac{1}{2}\sqrt{\frac{a^2k^2p_0^4}{b^2c^2} + \frac{4p_0^6}{27}}} \;\; .e^{\frac{2K\pi}{3}i}, \quad K = 0, 1, 2, \\ u_{4,5,6} &= \sqrt[3]{\frac{akp_0^2}{2bc} - \frac{1}{2}\sqrt{\frac{a^2k^2p_0^4}{b^2c^2} + \frac{4p_0^6}{27}}} \;\; .e^{\frac{\pi+2K\pi}{3}i}, \quad K = 0, 1, 2. \end{aligned} \tag{1.14}$$

A positive real steady state is required in order for it to be biologically relevant, so we

only need to look at u_1 in (1.14) (where $K = 0$):

$$u = \sqrt[3]{\frac{akp_0^2}{2bc} + \frac{1}{2}\sqrt{\frac{a^2k^2p_0^4}{b^2c^2} + \frac{4p_0^6}{27}}}. \tag{1.15}$$

Substituting (1.15) back into $\bar{p} = u - \frac{p_0^2}{3u}$, we are able to express the steady states $\bar{p}$ and $\bar{m}$ of system (1.11) as follows:

$$\bar{p} = \frac{\left(\frac{F}{2} + \frac{1}{2}\sqrt{F^2 + \frac{4p_0^6}{27}}\right)^{2/3} - \frac{p_0^2}{3}}{\left(\frac{F}{2} + \frac{1}{2}\sqrt{F^2 + \frac{4p_0^6}{27}}\right)^{1/3}}, \qquad \bar{m} = \frac{\frac{b}{a}\left[\left(\frac{F}{2} + \frac{1}{2}\sqrt{F^2 + \frac{4p_0^6}{27}}\right)^{2/3} - \frac{p_0^2}{3}\right]}{\left(\frac{F}{2} + \frac{1}{2}\sqrt{F^2 + \frac{4p_0^6}{27}}\right)^{1/3}},$$

where $F = \frac{akp_0^2}{bc}$.

The equation for eigenvalues λ of the linearisation near the steady state $(\bar{p}, \bar{m})$ of system (1.11) has the form

$$\lambda^2 + (b + c)\lambda + bc + \gamma e^{-\lambda\tau} = 0, \tag{1.16}$$

where

$$\gamma = \frac{2ak\bar{p}/p_0^2}{(1 + (\bar{p}^2/p_0^2))^2} > 0.$$

In the limit $\tau = 0$, (1.16) reduces to the quadratic equation:

$$\lambda^2 + (b + c)\lambda + bc + \gamma = 0,$$

whose roots always have negative real parts since $b > 0$, $c > 0$, and $\gamma > 0$. This means that the steady state $(\bar{p}, \bar{m})$ is stable for any choice of parameters. Then to investigate if there is a point at which the steady state loses stability for $\tau > 0$, we notice that $\lambda = 0$ is not a valid solution to the characteristic equation (1.16). Thus, the only way in which the steady state $(\bar{p}, \bar{m})$ may lose stability is when a pair of complex conjugate roots of (1.16) cross the imaginary axis. We can investigate this by looking for solutions of the characteristic equation (1.16) in the form $\lambda = i\omega$ for some real $\omega > 0$. Substituting this

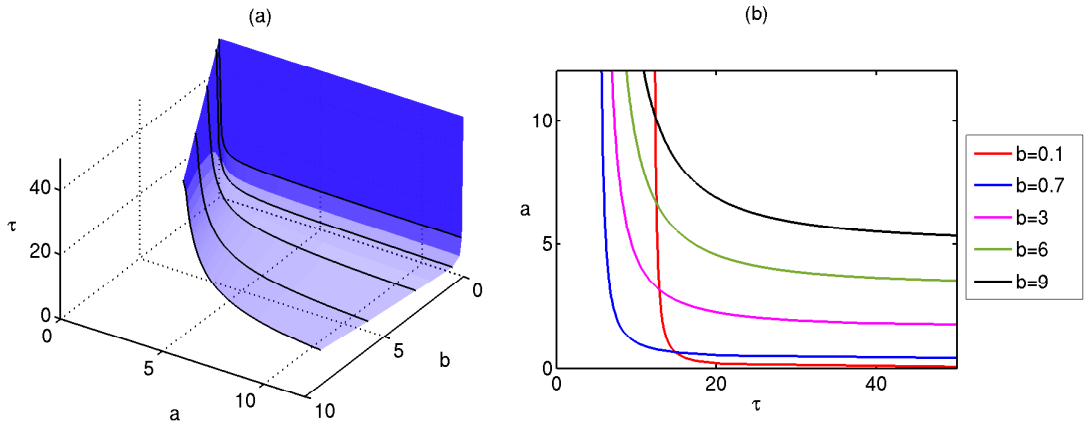

Figure 1.2: Stability boundary of the steady state $(\bar{p}, \bar{m})$ of system (1.11). The steady state is stable below the surface in (a) and to the left of the boundary curves shown in (b). Parameter values are $c = 0.23$, $k = 33$, and $p_0 = 40$.

into equation (1.16) and separating into real and imaginary parts gives

$$\begin{aligned} \gamma \cos(\omega\tau) &= \omega^2 - bc, \\ \gamma \sin(\omega\tau) &= (b + c)\omega. \end{aligned} \tag{1.17}$$

Squaring and adding these two equations together produces the following equation for $z = \omega^2$:

$$h(z) = z^2 + (b^2 + c^2)z + b^2c^2 - \gamma^2 = 0,$$

which can be solved to give the critical frequency:

$$\omega_0^2 = \frac{1}{2}\left[-(b^2 + c^2) + \sqrt{(b^2 - c^2)^2 + 4\gamma^2}\right]. \tag{1.18}$$

It should be noted that ω_0^2 will only give real values provided $bc < \gamma$. This means that for the values of parameters such that $bc \geq \gamma$, the steady state $(\bar{p}, \bar{m})$ is stable for all values of the time delay τ. Note that,

$$\frac{dh(z)}{dz} = 2z + b^2 + c^2 > 0, \quad \text{for any} \quad z \geq 0.$$

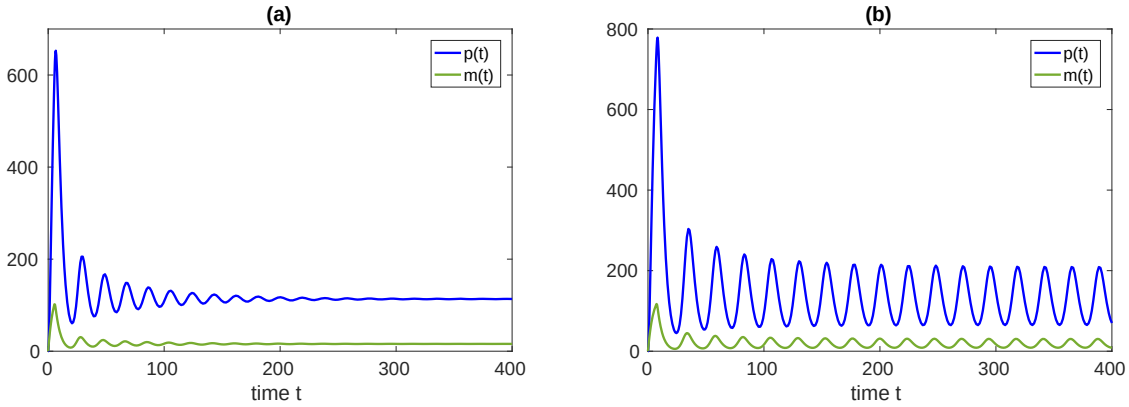

Figure 1.3: Numerical solution of system (1.11): (a) $\tau = 5$; (b) $\tau = 7$. Parameter values are $a = 5$, $b = 0.7$, $c = 0.23$, $k = 33$, and $p_0 = 40$. The critical time delay is $\tau_0 = 6.1271$.

The critical value of the time delay τ_0 can be calculated from (1.17) to give

$$\tau_{0,n} = \frac{1}{\omega_0}\left[\arctan\left(\frac{(b+c)\omega_0}{\omega_0^2 - bc}\right) + n\pi\right], \quad n = 0, 1, 2, ...,$$

where ω_0 is found from (1.18) and arctan corresponds to the principle value of arctan. When $\tau = \tau_{0,n}$ the complex conjugate roots of the characteristic equation (1.16) are on the imaginary axis. In order to determine if the roots do cross the imaginary axis, with positive speed, we consider the root $\lambda(\tau) = \mu(\tau) + i\omega(\tau)$, of (1.16) near $\tau = \tau_{0,n}$, satisfying $\mu(\tau_{0,n}) = 0$ and $\omega(\tau_{0,n}) = \omega_0$, $n = 0, 1, 2, ...$ Then substituting $\lambda = \lambda(\tau)$ into (1.16) and differentiating with respect to τ gives

$$\left(\frac{d\lambda}{d\tau}\right)^{-1} = \frac{(2\lambda + b + c)e^{\lambda\tau}}{\lambda\gamma} - \frac{\tau}{\lambda}.$$

Therefore, it can be found that

$$\begin{aligned}
\operatorname{sgn}\left\{\left[\frac{d(\mathrm{Re}\lambda)}{d\tau}\right]_{\tau=\tau_{0,n}}\right\} &= \operatorname{sgn}\left\{\mathrm{Re}\left[\left(\frac{d\lambda}{d\tau}\right)^{-1}\right]_{\tau=\tau_{0,n}}\right\} \\
&= \operatorname{sgn}\left\{\mathrm{Re}\left[\frac{(2\lambda + b + c)e^{\lambda\tau}}{\lambda\gamma}\right]_{\tau=\tau_{0,n}}\right\} \\
&= \operatorname{sgn}\left\{\frac{2\omega_0\cos(\omega_0\tau_{0,n}) + (b+c)\sin(\omega_0\tau_{0,n})}{\omega_0\gamma}\right\}.
\end{aligned}$$

Substituting the expressions for $\cos(\omega_0\tau_{0,n})$ and $\sin(\omega_0\tau_{0,n})$ given by (1.17) yields

$$\operatorname{sgn}\left\{\left[\frac{d(\mathrm{Re}\lambda)}{d\tau}\right]_{\tau=\tau_{0,n}}\right\} = \operatorname{sgn}\left\{\frac{2(\omega_0^2 - bc) + (b+c)^2}{\gamma^2}\right\} = \operatorname{sgn}\left\{\frac{h'(z_k)}{\gamma^2}\right\} > 0.$$

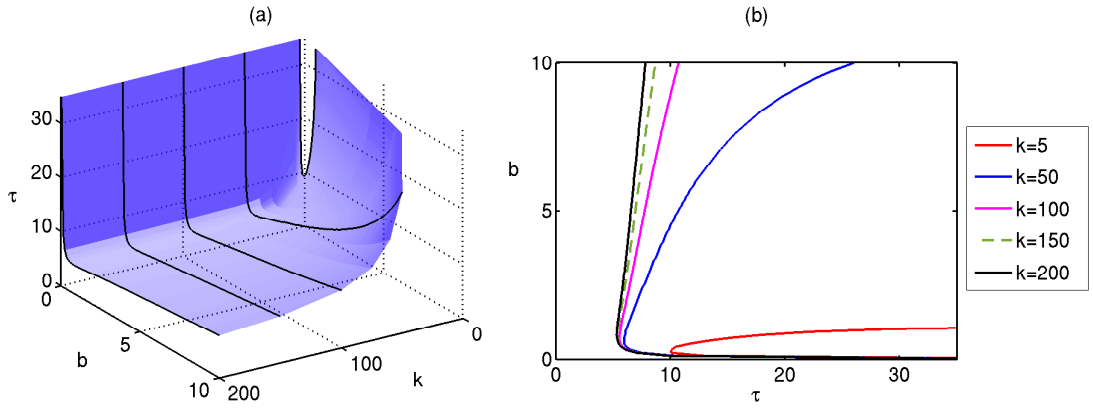

Figure 1.4: Stability boundary of the steady state $(\bar{p}, \bar{m})$ of system (1.11). The steady state is stable below the surface in (a) and to the left of the boundary curves shown in (b). Parameter values are $a = 4.5$, $c = 0.23$, and $p_0 = 40$.

Thus, the eigenvalues of the characteristic equation cross the imaginary axis at the point where $\tau = \tau_0$ and never goes back across the axis for larger values of τ. Therefore, we have proven the following result.

Theorem 1.1. *If $bc \geq \gamma$, the steady state $(\bar{p}, \bar{m})$ of the time delayed system (1.11) is stable for all values of time delay $\tau \geq 0$. If $bc < \gamma$, this steady state is stable for $0 \leq \tau < \tau_0$ and unstable for $\tau > \tau_0$ and undergoes a Hopf bifurcation at $\tau = \tau_0$.*

Figure 1.2 illustrates the stability boundary of the steady state $(\bar{p}, \bar{m})$ of system (1.11) depending on the time delay τ, protein synthesis initiation rate a, and protein degradation rate b, with parameter values taken from J. Lewis [92]. This Figure suggests that for a fixed value of the degradation rate b, the time delay required for the steady state to lose stability reduces as the protein synthesis initiation rate a, is increased. It also suggests that when b is fixed, there exists a value, $\hat{a}$, such that for $0 < a < \hat{a}$ the steady state is stable irrespective of the value of the time delay.

Figure 1.3 demonstrates the type of behaviour that is observed inside and outside of the stable region in Figure 1.2. It shows how increasing the time delay τ leads to a Hopf bifurcation of the steady state $(\bar{p}, \bar{m})$ inducing a stable periodic orbit. After stability is lost at the critical time delay, the system exhibits oscillatory behaviour for any larger value

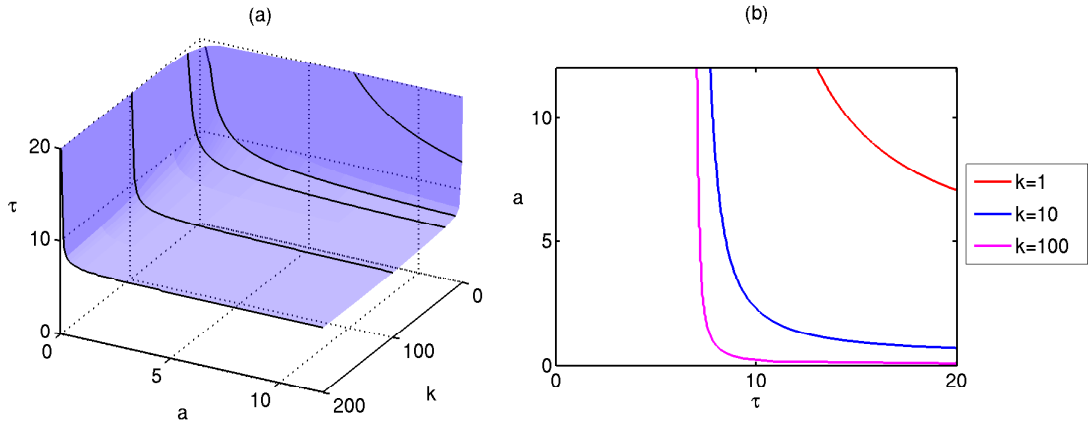

Figure 1.5: Stability boundary of the steady state $(\bar{p}, \bar{m})$ of system (1.11). The steady state is stable below the surface in (a) and to the left of the boundary curves shown in (b). Parameter values are $b = c = 0.23$, and $p_0 = 40$.

of τ.

In Figure 1.4 we show how the stability boundary for steady state $(\bar{p}, \bar{m})$ of system (1.11) varies depending on protein degradation rate b, the transcription rate k, and the time delay τ. One can see that by decreasing the value of k, there is a significant reduction in the range of b where an unstable steady state is possible. As k is increased the stability boundary tends towards a boundary curve limit as depicted for $k = 200$ and remains close to this for any larger value of k.

Figure 1.5 shows the stability boundary for steady state $(\bar{p}, \bar{m})$ of system (1.11), varying parameters for protein synthesis initiation rate a, transcription rate k and the time delay τ. It suggests that for large k, the region for a stable steady state is consistently small for most of the parameter space. However for very small values of k, and likewise for a, the region for a stable steady state increases exponentially.

1.2 Thesis Outline

The research in this thesis focuses on mathematical modelling of genetic regulatory networks with discrete time delays associated to transcription and translation processes.

In Chapter 2, I use a paradigmatic two-gene network to focus on the role played by time delays in the dynamics of gene regulatory networks. Dynamics of the reduced model arising in the limit of fast mRNA dynamics are contrasted with that of the full model.

Stability of steady states are established in terms of the system parameters and analytical conditions for a Hopf bifurcation are derived for both models. Numerical simulations are shown to illustrate the dynamical behaviour under different parameter schemes.

Chapter 3 discusses a mathematical model of a genetic regulatory network relevant for describing the dynamics of transcription factors in the immune system. A three-gene network is explored to examine the effects of time delays on its dynamics. Conditions for stability of each steady state are presented where a Hopf bifurcation is possible for one of the steady states. Numerical simulations help to further understand the results of the mathematical analysis.

In Chapter 4, I investigate a mathematical model of a genetic regulatory network which gives rise to oscillation and switch dynamics. A five-gene network is used to discuss the role of transcriptional and translational time delays on the dynamical behaviour of one protein in the gene regulatory network by comparing results with earlier literature. Numerical simulations are used to depict the existence of new behaviour due to the inclusion of time delays.

Chapter 5 contains a summary of the main results of the thesis and a discussion of some open problems.

Chapter 2

Time-Delayed Models of Gene Regulatory Networks

Cancer is a complex disease, triggered by multiple mutations in various genes and exacerbated by a number of different behavioural and environmental factors. Some risk factors associated with possible onset and development of cancer are preventable, such as, inappropriate diet, physical inactivity, smoking and drinking [94], while other causes include pathogens (HPV16 and HPV18 are known to cause up to 70% of cervical cancer cases [95]), as well as genetic pre-disposition. Many studies have focussed on identifying efficient genetic cancer biomarkers, such as, specific genes and groups of genes associated with significant number of cases of breast cancer [96], prostate [97] and pancreatic cancer [98]. Despite this progress, due to significant complexity associated with mutations of various cancer genes, many molecular mechanisms of oncogenesis remain poorly understood.

Recent advances in microarray and high-throughput sequencing technologies have provided pathways for measuring the expression of thousands of genes and mapping most crucial genes and groups of genes controlling different types of cancer.

In order to make progress in understanding the onset and development of cancer, as well as to develop effective drug targets, it is essential to be able to reconstruct GRNs pertinent to particular types of cancer from available data. Yeh et al. [99] have used a K-nearest-neighbours algorithm to identify GRNs correlated with cancer, tumour grade and stage in prostate cancer. As an alternative approach, Bonnet et al. [100] have utilised

LeMoNe (Learning Module Networks) algorithms to derive GRNs from gene and mRNA expression, as measured in lymphoblastoid cell lines of prostate cancer patients. A rule-based algorithm has been successfully used to determine GRNs in colon cancer [101], and similar kinds of networks have been identified from microarray data using neural fuzzy networks [102]. Madhamshettiwar et al. [103] discuss different approaches to infer GRNs in ovarian cancer, as well as the potential of using these GRNs to develop optimal drug targets. Bayesian network techniques have been employed to construct GRNs from microarray data for breast cancer [104]. In a recent paper, Emmert-Streib et al. [105] have successfully used a BC3Net inference algorithm to analyse a large-scale breast cancer gene expression data set and reconstruct the associated GRN.

This chapter is devoted to consideration of the effects of transcriptional and translational time delays on the dynamics of GRNs. We introduce the time-delayed model of a two-gene activation-inhibition network together with its quasi-steady state simplification, and estabilish the well-posedness of both models. We derive analytical conditions for stability and a Hopf bifurcation in the case of very fast mRNA dynamics, before extending analysis to the full time-delayed system.

2.1 Time-Delayed Models: Derivation and Positivity

To motivate the analysis of time-delayed effects in gene regulatory dynamics, following Polynikis et al. [32], we consider an activation-inhibition two-gene GRN consisting of two genes a and b, which are assumed to have no effect on their own expression; at the same time, protein P_b is assumed to activate the expression of gene a, while protein P_a inhibits the expression of gene b. This is one of the fundamental motifs, which has been shown to be functionally relevant in GRNs [50, 106]. Denoting the concentrations of proteins P_a and P_b as p_a and p_b, and concentrations of transcribed mRNAs as r_a and r_b, the following system of equations can be derived for the dynamics of this GRN [32]:

$$\begin{aligned}
\dot{r}_a &= m_a h^+(p_b;\theta_b,n_b) - \gamma_a r_a,\\
\dot{r}_b &= m_b h^-(p_a;\theta_a,n_a) - \gamma_b r_b,\\
\dot{p}_a &= k_a r_a - \delta_a p_a,\\
\dot{p}_b &= k_b r_b - \delta_b p_b,
\end{aligned} \tag{2.1}$$

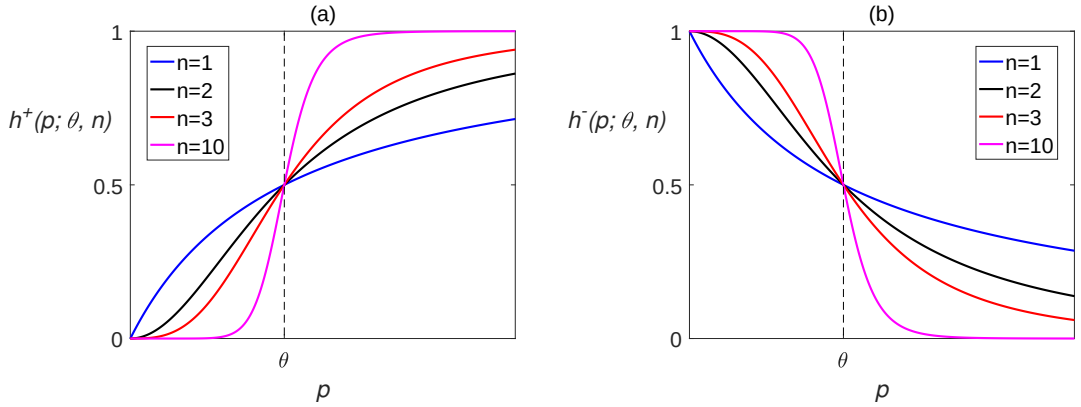

Figure 2.1: Hill functions for activation and inhibition of transcription in system (2.1), varying the Hill coefficient, n. (a) Activation function. (b) Inhibition function.

where m_i are the maximum transcription rates, k_i are the translation rates, γ_i are the mRNA degradation rates, and δ_i are the protein degradation rates for $i = a, b$. Equations (2.1) are called the complete nonlinear model (CNM). To make further analytical progress, the activation and inhibition functions in the system (2.1) can be written as the following Hill functions:

$$h^+(p_i;\theta_i,n_i) = \frac{p_i^{n_i}}{p_i^{n_i}+\theta_i^{n_i}},$$
$$h^-(p_i;\theta_i,n_i) = 1 - h^+(p_i;\theta_i,n_i) = \frac{\theta_i^{n_i}}{p_i^{n_i}+\theta_i^{n_i}}, \qquad i = a, b,$$

where θ_a and θ_b are known as activation and inhibition coefficients, and the integer parameters n_a and n_b, known as Hill coefficients, determine the steepness of Hill curves [1]. The parameters θ_a and θ_b give the values of protein concentrations p_a and p_b, at which the corresponding Hill function achieves half of its maximum value. Depending on the values of transcription rates, this would then lead to a significant increase in the respective mRNAs regulated by these proteins [3, 32]. A qualitative illustration of the activation and inhibition Hill functions is given in Figure 2.1.

Due to the fact that the dynamics of mRNA is normally much faster than that of related proteins, one can use a quasi-steady state assumption to simplify the CNM (2.1) by reducing the number of equations. Effectively, this means assuming that mRNAs have already reached their steady-state concentrations, i.e. taking $\dot{r}_i \approx 0$, $i = a, b$ in the CNM (2.1), and then focusing on the dynamics of proteins only, as given by the following

simplified nonlinear model (SNM):

$$\dot{p}_a = k'_a h^+(p_b; \theta_b, n_b) - \delta_a p_a,$$
$$\dot{p}_b = k'_b h^-(p_a; \theta_a, n_a) - \delta_b p_b,$$

where

$$k'_a = \frac{m_a k_a}{\gamma_a}, \quad k'_b = \frac{m_b k_b}{\gamma_b}. \tag{2.2}$$

Polynikis et al. [32] have shown that while the CNM exhibits Hopf bifurcation of a positive equilibrium, leading to persistent oscillations, in the case of the SNM model this behaviour can disappear. They have also demonstrated an important role played by the Hill coefficients, as well as the separation of timescales between mRNA and proteins, with a larger scale separation favouring a stable equilibrium rather than oscillatory behaviour.

While the transcription and translation may be faster than characteristic times associated with significant changes in protein concentrations (of the order of 5 minutes for transcription + translation and 1 hour for a 50% change in the concentration of translated protein for *E. coli.* [1]), these are, in fact, multi-step processes consisting of thousands of consecutive chemical reactions. Hence, the duration of transcription and translation is non-negligible when considered in the context of GRN dynamics [72, 84], and has to be correctly accounted for in mathematical models. To analyse the effects of transcriptional and translational time delays we introduce the following model [107]:

$$\begin{aligned}
\dot{r}_a &= m_a h^+(p_b(t - \tau_{r_a}); \theta_b, n_b) - \gamma_a r_a, \\
\dot{r}_b &= m_b h^-(p_a(t - \tau_{r_b}); \theta_a, n_a) - \gamma_b r_b, \\
\dot{p}_a &= k_a r_a(t - \tau_{p_a}) - \delta_a p_a, \\
\dot{p}_b &= k_b r_b(t - \tau_{p_b}) - \delta_b p_b,
\end{aligned} \tag{2.3}$$

where τ_{r_a} and τ_{r_b} are the delays during transcription of mRNAs r_a and r_b, and τ_{p_a} and τ_{p_b} are the delays during translation of proteins p_a and p_b, respectively. This model will be referred to as the delayed complete non-linear model (DCNM). Similar to the case of instantaneous transcription and translation, the quasi-steady-state assumption simplifies

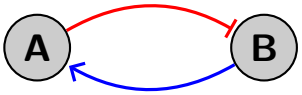

Figure 2.2: Network motif for the activation-inhibition model of the DCNM and DSNM. The nodes are genes A and B where expression of gene B is inhibited by gene A, whilst expression of gene A is activated by gene B.

the system (2.3) to the following delayed simplified non-linear model (DSNM):

$$\begin{aligned} \dot{p}_a &= k'_a h^+(p_b(t-\tau_{r_a}-\tau_{p_a});\theta_b,n_b)-\delta_a p_a, \\ \dot{p}_b &= k'_b h^-(p_a(t-\tau_{r_b}-\tau_{p_b});\theta_a,n_a)-\delta_b p_b, \end{aligned} \tag{2.4}$$

with parameters k'_a and k'_b defined in (2.2).

Before proceeding with the analysis, one has to augment the models (2.3) and (2.4) with the appropriate initial conditions and establish that these models are well-posed, i.e. that their solutions remain non-negative for all time to ensure their biological feasibility. The initial conditions for the DCNM model (2.3) are given by

$$\begin{aligned} r_a(s) &= \phi_1(s), \quad s\in[-\tau_{\max},0], \\ r_b(s) &= \phi_2(s), \quad s\in[-\tau_{\max},0], \\ p_a(s) &= \phi_3(s), \quad s\in[-\tau_{\max},0], \\ p_b(s) &= \phi_4(s), \quad s\in[-\tau_{\max},0], \end{aligned} \tag{2.5}$$

where $\tau_{\max}=\max(\tau_{r_a},\tau_{r_b},\tau_{p_a},\tau_{p_b})$ and $\phi_i(s)\in C([-\tau_{\max},0],\mathbb{R})$ with $\phi_i(s)\geq 0$ ($-\tau_{\max}\leq s\leq 0$, $i=1,..,4$), and similarly for the DSNM model (2.4). Here, $C([-\tau_{\max},0],\mathbb{R})$ is the Banach space of continuous mappings of the interval $[-\tau_{\max},0]$ into $\mathbb{R}$. It is further assumed that $r_a(0)>0$, $r_b(0)>0$ to ensure that at least some amount of proteins will be produced.

We now prove that the solution $(r_a(t),r_b(t),p_a(t),p_b(t))$ of the DCNM model (2.3) with the initial condition (2.5) is positive for all $t>0$. This result can be proven by contradiction, following the methodology used in [93]. As a first step, let us show that $r_b(t)\geq 0$ for all $t>0$. Let $t_1>0$ be the first time when $p_a(t_1)r_b(t_1)=0$; assuming that $r_b(t_1)=0$ implies $p_a(t)\geq 0$ for all $t\in[0;t_1]$, and since t_1 is the first time when $r_b(t_1)=0$, this also means $dr_b(t_1)/dt\leq 0$; that is, the function $r_b(t)$ is decreasing at $t=t_1$. On the

other hand, evaluating the second equation of the system (2.3) at $t = t_1$ yields

$$\frac{dr_b(t_1)}{dt} = \frac{m_b \theta_a^{n_a}}{p_a(t_1 - \tau_{r_b})^{n_a} + \theta_a^{n_a}} > 0,$$

which gives a contradiction. Since $r_b(0) > 0$, this implies $r_b(t) > 0$ for all $t > 0$. Now that the positivity of $r_b(t)$ has been established, let $t_2 > 0$ be the first time when $p_b(t_2) = 0$. In order for this to happen, one must have $dp_b(t_2)/dt \leq 0$; that is, the function $p_b(t)$ should be decreasing at $t = t_2$. At the same time, evaluating the last equation of the system (2.3) at $t = t_2$ yields

$$\frac{dp_b(t_2)}{dt} = k_b r_b(t_2 - \tau_{p_b}) > 0,$$

which gives a contradiction and, therefore, $p_b(t) > 0$ for all $t > 0$. In a similar manner, the positivity of $p_b(t)$ implies the positivity of $r_a(t)$, which in turn implies the positivity of $p_a(t)$. Hence, all solutions $r_a(t)$, $r_b(t)$, $p_a(t)$ and $p_b(t)$ of the DCNM model (2.3) are positive for all $t > 0$. The same approach can be employed to show positivity of solutions of DSNM model (2.4).

Steady states $(\bar{r}_a, \bar{r}_b, \bar{p}_a, \bar{p}_b)$ of the DCNM model can be found as roots of the following system of algebraic equations:

$$\begin{aligned} m_a h^+(\bar{p}_b; \theta_b, n_b) - \gamma_a \bar{r}_a &= 0, \\ m_b h^-(\bar{p}_a; \theta_a, n_a) - \gamma_b \bar{r}_b &= 0, \\ k_a \bar{r}_a - \delta_a \bar{p}_a &= 0, \\ k_b \bar{r}_b - \delta_b \bar{p}_b &= 0. \end{aligned}$$

This gives

$$\bar{r}_a = \frac{\delta_a}{k_a}\bar{p}_a, \qquad \bar{r}_b = \frac{\delta_b}{k_b}\bar{p}_b, \qquad \bar{p}_b = \frac{\phi_b \theta_a^{n_a}}{\theta_a^{n_a} + \bar{p}_a^{n_a}},$$

where $\bar{p}_a$ satisfies the polynomial equation

$$\theta_b^{n_b} \sum_{k=0}^{n_b} \binom{n_b}{k} \bar{p}_a^{n_a(n_b-k)+1} \theta_a^{n_a k} + (\bar{p}_a - \phi_a)(\phi_b \theta_a^{n_a})^{n_b} = 0, \tag{2.6}$$

and we used the notation

$$\phi_a = \frac{m_a k_a}{\gamma_a \delta_a}, \qquad \phi_b = \frac{m_b k_b}{\gamma_b \delta_b}.$$

Even for realistically small values of Hill coefficients, such as $n = 2, 3$ [108] or $n = 4$-8 [109], (2.6) is too complicated to allow one to analytically find closed form expressions for $\bar{p}_a$ and other state variables. Despite not having explicit formulae for possible steady states $(\bar{r}_a, \bar{r}_b, \bar{p}_a, \bar{p}_b)$, one can still perform the analysis of stability in terms of system parameters, and such results would be valid for the values of steady state variables that can be accurately and efficiently determined through numerical solution of the polynomial equation (2.6).

2.2 Analysis of the Delayed Simplified Nonlinear Model (DSNM)

In order to gain some first insights into the role of transcriptional and translational delays on the dynamics of GRN, we focus on the behaviour of the delayed simplified nonlinear model (DSNM) (2.4). To reduce the number of free parameters in the model, we introduce the new variables:

$$\hat{p}_a(t) = p_a(t), \quad \hat{p}_b(t) = p_b(t - \tau_{r_a} - \tau_{p_a}), \tag{2.7}$$

which transform the first equation of system (2.4) into

$$\dot{p}_a = k'_a h^+(p_b(t - \tau_{r_a} - \tau_{p_a}); \theta_b, n_b) - \delta_a p_a \quad \Longleftrightarrow \quad \dot{\hat{p}}_a(t) = k'_a h^+(\hat{p}_b(t); \theta_b, n_b) - \delta_a \hat{p}_a(t).$$

The second equation of system (2.4) evaluated at $t - \tau_{r_a} - \tau_{p_a}$ has the form

$$\dot{p}_b(t - \tau_{r_a} - \tau_{p_a}) = k'_b h^-(p_a(t - \tau_{r_a} - \tau_{p_a} - \tau_{r_b} - \tau_{p_b}); \theta_a, n_a) - \delta_b p_b(t - \tau_{r_a} - \tau_{p_a}),$$

and in terms of the new variables (2.7) this can be rewritten as

$$\dot{\hat{p}}_b(t) = k'_b h^-(\hat{p}_a(t - \tau_{r_a} - \tau_{p_a} - \tau_{r_b} - \tau_{p_b}); \theta_a, n_a) - \delta_b \hat{p}_b(t).$$

Thus, system (2.4) takes form

$$\begin{aligned} \dot{\hat{p}}_a(t) &= k'_a h^+(\hat{p}_b(t); \theta_b, n_b) - \delta_a \hat{p}_a(t), \\ \dot{\hat{p}}_b(t) &= k'_b h^-(\hat{p}_a(t - \tau); \theta_a, n_a) - \delta_b \hat{p}_b(t), \end{aligned} \tag{2.8}$$

where

$$\tau = \tau_{r_a} + \tau_{p_a} + \tau_{r_b} + \tau_{p_b}$$

is the new combined time delay. The equation for eigenvalues λ of the linearisation near a steady state $(\bar{p}_a, \bar{p}_b)$ of system (2.8) has the form

$$(\lambda + \delta_a)(\lambda + \delta_b) + D_{\mathrm{DSNM}} e^{-\lambda\tau} = 0, \tag{2.9}$$

where

$$D_{\mathrm{DSNM}} = k'_a k'_b n_a n_b \frac{\theta_a^{n_a} \theta_b^{n_b} \bar{p}_a^{(n_a-1)} \bar{p}_b^{(n_b-1)}}{(\theta_a^{n_a} + \bar{p}_a^{n_a})^2 (\theta_b^{n_b} + \bar{p}_b^{n_b})^2} = n_a n_b \delta_a \delta_b \frac{\bar{p}_a^{n_a}}{\theta_a^{n_a} + \bar{p}_a^{n_a}} \frac{\theta_b^{n_b}}{\theta_b^{n_b} + \bar{p}_b^{n_b}}.$$

In the limit $\tau = 0$, this equation reduces to the quadratic equation [32]:

$$\lambda^2 + (\delta_a + \delta_b)\lambda + \delta_a \delta_b + D_{\mathrm{DSNM}} = 0,$$

whose roots always have negative real parts, since $\delta_a > 0$, $\delta_b > 0$ and $D_{\mathrm{DSNM}} > 0$. This implies that, for $\tau = 0$, the steady state $(\bar{p}_a, \bar{p}_b)$ is stable for any values of parameters. To investigate whether this steady state can lose stability for $\tau > 0$, one can note that $\lambda = 0$ is not a solution of the characteristic equation (2.9). Hence, the only possible way that the steady state $(\bar{p}_a, \bar{p}_b)$ can lose its stability is when a pair of complex conjugate eigenvalues crosses the imaginary axis. In the light of this observation, one can look for eigenvalues of (2.9) in form $\lambda = i\omega$ for some real $\omega > 0$. Substituting this into (2.9) and separating into real and imaginary parts gives

$$\begin{aligned} \omega^2 - \delta_a \delta_b &= D_{\mathrm{DSNM}} \cos(\omega\tau), \\ (\delta_a + \delta_b)\omega &= D_{\mathrm{DSNM}} \sin(\omega\tau). \end{aligned} \tag{2.10}$$

Squaring and adding these two equations yields the following equation for $z = \omega^2$:

$$h(z) = z^2 + (\delta_a^2 + \delta_b^2)z + \delta_a^2 \delta_b^2 - D_{\mathrm{DSNM}}^2 = 0,$$

which can be solved to give the critical frequency as

$$\omega_0^2 = \frac{1}{2}\left[-(\delta_a^2 + \delta_b^2) + \sqrt{(\delta_a^2 + \delta_b^2)^2 - 4(\delta_a^2 \delta_b^2 - D_{\mathrm{DSNM}}^2)}\right]. \tag{2.11}$$

One should note that ω_0^2 will only admit positive real values, provided $\delta_a\delta_b < D_{\text{DSNM}}$, which implies that, for $\delta_a\delta_b \geq D_{\text{DSNM}}$, the steady state $(\bar{p}_a, \bar{p}_b)$ is stable for all values of the time delay τ. Note that

$$\frac{dh(z)}{dz} = 2z + \delta_a^2 + \delta_b^2 > 0 \quad \text{for any} \quad z \geq 0.$$

The critical value of the time delay τ can be found from (2.10), which gives

$$\tau_{0,n} = \frac{1}{\omega_0}\left[\arctan\left(\frac{(\delta_a + \delta_b)\omega_0}{\omega_0^2 - \delta_a\delta_b}\right) + n\pi\right], \qquad n = 0, 1, 2, ...,$$

where ω_0 is determined by (2.11), and arctan corresponds to the principal value of arctan. When $\tau = \tau_{0,n}$, the characteristic equation (2.9) has a pair of purely imaginary roots. To determine whether or not these roots do indeed cross the imaginary axis, we consider $\lambda(\tau) = \mu(\tau) + i\omega(\tau)$ as a root of (2.9) near $\tau = \tau_{0,n}$, satisfying $\mu(\tau_{0,n}) = 0$, $\omega(\tau_{0,n}) = \omega_0$, and $j = 0, 1, 2, ...$ Substituting $\lambda = \lambda(\tau)$ into (2.9) and differentiating with respect to τ yields

$$\left(\frac{d\lambda}{d\tau}\right)^{-1} = \frac{(2\lambda + \delta_a + \delta_b)e^{\lambda\tau}}{\lambda D_{\text{DSNM}}} - \frac{\tau}{\lambda}.$$

From this equation, one can find

$$\begin{aligned}
\operatorname{sgn}\left\{\left[\frac{d(\text{Re}\lambda)}{d\tau}\right]_{\tau=\tau_{0,n}}\right\} &= \operatorname{sgn}\left\{\text{Re}\left[\left(\frac{d\lambda}{d\tau}\right)^{-1}\right]_{\tau=\tau_{0,n}}\right\} \\
&= \operatorname{sgn}\left\{\text{Re}\left[\frac{(2\lambda + \delta_a + \delta_b)e^{\lambda\tau}}{\lambda D_{\text{DSNM}}}\right]_{\tau=\tau_{0,n}}\right\} \\
&= \operatorname{sgn}\left\{\frac{2\omega_0\cos(\omega_0\tau_{0,n}) + (\delta_a + \delta_b)\sin(\omega_0\tau_{0,n})}{\omega_0 D_{\text{DSNM}}}\right\}.
\end{aligned}$$

Substituting the expressions for $\cos(\omega_0\tau_{0,n})$ and $\sin(\omega_0\tau_{0,n})$ from system (2.10) gives

$$\operatorname{sgn}\left\{\left[\frac{d(\text{Re}\lambda)}{d\tau}\right]_{\tau=\tau_{0,n}}\right\} = \operatorname{sgn}\left\{\frac{2(\omega_0^2 - \delta_a\delta_b) + (\delta_a + \delta_b)^2}{D_{\text{DSNM}}^2}\right\} = \operatorname{sgn}\left\{\frac{h'(\omega_0^2)}{D_{\text{DSNM}}^2}\right\} > 0.$$

Hence, the eigenvalues of the characteristic equation cross the imaginary axis at $\tau = \tau_0$ (here, $\tau_0 = \tau_{0,0}$) and never cross back for higher values of τ. Thus, we have proved the following result.

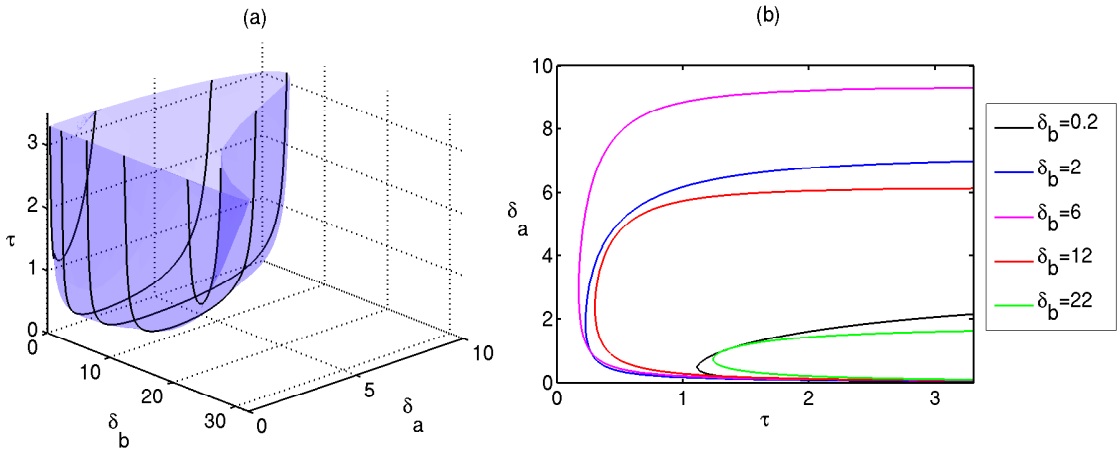

Figure 2.3: Stability boundary of the steady state $(\bar{p}_a, \bar{p}_b)$ of DSNM system (2.8). The steady state is stable below the surface in (a) and to the left of the boundary curves shown in (b). Parameter values are $m_a = m_b = 2.35$, $\theta_a = \theta_b = 0.21$, $n_a = n_b = 3$, and $k_a = k_b = \gamma_a = \gamma_b = 1$.

Theorem 2.1. *If $\delta_a \delta_b \geq D_{DSNM}$, the steady state $(\bar{p}_a, \bar{p}_b)$ of DSNM system (2.8) is stable for all values of the time delay $\tau \geq 0$. If $\delta_a \delta_b < D_{DSNM}$, this steady state is stable for $0 \leq \tau < \tau_0$ and unstable for $\tau > \tau_0$ and undergoes a Hopf bifurcation at $\tau = \tau_0$.*

Figure 2.3 illustrates the stability boundary of the steady state $(\bar{p}_a, \bar{p}_b)$ of the DSNM system (2.8) depending on the time delay τ and the protein degradation rates δ_a and δ_b, with the parameter values taken from Polynikis et al. [32]. This Figure suggests that, for any fixed value of one of such rates, there is only a limited range of positive values of the other degradation rate, for which, at a given time delay τ, the positive equilibrium is unstable. For sufficiently high values of δ_a and δ_b, this steady state is stable regardless of the value of the time delay τ, confirming the result proved in Theorem 2.1.

In Figure 2.4 we show how the stability boundary varies depending on the parameters θ_a and θ_b, and the time delay τ. One observes that, for sufficiently high values of θ_b, the range of possible values of θ_a for which the steady state is unstable is significantly reduced, thus making the system more prone to support a stable positive equilibrium rather than exhibit oscillations. At the Hopf bifurcation, the associated critical value of the time delay τ monotonically increases with the parameter θ_a. At the same time, there is a minimum

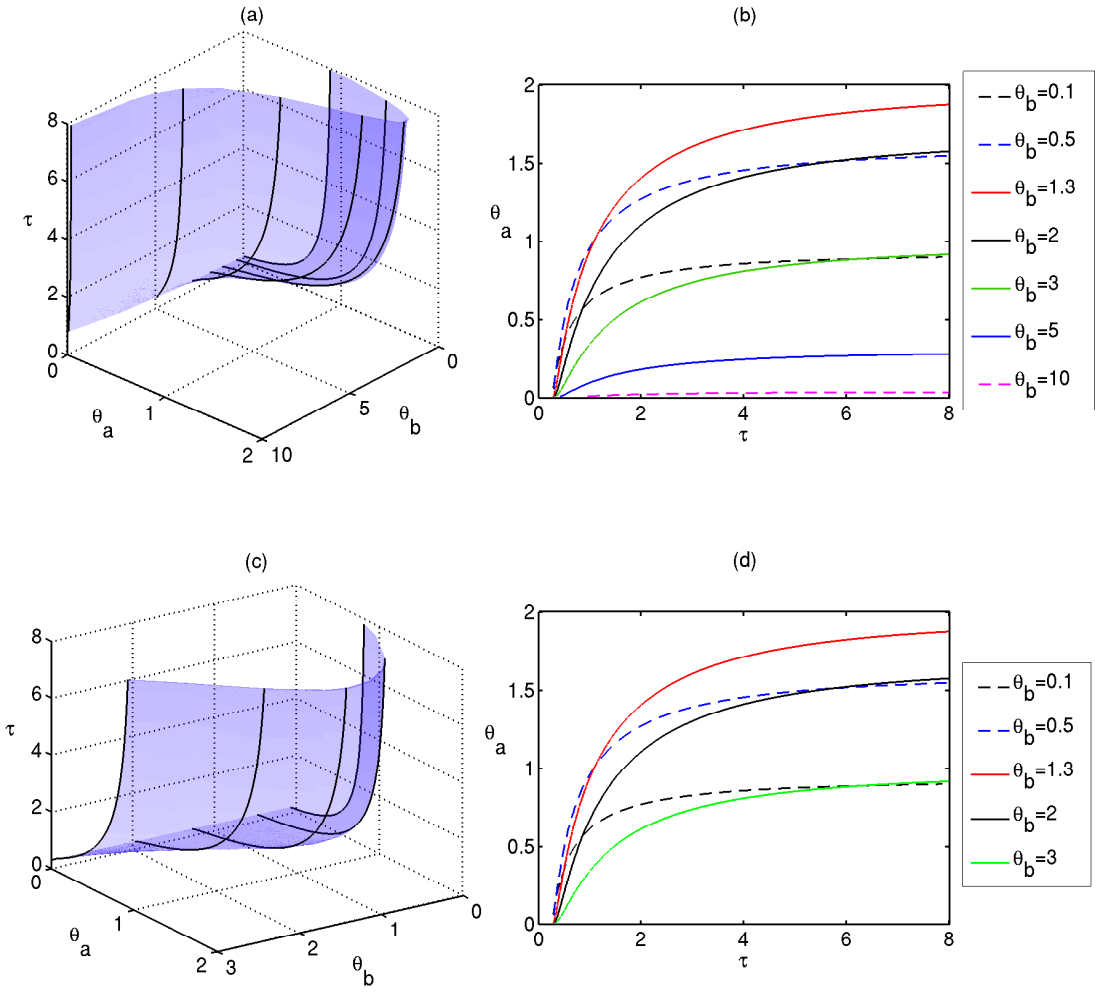

Figure 2.4: Stability boundary of the steady state $(\bar{p}_a, \bar{p}_b)$ of DSNM system (2.8). The steady state is stable below the surface in (a) and (c) and to the left of the boundary curves shown in (b) and (d). Parameter values are $m_a = m_b = 2.35$, $n_a = n_b = 3$, and $k_a = k_b = \delta_a = \delta_b = \gamma_a = \gamma_b = 1$.

value of the time delay τ, such that for τ smaller than this value the steady state $(\bar{p}_a, \bar{p}_b)$ is stable for any value of θ_a.

In a similar way, the effects of the transcription rates m_a and m_b are illustrated in Figure 2.5, which shows that the critical transcription rate of the inhibitor m_a increases with decreasing τ, and, similar to Figure 2.4, below certain value of τ, the steady state $(\bar{p}_a, \bar{p}_b)$ is stable for any value of m_a. Qualitatively similar dependence is observed between the critical value of τ and the transcription rate m_b, though this dependence is not completely monotonic.

Figure 2.6 demonstrates how increasing the overall time delay τ results in a Hopf bifurcation of the steady state $(\bar{p}_a, \bar{p}_b)$ and the emergence of a stable periodic orbit. The

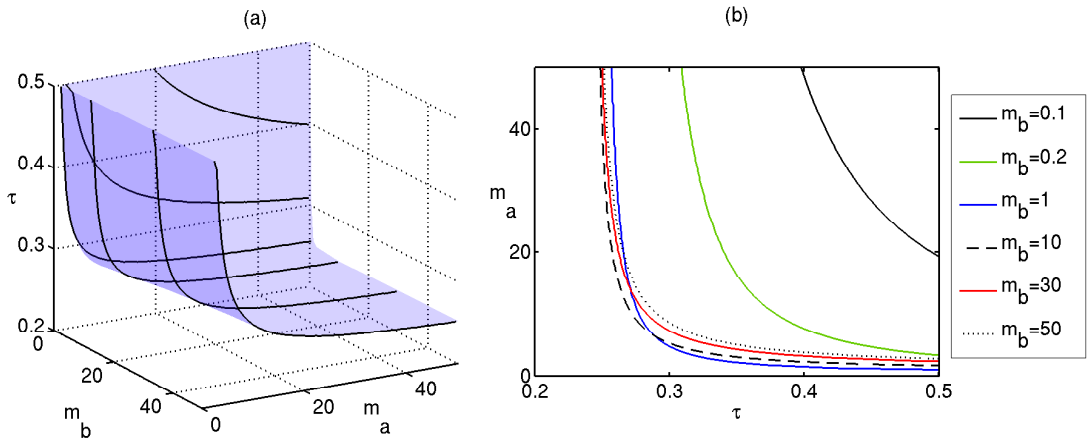

Figure 2.5: Stability boundary of the steady state $(\bar{p}_a, \bar{p}_b)$ of DSNM system (2.8). The steady state is stable below the surface in (a), and to the left of the boundary curves shown in (b). Parameter values are $\theta_a = \theta_b = 0.21$, $n_a = n_b = 3$, and $k_a = k_b = \delta_a = \delta_b = \gamma_a = \gamma_b = 1$.

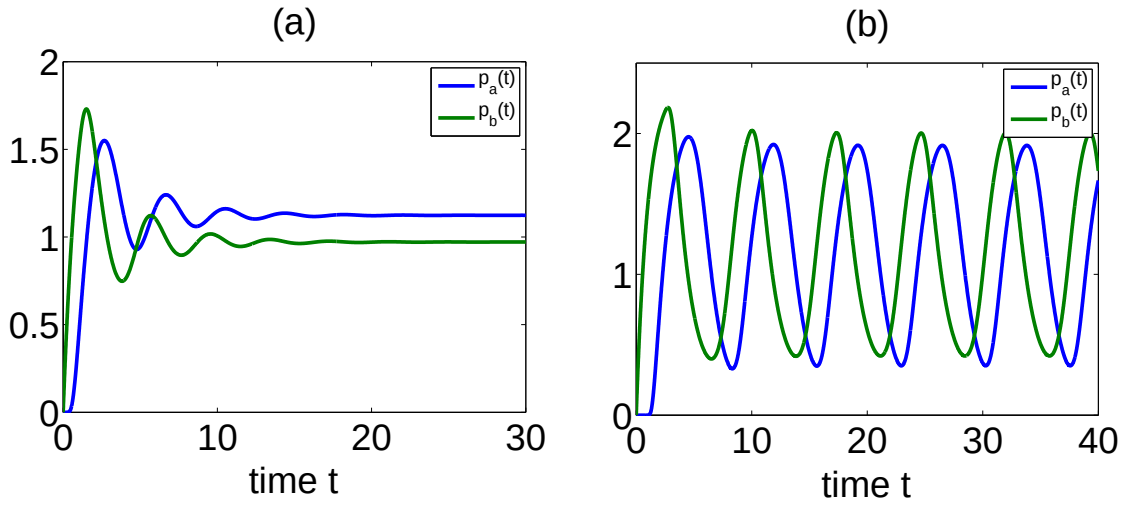

Figure 2.6: Numerical solution of DSNM system (2.8): (a) $\tau = 0.5$; (b) $\tau = 2$. Parameter values are $m_a = m_b = 2.35$, $\theta_a = \theta_b = 1$, $n_a = n_b = 3$, and $k_a = k_b = \delta_a = \delta_b = \gamma_a = \gamma_b = 1$. The critical time delay is $\tau_0 = 0.9762$.

shift between individual time series for p_a and p_b can be interpreted in the same way as in predator-prey or activator-inhibitor systems [110]. In accordance with Theorem 2.1, once the stability of the steady state $(\bar{p}_a, \bar{p}_b)$ is lost, it can never be regained for higher values of τ, so the system will be exhibiting oscillatory behaviour. This result highlights the significance of correct mathematical representation of the transcription and translation processes, since inclusion of transcriptional and translational delays can lead to sustained periodic oscillations even in the simplified model, where such oscillations were impossible when the time delays were neglected.

2.3 Analysis of the Delayed Complete Nonlinear Model (DCNM)

Linearisation of the full nonlinear DCNM model (2.3) near the steady state $(\bar{r}_a, \bar{r}_b, \bar{p}_a, \bar{p}_b)$ results in the following characteristic equation:

$$(\lambda+\gamma_a)(\lambda+\gamma_b)(\lambda+\delta_a)(\lambda+\delta_b)+D_{\mathrm{DCNM}}e^{-\lambda\tau}=0, \tag{2.12}$$

where

$$D_{\mathrm{DCNM}}=m_a m_b k_a k_b \theta_a^{n_a}\theta_b^{n_b}\frac{n_a n_b \bar{p}_a^{(n_a-1)}\bar{p}_b^{(n_b-1)}}{(\theta_a^{n_a}+\bar{p}_a^{n_a})^2(\theta_b^{n_b}+\bar{p}_b^{n_b})^2}=n_a n_b \delta_a\delta_b\gamma_a\gamma_b\frac{\bar{p}_a^{n_a}}{\theta_a^{n_a}+\bar{p}_a^{n_a}}\frac{\theta_b^{n_b}}{\theta_b^{n_b}+\bar{p}_b^{n_b}},$$

and

$$\tau=\tau_{r_a}+\tau_{r_b}+\tau_{p_a}+\tau_{p_b}.$$

It immediately follows from the form of the characteristic equation (2.12) that stability of the steady state $(\bar{r}_a, \bar{r}_b, \bar{p}_a, \bar{p}_b)$ is determined not by individual transcriptional and translational delays but rather by their overall combined duration. In the case $\tau_{r_a}=\tau_{r_b}=\tau_{p_a}=\tau_{p_b}=0$, the characteristic equation of the DCNM model reduces to the one analysed in Polynikis et al. [32].

The characteristic equation (2.12) can be recast in the form

$$\lambda^4+A\lambda^3+B\lambda^2+C\lambda+(D+D_{\mathrm{DCNM}}e^{-\lambda\tau})=0, \tag{2.13}$$

where

$$\begin{aligned}
A&=\gamma_a+\gamma_b+\delta_a+\delta_b,\\
B&=\gamma_a\gamma_b+\gamma_a\delta_a+\gamma_a\delta_b+\gamma_b\delta_a+\gamma_b\delta_b+\delta_a\delta_b,\\
C&=\gamma_a\gamma_b\delta_a+\gamma_a\gamma_b\delta_b+\gamma_a\delta_a\delta_b+\gamma_b\delta_a\delta_b,\\
D&=\gamma_a\gamma_b\delta_a\delta_b.
\end{aligned} \tag{2.14}$$

At $\tau=0$, (2.13) reduces to a quartic

$$\lambda^4+A\lambda^3+B\lambda^2+C\lambda+(D+D_{\mathrm{DCNM}})=0. \tag{2.15}$$

By the Routh-Hurwitz criterion [110], the necessary and sufficient conditions for all roots of (2.15) to have negative real parts are given by

$$\Delta_1 = A > 0,$$
$$\Delta_2 = AB - C > 0,$$
$$\Delta_3 = ABC - A^2(D + D_{\mathrm{DCNM}}) > 0,$$
$$\Delta_4 = (D + D_{\mathrm{DCNM}})(ABC - A^2(D + D_{\mathrm{DCNM}}) - C^2) = (D + D_{\mathrm{DCNM}})(\Delta_3 - C^2) > 0.$$

From the fact that all system parameters are positive and using the definitions of A, B, and C in (2.14), it follows that $\Delta_1 > 0$ and $\Delta_2 > 0$ for any values of the parameters. Since $D + D_{\mathrm{DCNM}} > 0$, it is sufficient to require $\Delta_4 > 0$ to ensure that condition $\Delta_3 > 0$ is also satisfied. This leads to the following result.

Lemma 2.1. *Let $\tau = 0$. The steady state $(\bar{r}_a, \bar{r}_b, \bar{p}_a, \bar{p}_b)$ of the system (2.3) is stable whenever the condition $ABC - A^2(D + D_{\mathrm{DCNM}}) - C^2 > 0$ holds.*

From now on, we will assume that the condition in Lemma 2.1 holds and analyse whether stability can be lost as τ increases. Since both D and D_{DCNM} are positive, this means that $\lambda = 0$ is not a root of the characteristic equation (2.13), so once again the stability can only be lost through a possible Hopf bifurcation. To investigate this possibility, we look for solutions of (2.13) in the form $\lambda = i\omega$ for some real $\omega > 0$. Substituting this into (2.13) and separating into the real and imaginary parts gives

$$\begin{aligned} \omega^4 - B\omega^2 + D &= -D_{\mathrm{DCNM}} \cos(\omega\tau), \\ -A\omega^3 + C\omega &= D_{\mathrm{DCNM}} \sin(\omega\tau). \end{aligned} \tag{2.16}$$

Squaring and adding these equations yields a quartic equation as follows:

$$g(z) = z^4 + az^3 + bz^2 + cz + d = 0, \tag{2.17}$$

where $z = \omega^2$ and

$$\begin{aligned} a &= A^2 - 2B, \\ b &= B^2 + 2D - 2AC, \\ c &= C^2 - 2BD, \\ d &= D^2 - D_{\text{DCNM}}^2. \end{aligned}$$

Without loss of generality, suppose that (2.17) has four positive real roots, denoted by z_1, z_2, z_3, z_4, respectively, which would give four possible values of ω:

$$\omega_1 = \sqrt{z_1}, \;\; \omega_2 = \sqrt{z_2}, \;\; \omega_3 = \sqrt{z_3}, \;\; \omega_4 = \sqrt{z_4}.$$

Dividing the two equations in (2.16) gives

$$\tan(\omega_k \tau_k) = \frac{A\omega_k^3 - C\omega_k}{\omega_k^4 - B\omega_k^2 + D} \implies \tau_{k,j} = \frac{1}{\omega_k}\left[\arctan\left(\frac{A\omega_k^3 - C\omega_k}{\omega_k^4 - B\omega_k^2 + D}\right) + j\pi\right], \quad k = 1, .., 4, \;\; j = 0, 1, 2, ...$$

Define

$$\tau_0 = \min_{1 \le k \le 4} \{\tau_{k,0}\}, \quad \omega_0 = \omega_{k_0}, \quad k_0 \in \{1, 2, 3, 4\},$$

and then τ_0 is the first value of $\tau > 0$ such that the characteristic equation (2.13) has a pair of purely imaginary roots. We have the following result.

Theorem 2.2. *Suppose the conditions of Lemma 2.1 hold and $g'(z_0) > 0$, where $g(z)$ is defined in (2.17). Then the steady state $(\bar{r}_a, \bar{r}_b, \bar{p}_a, \bar{p}_b)$ of system (2.3) is stable for $0 \le \tau < \tau_0$ and unstable for $\tau > \tau_0$ and undergoes a Hopf bifurcation at $\tau = \tau_0$.*

Proof. The conclusion of Lemma 2.1 ensures the steady state $(\bar{r}_a, \bar{r}_b, \bar{p}_a, \bar{p}_b)$ of system (2.3) is stable at $\tau = 0$, and the fact that the roots of the characteristic equation (2.13) depend continuously on τ implies that the steady state $(\bar{r}_a, \bar{r}_b, \bar{p}_a, \bar{p}_b)$ is also stable for sufficiently small positive values of τ. Since τ_0 is the first positive τ, for which the eigenvalues lie on the imaginary axis, in order to verify whether or not the steady state actually loses stability

at $\tau = \tau_0$, one has to compute the sign of $d\mathrm{Re}(\lambda)/d\tau|_{\tau=\tau_0}$. Let $\lambda(\tau) = \mu(\tau) + i\omega(\tau)$ be the root of the characteristic equation (2.13) near $\tau = \tau_0$, satisfying $\mu(\tau_0) = 0$ and $\omega(\tau_0) = \omega_0$. Substituting $\lambda = \lambda(\tau)$ into (2.13) and differentiating both sides with respect to τ gives

$$\left(\frac{d\lambda}{d\tau}\right)^{-1} = \frac{(4\lambda^3 + 3A\lambda^2 + 2B\lambda + C)e^{\lambda\tau}}{\lambda D_{\mathrm{DCNM}}} - \frac{\tau}{\lambda}.$$

This implies, with $\lambda(\tau_0) = i\omega_0$,

$$\begin{aligned}
\mathrm{sgn}\left\{\left[\frac{d(\mathrm{Re}\lambda)}{d\tau}\right]_{\tau=\tau_0}\right\} &= \mathrm{sgn}\left\{\mathrm{Re}\left[\left(\frac{d\lambda}{d\tau}\right)^{-1}\right]_{\tau=\tau_0}\right\} \\
&= \mathrm{sgn}\left\{\mathrm{Re}\left[\frac{(4\lambda^3 + 3A\lambda^2 + 2B\lambda + C)e^{\lambda\tau}}{\lambda D_{\mathrm{DCNM}}}\right]_{\tau=\tau_0}\right\} \\
&= \mathrm{sgn}\left\{\frac{(2B\omega_0 - 4\omega_0^3)\cos(\omega_0\tau_0) + (C - 3A\omega_0^2)\sin(\omega_0\tau_0)}{\omega_0 D_{\mathrm{DCNM}}}\right\}.
\end{aligned}$$

Using the expressions for $\cos(\omega_0\tau_0)$ and $\sin(\omega_0\tau_0)$ from (2.16) gives

$$\begin{aligned}
\mathrm{sgn}\left\{\left[\frac{d(\mathrm{Re}\lambda)}{d\tau}\right]_{\tau=\tau_0}\right\} &= \mathrm{sgn}\left\{\frac{4\omega_0^6 + (3A^2 - 6B)\omega_0^4 + (2B^2 + 4D - 4AC)\omega_0^2 + C^2 - 2BD}{D_{\mathrm{DCNM}}^2}\right\} \\
&= \mathrm{sgn}\left\{\frac{g'(\omega_0^2)}{D_{\mathrm{DCNM}}^2}\right\} > 0,
\end{aligned}$$

which means that at $\tau = \tau_0$ a pair of complex conjugate eigenvalues of the characteristic equation (2.13) crosses the imaginary axis with a positive speed. This implies that the steady state $(\bar{r}_a, \bar{r}_b, \bar{p}_a, \bar{p}_b)$ of system (2.3) does lose its stability at $\tau = \tau_0$. □

Figure 2.7 shows the stability boundary of the steady state $(\bar{r}_a, \bar{r}_b, \bar{p}_a, \bar{p}_b)$ of system (2.3) depending on the transcription rates m_a and m_b and the total time delay τ. In a manner similar to that for the simplified model, the critical value of the transcription rate m_a at the Hopf bifurcation reduces with increasing τ. However, a major difference from the DSNM model, as shown in Figure 2.5, is that now the Hopf bifurcation can take place even at $\tau = 0$, as the DCNM system is able to support sustained oscillations [32]. In Figure 2.8 we illustrate the transition from a stable steady state $(\bar{r}_a, \bar{r}_b, \bar{p}_a, \bar{p}_b)$ to a stable periodic solution around this steady state as the time delay passes through the critical value of $\tau = \tau_0$.

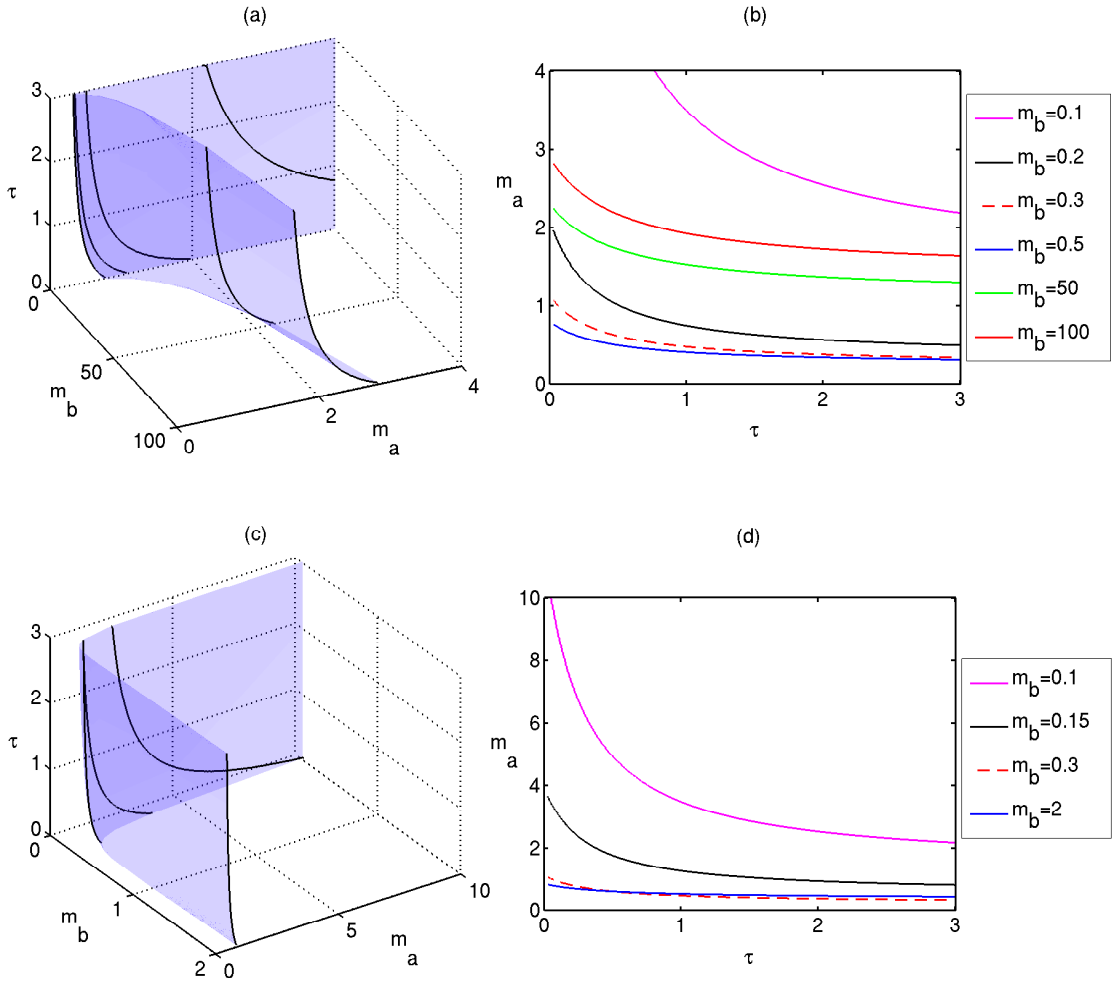

Figure 2.7: Stability boundary of the steady state $(\bar{r}_a, \bar{r}_b, \bar{p}_a, \bar{p}_b)$ of DCNM system (2.3). The steady state is stable below the surface in (a), (c), and below the boundary curves shown in (b), (d). Parameter values: $\theta_a = \theta_b = 0.21$, $n_a = n_b = 3$ and $k_a = k_b = \delta_a = \delta_b = \gamma_a = \gamma_b = 1$.

2.4 Discussion

In this chapter we have discussed mathematical models for the analysis of GRNs and focussed on the role played by the transcriptional and translational time delays in the dynamics of a two-gene activator-inhibitor GRN. By reducing the model to the one with a single time delay, we have considered possible behaviour in the quasi-steady state approximation of very fast mRNA dynamics, which has resulted in a lower-dimensional system of DDEs. Due to the presence of time delays, even this simplified model is able to exhibit loss of stability of the positive equilibrium through a Hopf bifurcation and a subsequent emergence of sustained periodic oscillations, which was not possible in the absence of the

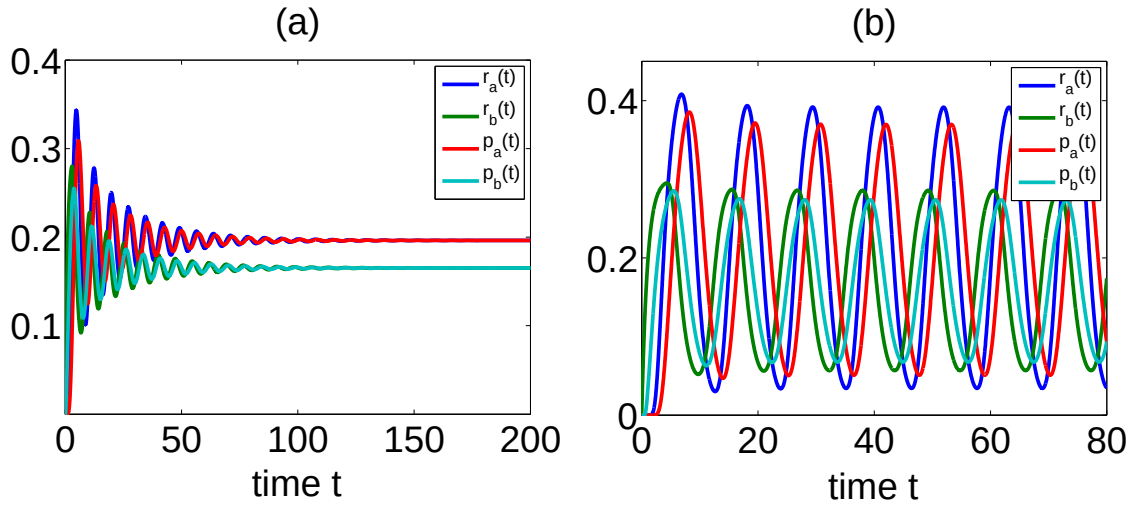

Figure 2.8: Numerical solution of DCNM system (2.3): (a) $\tau = 0.25$; (b) $\tau = 2$. Parameter values: $m_a = 0.6$, $m_b = 0.3$, $\theta_a = \theta_b = 0.21$, $n_a = n_b = 3$, and $k_a = k_b = \delta_a = \delta_b = \gamma_a = \gamma_b = 1$. The critical time delay is $\tau_0 = 0.5314$.

time delays, as discussed in Polynikis et al. [32]. We have found analytically the boundary of the Hopf bifurcation depending on the total time delay and other system parameters and illustrated different types of behaviour by direct numerical simulations. Our results suggest that once the positive steady state loses its stability, it can never regain it for higher values of the time delay.

We have also studied the stability of a positive steady state in the full system and showed that this steady state can also undergo a Hopf bifurcation depending on the time delay and system parameters. Our analysis extends an earlier result of Polynikis et al. [32] by showing how the critical values of the parameters at the Hopf boundary change when the time delay increases from zero. Numerical simulations have illustrated the transition from a stable positive steady state to a stable periodic solution as the time delay exceeds its critical value.

Besides providing insights into the dynamics of GRNs, there are several practical ways in which models similar to the one described in this chapter are helpful for monitoring and treatment of cancer. GRN models based on differential equations coupled with other techniques, such as machine learning and Bayesian networks, have proved effective in identifying specific oncogenes that can be used as biomarkers or drug targets [50, 104, 111–114]. Similar kinds of models are useful for modelling cancer cell growth and understanding interactions between tumour growth and immune response and for analysis of the effects of

chemotherapy (or immunotherapy) and drug resistance [50,51,115,116]. The methodology described in this chapter can be directly used to improve the performance of these models by elucidating the role of transcriptional and translational time delays in GRN dynamics and its impact on various aspects of cancer onset and development.

Chapter 3

Time-Delayed Model of a Genetic Regulatory Network in the Immune System

Recent studies have highlighted the physical applications of GRNs to model cell dynamics in the immune system [117]. The immune system is a complex system of cells and molecules that can provide us with a basic defence against pathogenic organisms. Like the nervous system, the immune system performs pattern recognition tasks, learns, and retains a memory of the antigens that it has fought. Furthermore, the immune response develops in time and the description of its time evolution is an interesting problem in dynamical systems [118].

An area of research in immunology that is of particular interest is the ability to develop deterministic models for cell fates. Sciammas et al. [119] have used a chemical kinetic approach based on ordinary differential equations (ODEs) to develop a model for a GRN that regulates the cell fate dynamics of activated B cells undergoing a germinal centre (GC) response and then differentiating into plasma cells. The architecture of this GRN involves the mutual repression of several transcription factors (TFs), namely a TF of the plasma-cell program, Blimp1, as well as Bcl6 which is essential for GC B cells. In this network design there exists a TF, IRF4, which activates both genes, and also positive feedback based on the mutual activation of Blimp1 and IRF4 [117]. The dynamics that appear as a result of the varied connections between transcription factors provide valuable

insight into the behaviour of proteins in the immune system.

Modelling dynamics of T cells have also been extensively studied [120–123]. H. J. van den Ham et al. developed a simple master regulator for the T_h1/T_h2 paradigm, which can be extended to higher dimensions for larger networks and enables the analysis of other cell types. This general model, however, is mechanistic in characterising binding of transcription factors but due to its simplicity, allows for the study of larger networks. A more deterministic approach was carried out by W. C. Lo [123], who modelled the concentrations of the transcription factors T-Bet (Th1), Gata3 (Th2), and Foxp3 (Treg) in a cell using ODEs. This meant they were able to account for influences from external activators, mutual inhibition, and auto-activation which is modelled using Hill functions. However, mathematical analysis of larger networks using this approach would be very challenging.

Due to the vast number of connections between transcription factors in the immune system, the aim is to be able to model complex networks whilst still capturing useful information about the system dynamics. There have been many different network motifs explored and analysed to various degrees of complexity [124–127]. T. Hong et al. build on their previous work by exploring a three and four master regulator symmetric motif, to describe the interactions between the master transcription factors T-Bet, Gata3, Foxp3 and Rorγt (Th17). It is shown that mathematical analysis and numerical simulation agree with experimental data. This observation motivates investigation into networks with multiple nodes, where inhibition and positive feedback loops are present, to model the dynamics of GRNs in the immune system.

This chapter focuses on the transcriptional and translational delays in a system of three genes, each of which promotes the growth of its own proteins, and expresses unidirectional inhibition. We discuss the works of Andrecut et al. [128] and H. El Samad et al. [129] and derive a delayed model based on the so-called *Repressilator*. We analyse the model and derive conditions for the existence of a Hopf bifurcation leading to periodic oscillations, which could not be present for such a low Hill coefficient in the symmetric *Repressilator* model. Numerical simulations are discussed, which give rise to interesting patterns of stability regions in the parameter space due to the inclusion of multiple time delays. It is also illustrated that only one of the possible 9 steady states has the potential to lose stability.

3.1 Derivation of the Time-Delayed Model

We take insight from the general model studied by Andrecut et al. [128] for describing auto-activation and mutual repression between two general proteins, which has equations given by

$$\begin{aligned} \frac{dx}{dt} &= \frac{ax}{xy + bx + cy + d} - fx, \\ \frac{dy}{dt} &= \frac{ay}{xy + by + cx + d} - fy, \end{aligned} \tag{3.1}$$

where x and y are the two system variables of the generic dynamical system, which can be taken to describe the concentrations of protein x and protein y. The first term of each equation in (3.1) describe both auto-activation and mutual inhibition, and the second terms are degradation for each protein. Note that the growth terms are of the form

$$\left(\frac{x}{\theta_x + x}\right)\left(\frac{\theta_{xy}}{\theta_{xy} + y}\right) = \frac{\theta_{xy}x}{xy + \theta_{xy}x + \theta_x y + \theta_x\theta_{xy}}, \tag{3.2}$$

where the left hand side of the equation consists of two Hill functions with Hill coefficient $n = 1$; the first term representing auto-activation of protein x, and the second is repression of x by protein y.

Here we investigate a three-gene asymmetric model with time delays accounting for those present in auto-activation and mutual repression processes. The model is given by the following set of delay differential equations:

$$\begin{aligned} \frac{dx}{dt} &= \frac{a_1 x(t-\tau_{ax})}{x(t-\tau_{ax})z(t-\tau_{rx}) + b_1 x(t-\tau_{ax}) + c_1 z(t-\tau_{rx}) + d_1} - f_1 x, \\ \frac{dy}{dt} &= \frac{a_2 y(t-\tau_{ay})}{y(t-\tau_{ay})x(t-\tau_{ry}) + b_2 y(t-\tau_{ay}) + c_2 x(t-\tau_{ry}) + d_2} - f_2 y, \\ \frac{dz}{dt} &= \frac{a_3 z(t-\tau_{az})}{z(t-\tau_{az})y(t-\tau_{rz}) + b_3 z(t-\tau_{az}) + c_3 y(t-\tau_{rz}) + d_3} - f_3 z, \end{aligned} \tag{3.3}$$

where τ_{ax}, τ_{ay} and τ_{az} are the transcriptional delays associated to the auto-activation of proteins x, y, and z, while τ_{rx}, τ_{ry}, and τ_{rz} are the transcriptional delays associated to the repression of proteins x, y, and z respectively.

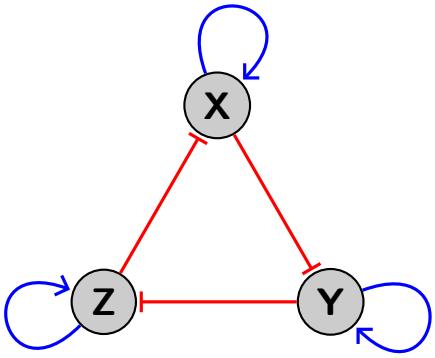

Figure 3.1: Network motif of the *Repressilator* with auto-activation model. The nodes are genes X, Y, and Z, which are connected by edges, in red, representing regulation of each gene by inhibition from the preceding gene in the cycle. The loops, in blue, represent self activation of each gene.

In the work by H. El Samad et al. [129], they discuss a two-gene network given by

$$\begin{aligned}
\dot{r}_1 &= -\delta_1 r_1 + f_1(p2), \\
\dot{p}_1 &= r_1 - \delta_2 p_1, \\
\dot{r}_2 &= -\delta_1 r_2 + f_2(p1), \\
\dot{p}_2 &= r_2 - \delta_2 p_2,
\end{aligned}$$

where $f_1(p_2) = \dfrac{a_2^2}{1+p_2^n}$ and $f_2(p_1) = \dfrac{a_1^2 p_1^n}{1+p_1^n}$ are Hill functions with n being the Hill coefficient. They show that the linearisation of the system does not have positive eigenvalues if $n \leq 2$. Thus, oscillations do not occur unless the Hill coefficient exceeds $n = 2$. H. El Samad et al. then look at a three-gene fully symmetric circuit, where the Hill functions are all of the form $f_i(p) = \dfrac{a^2}{1+p^n}$ and therefore represents a network where each protein represses the transcription of the next. This network is known as the symmetric *Repressilator* [74]. It is shown that periodic solutions are possible for certain choices of the system parameters. Oscillations can occur provided that $n > 4/3$.

The model described by (3.3) is essentially an asymmetric repressilator where each gene also promotes the transcription of its own proteins. As demonstrated in equation (3.2), the growth term in each equation of system (3.3) is composed of two Hill functions with Hill coefficient $n = 1$. Figure 3.2 shows a time profile of system (3.3) where all time delays are equal to zero. We see there are sustained oscillations, which illustrates that

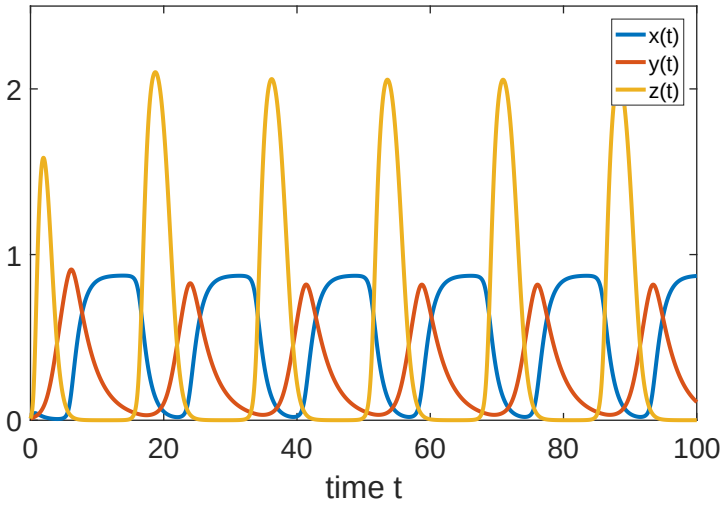

Figure 3.2: Numerical solution of three-gene *Repressilator* model with auto-activation and without time delays. Parameter values: $\tau_x = \tau_y = \tau_z = 0$, $\alpha_1 = 4$, $\alpha_2 = 5$, $\alpha_3 = 6$, $b_1 = 4$, $b_2 = 3$, $b_3 = 1$, $c_1 = 8$, $c_2 = 10$, $c_3 = 15$, $d_1 = 0.5$, $d_2 = 2$, $d_3 = 0.2$, $\gamma_2 = 0.8$, $\gamma_3 = 2$.

the inclusion of auto-activation and asymmetry within the repressilator model can lead to periodic solutions, even with Hill coefficients $n = 1$. Without time delays, system (3.3) can still give rise to sustained oscillations given a small Hill coefficient.

In (3.3) we assume, for simplicity, that the time delays associated with auto-activation and inhibition are equal for each respective gene. Thus, let $\tau_{ax} = \tau_{rx} = \tau_x$ and $\tau_{ay} = \tau_{ry} = \tau_y$ and $\tau_{az} = \tau_{rz} = \tau_z$. We may also rescale the system to reduce the number of free parameters by introducing

$$t = \frac{1}{f_1}\bar{t}.$$

Omitting the bar $\bar{\cdot}$, model (3.3) can be rewritten as follows:

$$\begin{aligned}
\frac{dx}{dt} &= \frac{\alpha_1 x(t-\tau_x)}{x(t-\tau_x)z(t-\tau_x) + b_1 x(t-\tau_x) + c_1 z(t-\tau_x) + d_1} - x, \\
\frac{dy}{dt} &= \frac{\alpha_2 y(t-\tau_y)}{y(t-\tau_y)x(t-\tau_y) + b_2 y(t-\tau_y) + c_2 x(t-\tau_y) + d_2} - \gamma_2 y, \\
\frac{dz}{dt} &= \frac{\alpha_3 z(t-\tau_z)}{z(t-\tau_z)y(t-\tau_z) + b_3 z(t-\tau_z) + c_3 y(t-\tau_z) + d_3} - \gamma_3 z,
\end{aligned} \tag{3.4}$$

where $\alpha_1 = \frac{a_1}{f_1}$, $\alpha_2 = \frac{a_2}{f_1}$, $\alpha_3 = \frac{a_3}{f_1}$, $\gamma_2 = \frac{f_2}{f_1}$, $\gamma_3 = \frac{f_3}{f_1}$, and all system parameters have positive real values. This model will be referred to as the delayed repressilator with auto-activation model (DRAM). We investigate analytically the conditions for oscillations to occur and also examine as to what extent the inclusion of time delays affect steady state stability.

3.2 Time Delayed Model: Positivity and Steady States

Before continuing with any analysis of the DRAM model, first we must define initial conditions where appropriate and address whether all solutions to the model give positive values for all time to guarantee it's biological feasibility. The initial conditions for the DRAM model are

$$\begin{aligned} x(s) &= \phi_1(s), \quad s \in [-\tau_{\max}, 0], \\ y(s) &= \phi_2(s), \quad s \in [-\tau_{\max}, 0], \\ z(s) &= \phi_3(s), \quad s \in [-\tau_{\max}, 0], \end{aligned} \tag{3.5}$$

where $\tau_{\max} = \max(\tau_x, \tau_y, \tau_z)$ and $\phi_i(s) \in C([-\tau_{\max}, 0], \mathbb{R})$ with $\phi_i(s) \geq 0$ ($-\tau_{\max} \leq s \leq 0$, $i = 1, 2, 3$). $C([-\tau_{\max}, 0], \mathbb{R})$ is the Banach space of continuous mappings of the interval $[-\tau_{\max}, 0]$ into $\mathbb{R}$. It is also assumed that $x(0) > 0$, $y(0) > 0$, and $z(0) > 0$ to be sure that some proteins are produced.

Now we prove that the solution $(x(t), y(t), z(t))$ of system (3.4) with initial condition (3.5) is positive for all $t > 0$. As we did in the last chapter, the proof for this makes use of the methodology applied in [93]. First, we show $x(t) > 0$ for all $t > 0$ by contradiction. Let $t_1 > 0$ be the first time that $x(t_1)z(t_1) = 0$; assuming that $x(t_1) = 0$ implies $z(t) \geq 0$ for all $t \in [0; t_1]$ and since t_1 is the first time when $x(t_1) = 0$, this also means that $dx(t_1)/dt \leq 0$, meaning the function $x(t)$ is decreasing at $t = t_1$. However, evaluating the first equation of system (3.4) at $t = t_1$ gives

$$\frac{dx(t_1)}{dt} = \frac{\alpha_1 x(t_1 - \tau_x)}{x(t_1 - \tau_x)z(t_1 - \tau_x) + b_1 x(t_1 - \tau_x) + c_1 z(t - \tau_x) + d_1} > 0,$$

which yields a contradiction. This implies that $x(t) \geq 0$ for all $t > 0$. In a similar way to this, we can prove the positivity of $y(t)$ and $z(t)$. Hence, all solutions $x(t)$, $y(t)$, and $z(t)$ of model (3.4) are positive for all $t > 0$, that is, the model is well posed.

The steady states $(\bar{x}, \bar{y}, \bar{z})$ of (3.4) can be found as roots of the following system of

algebraic equations:

$$\begin{aligned}
\frac{\alpha_1\bar{x}}{\bar{x}\bar{z}+b_1\bar{x}+c_1\bar{z}+d_1}-\bar{x}&=0,\\
\frac{\alpha_2\bar{y}}{\bar{y}\bar{x}+b_2\bar{y}+c_2\bar{x}+d_2}-\gamma_2\bar{y}&=0,\\
\frac{\alpha_3\bar{z}}{\bar{z}\bar{y}+b_3\bar{z}+c_3\bar{y}+d_3}-\gamma_3\bar{z}&=0.
\end{aligned} \tag{3.6}$$

This gives

$$\begin{aligned}
&(1)\quad (x_1,y_1,z_1)=(0,0,0),\\
&(2)\quad (x_2,y_2,z_2)=\left(0,0,\frac{\alpha_3-d_3\gamma_3}{b_3\gamma_3}\right),\\
&(3)\quad (x_3,y_3,z_3)=\left(0,\frac{\alpha_2-d_2\gamma_2}{b_2\gamma_2},0\right),\\
&(4)\quad (x_4,y_4,z_4)=\left(0,\frac{\alpha_2-d_2\gamma_2}{b_2\gamma_2},\frac{\gamma_3(\gamma_2(c_3d_2-b_2d_3)-\alpha_2c_3)+\alpha_3b_2\gamma_2}{\gamma_3(\gamma_2(b_2b_3-d_2)+\alpha_2)}\right),\\
&(5)\quad (x_5,y_5,z_5)=\left(\frac{\alpha_1-d_1}{b_1},0,0\right),\\
&(6)\quad (x_6,y_6,z_6)=\left(\frac{\gamma_3(b_3(\alpha_1-d_1)+c_1d_3)-\alpha_3c_1}{\gamma_3(b_1b_3-d_3)+\alpha_3},0,\frac{\alpha_3-d_3\gamma_3}{b_3\gamma_3}\right),\\
&(7)\quad (x_7,y_7,z_7)=\left(\frac{\alpha_1-d_1}{b_1},\frac{\gamma_2(c_2(d_1-\alpha_1)-b_1d_2)+\alpha_2b_1}{\gamma_2(\alpha_1+b_1b_2-d_1)},0\right),
\end{aligned}$$

and the final two $\bar{x}$ steady states are found by solving the following quadratic for x_8 and x_9:

$$\zeta x_{8,9}^2+\rho x_{8,9}+\phi=0,$$

where

$$\begin{aligned}
\zeta&=\gamma_2(\gamma_3(b_1b_3+c_2c_3-d_3)+\alpha_3-b_1c_2\gamma_2),\\
\rho&=\gamma_2(\gamma_3(b_3(b_1b_2+d_1-\alpha_1)+c_1(c_2c_3-d_3)+c_3d_2-b_2d_3)+\gamma_2(\alpha_1c_2-b_1d_2-c_2d_1)\\
&\quad+\alpha_3(b_2+c_1)+\alpha_2b_1)-\alpha_2c_2\gamma_3,\\
\phi&=\gamma_2(\gamma_3(b_2(b_3(d_1-\alpha_1)-c_1d_3)+c_1c_3d_2)+(\alpha_1-d_1)(d_2\gamma_2-\alpha_2)+\alpha_3b_2c_1)-\alpha_2c_1c_3\gamma_3,
\end{aligned}$$

with respective $\bar{y}$ and $\bar{z}$ components given by

$$y_{8,9}=\frac{\alpha_2-\gamma_2(c_2x_{8,9}+d_2)}{\gamma_2(x_{8,9}+b_2)},\qquad z_{8,9}=\frac{\alpha_3-\gamma_3(c_3y_{8,9}+d_3)}{\gamma_3(y_{8,9}+b_3)}.$$

Now that we have explicit formulae for steady states (1)-(7) and implicit forms for the final two steady states, we can use these to perform the stability analysis in terms of the system parameters.

3.3 Analysis of the Delayed Repressilator with Auto-activation Model (DRAM)

The equation for eigenvalues λ of the linearisation near a steady state $(\bar{x}, \bar{y}, \bar{z})$ of system (3.4) has the form

$$\left(\frac{\alpha_1(c_1\bar{z}+d_1)e^{-\lambda\tau_x}}{(\bar{x}\bar{z}+b_1\bar{x}+c_1\bar{z}+d_1)^2}-1-\lambda\right)\left(\frac{\alpha_2(c_2\bar{x}+d_2)e^{-\lambda\tau_y}}{(\bar{y}\bar{x}+b_2\bar{y}+c_2\bar{x}+d_2)^2}-\gamma_2-\lambda\right)\left(\frac{\alpha_3(c_3\bar{y}+d_3)e^{-\lambda\tau_z}}{(\bar{z}\bar{y}+b_3\bar{z}+c_3\bar{y}+d_3)^2}-\gamma_3-\lambda\right)$$
$$-\left(\frac{\alpha_1\bar{x}(\bar{x}+c_1)e^{-\lambda\tau_x}}{(\bar{x}\bar{z}+b_1\bar{x}+c_1\bar{z}+d_1)^2}\right)\left(\frac{\alpha_2\bar{y}(\bar{y}+c_2)e^{-\lambda\tau_y}}{(\bar{y}\bar{x}+b_2\bar{y}+c_2\bar{x}+d_2)^2}\right)\left(\frac{\alpha_3\bar{z}(\bar{z}+c_3)e^{-\lambda\tau_z}}{(\bar{z}\bar{y}+b_3\bar{z}+c_3\bar{y}+d_3)^2}\right)=0. \tag{3.7}$$

For the zero steady state $(\bar{x}, \bar{y}, \bar{z}) = (0, 0, 0)$, equation (3.7) simplifies to

$$\left(\frac{\alpha_1}{d_1}e^{-\lambda\tau_x}-1-\lambda\right)\left(\frac{\alpha_2}{d_2}e^{-\lambda\tau_y}-\gamma_2-\lambda\right)\left(\frac{\alpha_3}{d_3}e^{-\lambda\tau_z}-\gamma_3-\lambda\right)=0. \tag{3.8}$$

For the non-zero steady states, substitutions can be made to simplify analysis of the characteristic equation (3.7). Using the system of equations (3.6), we have

$$\begin{aligned}\bar{x}\bar{z}+b_1\bar{x}+c_1\bar{z}+d_1&=\alpha_1,\\ \bar{y}\bar{x}+b_2\bar{y}+c_2\bar{x}+d_2&=\alpha_2/\gamma_2,\\ \bar{z}\bar{y}+b_3\bar{z}+c_3\bar{y}+d_3&=\alpha_3/\gamma_3,\end{aligned}$$

so that the characteristic equation for non-zero steady states reads

$$\left(\frac{c_1\bar{z}+d_1}{\alpha_1}e^{-\lambda\tau_x}-1-\lambda\right)\left(\frac{\gamma_2^2(c_2\bar{x}+d_2)}{\alpha_2}e^{-\lambda\tau_y}-\gamma_2-\lambda\right)\left(\frac{\gamma_3^2(c_3\bar{y}+d_3)}{\alpha_3}e^{-\lambda\tau_z}-\gamma_3-\lambda\right)$$
$$-\left(\frac{\bar{x}(\bar{x}+c_1)}{\alpha_1}e^{-\lambda\tau_x}\right)\left(\frac{\gamma_2^2\bar{y}(\bar{y}+c_2)}{\alpha_2}e^{-\lambda\tau_y}\right)\left(\frac{\gamma_3^2\bar{z}(\bar{z}+c_3)}{\alpha_3}e^{-\lambda\tau_z}\right)=0. \tag{3.9}$$

3.3.1 Stability of Steady States with a Zero Component

First we look at the characteristic equation (3.8) for the zero steady state, $(x_1, y_1, z_1) = (0, 0, 0)$. In the limit $\tau_x = \tau_y = \tau_z = 0$, equation (3.8) reduces to

$$\left(\frac{\alpha_1}{d_1} - 1 - \lambda\right)\left(\frac{\alpha_2}{d_2} - \gamma_2 - \lambda\right)\left(\frac{\alpha_3}{d_3} - \gamma_3 - \lambda\right) = 0,$$

which gives the following result.

Lemma 3.1. *Let $\tau_x = \tau_y = \tau_z = 0$. The steady state $(x_1, y_1, z_1) = (0, 0, 0)$ of system (3.4) is stable whenever the following conditions hold:*

$$\begin{aligned} &\text{i)} \quad \alpha_1 < d_1, \\ &\text{ii)} \quad \alpha_2 < \gamma_2 d_2, \\ &\text{iii)} \quad \alpha_3 < \gamma_3 d_3. \end{aligned}$$

We now assume that the conditions in Lemma 3.1 hold and analyse whether stability can be lost as τ_x, τ_y, and τ_z increases. To investigate whether this steady state loses stability for $\tau_x > 0$, $\tau_y > 0$, $\tau_z > 0$ one can note that $\lambda = 0$ is not a root of the characteristic equation (3.8). Therefore, the only way the steady state (x_1, y_1, z_1) can lose stability is if a pair of complex conjugate eigenvalues cross the imaginary axis. Hence, we can look for solutions of (3.8) of the form $\lambda = i\omega$, with real $\omega > 0$. We investigate the possible choices of τ_x, τ_y and τ_z, starting with the limit $\tau_y = \tau_z = 0$, and $\tau_x > 0$, to see whether the steady state (x_1, y_1, z_1) can lose stability. In the limit $\tau_y = \tau_z = 0$, and $\tau_x > 0$, equation (3.8) reduces to

$$\left(\frac{\alpha_1}{d_1} e^{-\lambda\tau_x} - 1 - \lambda\right)\left(\frac{\alpha_2}{d_2} - \gamma_2 - \lambda\right)\left(\frac{\alpha_3}{d_3} - \gamma_3 - \lambda\right) = 0.$$

Since Lemma 3.1 is satisfied the only way the steady state (x_1, y_1, z_1) can lose stability is if a pair of complex conjugate roots of $\frac{\alpha_1}{d_1} e^{-\lambda\tau_x} - 1 - \lambda = 0$ crosses the imaginary axis.

Substituting $\lambda = i\omega$ into this equation and separating into real and imaginary parts gives

$$\cos(\omega\tau_x) = \frac{d_1}{\alpha_1},$$
$$\sin(\omega\tau_x) = -\frac{d_1\omega}{\alpha_1}.$$

Squaring and adding these two equations together we have

$$\omega^2 = \frac{\alpha_1^2}{d_1^2} - 1,$$

which is a contradiction since ω is a positive real number however condition i) of Lemma 3.1 implies that $\frac{\alpha_1^2}{d_1^2} < 1$. Hence, in the limit $\tau_y = \tau_z = 0$, there does not exist a value of $\tau_x > 0$ that causes the steady state (x_1, y_1, z_1) to lose stability. Analogous to the above analysis, it follows that we have the same situation in the limit where one or more of τ_x, τ_y, or τ_z are zero, so this analysis is not shown here.

When $\tau_x > 0$, $\tau_y > 0$, and $\tau_z > 0$, the characteristic equation (3.8) reads

$$\left(\frac{\alpha_1}{d_1}e^{-\lambda\tau_x} - 1 - \lambda\right)\left(\frac{\alpha_2}{d_2}e^{-\lambda\tau_y} - \gamma_2 - \lambda\right)\left(\frac{\alpha_3}{d_3}e^{-\lambda\tau_z} - \gamma_3 - \lambda\right) = 0.$$

Again, since Lemma 3.1 is satisfied the only way the steady state (x_1, y_1, z_1) can lose stability is if a pair of complex conjugate roots of $\frac{\alpha_1}{d_1}e^{-\lambda_1\tau_x} - 1 - \lambda_1 = 0$ or $\frac{\alpha_2}{d_2}e^{-\lambda_2\tau_y} - \gamma_2 - \lambda_2 = 0$ or $\frac{\alpha_3}{d_3}e^{-\lambda_3\tau_z} - \gamma_3 - \lambda_3 = 0$ crosses the imaginary axis. Substituting $\lambda_1 = i\eta$ and $\lambda_2 = i\omega$ and $\lambda_3 = i\nu$, for some real $\eta, \omega, \nu > 0$, into the respective equations and performing the same type of analysis as before, we have equations for η, ω and ν given by

$$\eta^2 = \frac{\alpha_1^2}{d_1^2} - 1, \quad \omega^2 = \frac{\alpha_2^2}{d_2^2} - \gamma_2^2, \quad \nu^2 = \frac{\alpha_3^2}{d_3^2} - \gamma_3^2,$$

which again leads to a contradiction since Lemma 3.1 gives us that $\frac{\alpha_1^2}{d_1^2} < 1$, $\frac{\alpha_2^2}{d_2^2} < \gamma_2^2$ and $\frac{\alpha_3^2}{d_3^2} < \gamma_3^2$. It follows that there does not exist a value of τ_x, τ_y, $\tau_z > 0$ such that the steady state (x_1, y_1, z_1) loses stability.

Next we investigate the stability criteria for steady states (x_i, y_i, z_i), $i = 2, 3, ..., 7$. The characteristic equation for these steady states can be reduced from equation (3.9), taking

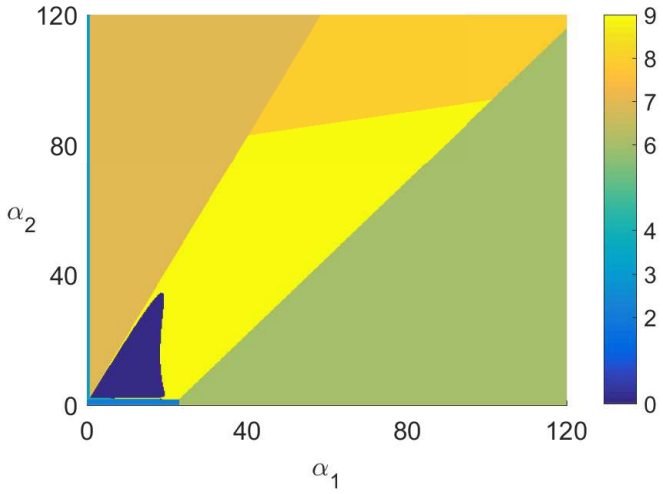

Figure 3.3: Parameter regions for stable and unstable steady states of DRAM system (3.4). Each colour coded number is the indice of the corresponding steady state which is stable in that region, whilst all other steady states are unstable or infeasible. The blue region labelled 0 is where all steady states are unstable, leading to sustained oscillations. Parameter values: $\tau_x = \tau_y = \tau_z = 0$, $\alpha_3 = 6$, $b_1 = 4$, $b_2 = 3$, $b_3 = 1$, $c_1 = 8$, $c_2 = 10$, $c_3 = 15$, $d_1 = 0.5$, $d_2 = 2$, $d_3 = 0.2$, $\gamma_2 = 0.8$, $\gamma_3 = 2$.

the form

$$\left(\frac{c_1\bar{z}+d_1}{\alpha_1}e^{-\lambda\tau_x}-1-\lambda\right)\left(\frac{\gamma_2^2(c_2\bar{x}+d_2)}{\alpha_2}e^{-\lambda\tau_y}-\gamma_2-\lambda\right)\left(\frac{\gamma_3^2(c_3\bar{y}+d_3)}{\alpha_3}e^{-\lambda\tau_z}-\gamma_3-\lambda\right)=0. \tag{3.10}$$

First we investigate (x_2, y_2, z_2), so that equation (3.10) reduces to

$$\left(\frac{c_1(\alpha_3-\gamma_3 d_3)+b_3\gamma_3 d_1}{\alpha_1 b_3\gamma_3}e^{-\lambda\tau_x}-1-\lambda\right)\left(\frac{\gamma_2^2 d_2}{\alpha_2}e^{-\lambda\tau_y}-\gamma_2-\lambda\right)\left(\frac{\gamma_3^2 d_3}{\alpha_3}e^{-\lambda\tau_z}-\gamma_3-\lambda\right)=0.$$

In the limit $\tau_x = \tau_y = \tau_z = 0$, the characteristic equation is given by

$$\left(\frac{c_1(\alpha_3-\gamma_3 d_3)+b_3\gamma_3 d_1}{\alpha_1 b_3\gamma_3}-1-\lambda\right)\left(\frac{\gamma_2^2 d_2}{\alpha_2}-\gamma_2-\lambda\right)\left(\frac{\gamma_3^2 d_3}{\alpha_3}-\gamma_3-\lambda\right)=0,$$

Lemma 3.2. *Let $\tau_x = \tau_y = \tau_z = 0$. The steady state (x_2, y_2, z_2) of system (3.4) is stable whenever the following conditions hold:*

i) $c_1(\alpha_3 - \gamma_3 d_3) < b_3\gamma_3(\alpha_1 - d_1)$,

ii) $\gamma_2 d_2 < \alpha_2$,

iii) $\gamma_3 d_3 < \alpha_3$.

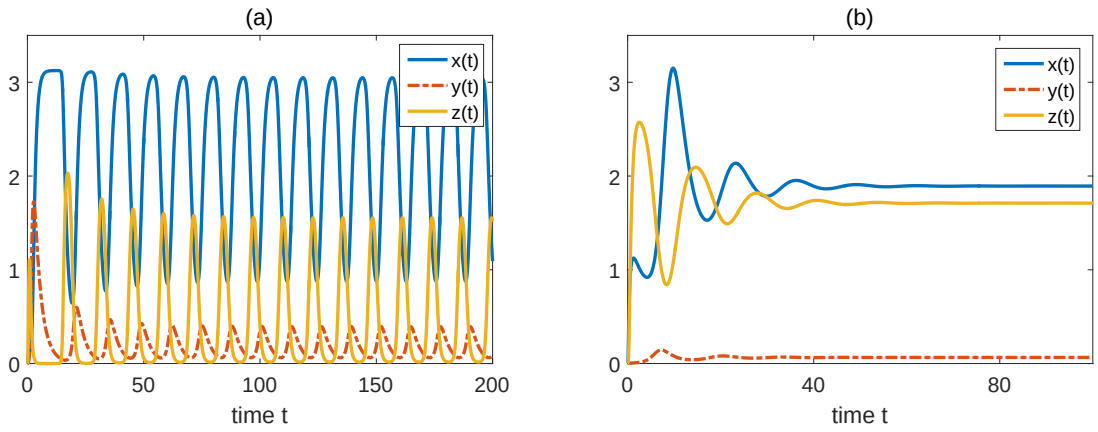

Figure 3.4: Numerical solutions of DRAM system (3.4): (a) $\alpha_1 = 13$. (b) $\alpha_1 = 25$. Parameter values: $\tau_x = \tau_y = \tau_z = 0$, $\alpha_2 = 17$, $\alpha_3 = 6$, $b_1 = 4$, $b_2 = 3$, $b_3 = 1$, $c_1 = 8$, $c_2 = 10$, $c_3 = 15$, $d_1 = 0.5$, $d_2 = 2$, $d_3 = 0.2$, $\gamma_2 = 0.8$, $\gamma_3 = 2$.

Assuming Lemma 3.2 is satisfied, we investigate whether the steady state can lose stability for possible choices of τ_x, τ_y, and τ_z. In the limit $\tau_y = \tau_z = 0$ and $\tau_x > 0$, the only way the steady state (x_2, y_2, z_2) can lose stability is if a pair of complex conjugate eigenvalues of $\frac{c_1(\alpha_3 - d_3\gamma_3) + b_3\gamma_3 d_1}{\alpha_1 b_3 \gamma_3} e^{-\lambda\tau_x} - 1 - \lambda = 0$ crosses the imaginary axis. Substituting $\lambda = i\omega$ into this equation and separating into real and imaginary parts we have

$$\cos(\omega\tau_x) = \frac{\alpha_1 b_3 \gamma_3}{c_1(\alpha_3 - \gamma_3 d_3) + b_3\gamma_3 d_1},$$
$$\sin(\omega\tau_x) = -\frac{\alpha_1 b_3 \gamma_3 \omega}{c_1(\alpha_3 - \gamma_3 d_3) + b_3\gamma_3 d_1}.$$

Squaring and adding these equations together yields

$$\omega^2 = \left(\frac{c_1(\alpha_3 - \gamma_3 d_3) + b_3\gamma_3 d_1}{\alpha_1 b_3 \gamma_3}\right)^2 - 1,$$

which, similarly to the steady state (x_1, y_1, z_1), leads to a contradiction as a result of i) and iii) in Lemma 3.2. This result shows that in the limit $\tau_y = \tau_z = 0$, there does not exist a value of $\tau_x > 0$ where the steady state (x_2, y_2, z_2) experiences a loss of stability. The same result arises for all other choices of τ_x, τ_y and τ_z, and also holds true for all steady states (x_i, y_i, z_i) where $i = 3, 4, ..., 7$. Assuming that the conditions for stability in the limit $\tau_x = \tau_y = \tau_z = 0$ are satisfied, each steady state remains stable for any time delay.

Figures 3.3, 3.5, 3.6, and 3.7 represent steady state stability regions of system (3.4)

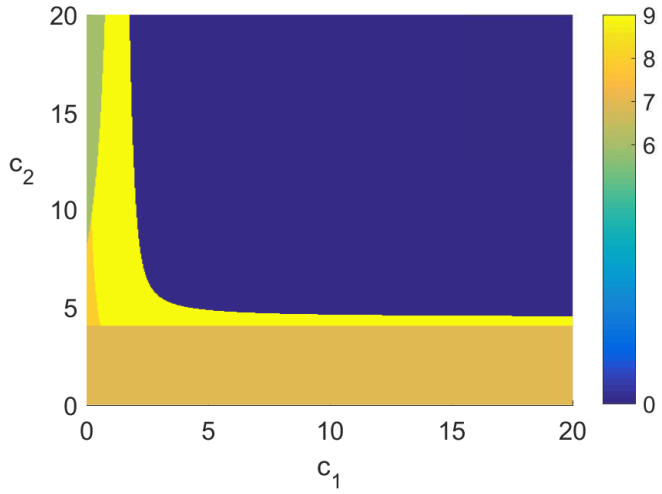

Figure 3.5: Parameter regions for stable and unstable steady states of DRAM system (3.4). Each colour coded number is the indice of the corresponding steady state which is stable in that region, whilst all other steady states are unstable or infeasible. The blue region labelled 0 is where all steady states are unstable, leading to sustained oscillations. Parameter values: $\tau_x = \tau_y = \tau_z = 0$, $\alpha_1 = 4$, $\alpha_2 = 5$, $\alpha_3 = 6$, $b_1 = 4$, $b_2 = 3$, $b_3 = 1$, $c_3 = 15$, $d_1 = 0.5$, $d_2 = 2$, $d_3 = 0.2$, $\gamma_2 = 0.8$, $\gamma_3 = 2$.

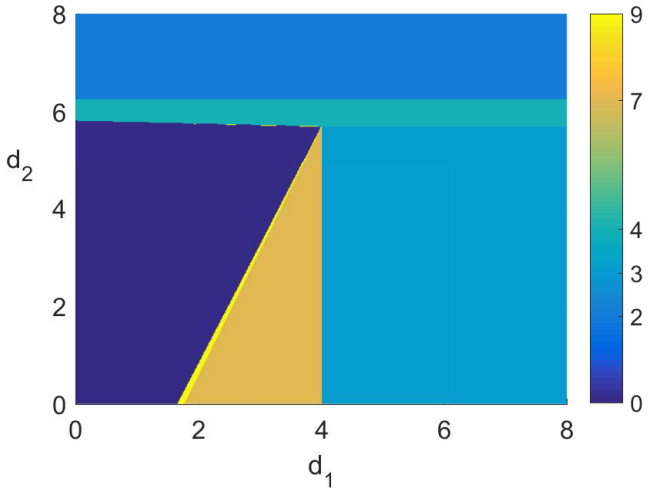

Figure 3.6: Parameter regions for stable and unstable steady states of DRAM system (3.4). Each colour coded number is the indice of the corresponding steady state which is stable in that region, whilst all other steady states are unstable or infeasible. The blue region labelled 0 is where all steady states are unstable, leading to sustained oscillations. Parameter values: $\tau_x = \tau_y = \tau_z = 0$, $\alpha_1 = 4$, $\alpha_2 = 5$, $\alpha_3 = 6$, $b_1 = 4$, $b_2 = 3$, $b_3 = 1$, $c_1 = 8$, $c_2 = 10$, $c_3 = 15$, $d_3 = 0.2$, $\gamma_2 = 0.8$, $\gamma_3 = 2$.

for the DRAM model, however the time delays have been equated to zero. These plots therefore depict the stability regions for the ODE description of the *Repressilator* with auto-activation. The numbers assigned to each colour coded region are the indices of the respective steady state, i.e. $1 = (x_1, y_1, z_1)$, $2 = (x_2, y_2, z_2)$, $\ldots$, $9 = (x_9, y_9, z_9)$. The

parameter regions that are represented by these colours signify where the corresponding steady state is stable. For example, if a region is colour coded with the number 2 then this means that steady state (x_2, y_2, z_2) is stable and all other steady states are either unstable or biologically infeasible in this region. The dark blue coloured regions labelled 0 are areas where system parameter choices that lie here lead to instability of all steady states, and give rise to oscillatory solutions.

In Figure 3.3, we can observe how the relationship between parameters α_1 and α_2 can lead to the destabilisation of steady state (x_9, y_9, z_9). For example if we fix $\alpha_2 = 17$ the system undergoes a Hopf bifurcation as α_1 is increased through $\alpha_1 = 8.4$. The system then reverts back as α_1 is increased beyond $\alpha_1 = 18.28$, to the stable steady state (x_9, y_9, z_9). We can also observe stability switching between many of the possible steady states throughout the parameter space. Figure 3.4 shows two solution diagrams. The parameter scheme for Figure 3.4(a) lies in the 0 region of Figure 3.3, and Figure 3.4(b) lies just to the right of the 0 region. In Figure 3.4(a) we see sustained oscillations around the steady state (x_9, y_9, z_9), then in Figure 3.4(b) we have a solution that tends towards the stable steady state (x_9, y_9, z_9).

In Figure 3.5 we see a strong dependence between parameters c_1 and c_2 for stability of steady states. For stability, either both parameters must be reasonably small or else if one grows, the other must remain small. We see therefore, a large parameter region exists where all steady states are unstable, and oscillations occur. Therefore, the model is not robust against variations in parameters c_1 and c_2 with regards to steady state stability.

Figure 3.6 shows that for $d_2 < 5.69$, the steady state (x_9, y_9, z_9) gains stability as d_1 is increased, followed by a subsequent switch of stability to (x_7, y_7, z_7) and then a switch to (x_3, y_3, z_3). For $5.69 < d_2 < 5.82$, as d_1 is increased, the steady states are unstable followed by a gain in stability of (x_9, y_9, z_9) for a very small parameter region before steady state (x_4, y_4, z_4) becomes stable and stays stable for any larger d_1. For $5.82 < d_2 < 6.25$, (x_4, y_4, z_4) is stable for any choice of parameter d_1, and likewise for (x_2, y_2, z_2) when $d_2 > 6.25$.

In a similar fashion to Figure 3.3, Figure 3.7 shows a small pocket in the parameter space where all steady states are unstable. This means that close to this region, if we increase γ_2, the steady state (x_9, y_9, z_9) switches from stable to unstable and then stable

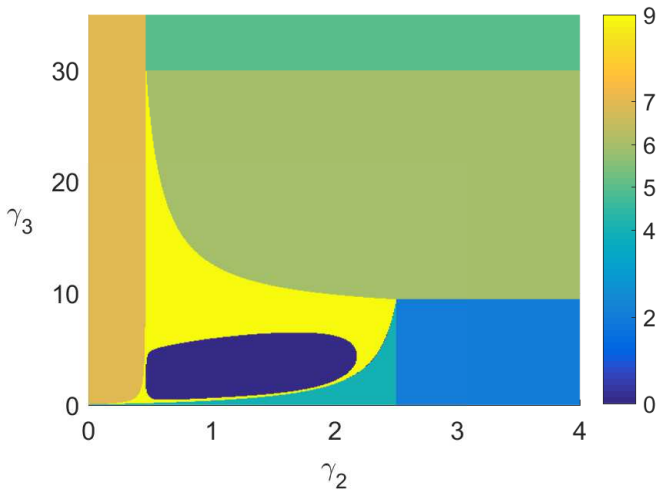

Figure 3.7: Parameter regions for stable and unstable steady states of DRAM system (3.4). Each colour coded number is the indice of the corresponding steady state which is stable in that region, whilst all other steady states are unstable or infeasible. The blue region labelled 0 is where all steady states are unstable, leading to sustained oscillations. Parameter values: $\tau_x = \tau_y = \tau_z = 0$, $\alpha_1 = 4$, $\alpha_2 = 5$, $\alpha_3 = 6$, $b_1 = 4$, $b_2 = 3$, $b_3 = 1$, $c_1 = 8$, $c_2 = 10$, $c_3 = 15$, $d_1 = 0.5$, $d_2 = 2$, $d_3 = 0.2$.

again. In the rest of the parameter space we notice switches of stability between the different steady states, so it can be inferred that the relationship between the parameters γ_2 and γ_3, i.e. the degradation rates of proteins y and z, have a strong impact on the long term behaviour of the system.

Even without time delays present it is not possible for any of the steady states (x_1, y_1, z_1), (x_2, y_2, z_3), $\ldots$, (x_7, y_7, z_7) to undergo a Hopf bifurcation and lose stability by varying the system parameters. The rest of this chapter investigates the stability properties of the remaining two steady states and the effect that time delays have on the long term system behaviour.

3.3.2 Stability of Steady States with Non-zero Components

We wish to investigate stability of the steady states (x_8, y_8, z_8) and (x_9, y_9, z_9), which have non zero values in all components. Here, the number of free parameters of system (3.4) is reduced in order to simplify analysis of the DRAM model which has 3 time delays. From here on, it is assumed that protein x is a different type to proteins y and z. Protein x is expressed under a smaller time scale to y and z, such that the time delays associated with protein x are negligible, relative to the delays associated with proteins y and z. Thus, we take the limit $\tau_x = 0$ and relabel $\tau_y = \tau_1$ and $\tau_z = \tau_2$. The system of equations for this

model is then given by

$$\begin{aligned}
\frac{dx}{dt} &= \frac{\alpha_1 x}{xz + b_1 + c_1 + d_1} - x, \\
\frac{dy}{dt} &= \frac{\alpha_2 y(t-\tau_1)}{y(t-\tau_1)x(t-\tau_1) + b_2 y(t-\tau_1) + c_2 x(t-\tau_1) + d_2} - \gamma_2 y, \\
\frac{dz}{dt} &= \frac{\alpha_3 z(t-\tau_2)}{z(t-\tau_2)y(t-\tau_2) + b_3 z(t-\tau_2) + c_3 y(t-\tau_2) + d_3} - \gamma_3 z.
\end{aligned} \tag{3.11}$$

This model will be referred to as the simplified delayed repressilator with auto-activation model (SDRAM). The initial conditions for model SDRAM are

$$\begin{aligned}
x(s) &= \phi_1(s), \quad s \in [-\tau_{\max}, 0], \\
y(s) &= \phi_2(s), \quad s \in [-\tau_{\max}, 0], \\
z(s) &= \phi_3(s), \quad s \in [-\tau_{\max}, 0],
\end{aligned}$$

where $\tau_{\max} = \max(\tau_1, \tau_2)$ and $\phi_i(s) \in C([-\tau_{\max}, 0], \mathbb{R})$ with $\phi_i(s) \geq 0$ ($-\tau_{\max} \leq s \leq 0$, $i = 1, 2, 3$). $C([-\tau_{\max}, 0], \mathbb{R})$ is the Banach space of continuous mappings of interval $[-\tau_{\max}, 0]$ into $\mathbb{R}$. It is also assumed that $x(0) > 0$, $y(0) > 0$, and $z(0) > 0$. The proof for the positivity of solutions follows the same methodology to that of system (3.4). Since time delays have no affect on the calculation of steady states, the equilibria of system (3.11) are the same as for system (3.4). Therefore, to investigate the stability properties of (x_8, y_8, z_8) and (x_9, y_9, z_9) with respect to the new reduced system, the characteristic equation of system (3.11) for non-zero steady states reads

$$\begin{aligned}
&\left(\frac{c_1\bar{z} + d_1}{\alpha_1} - 1 - \lambda\right)\left(\frac{\gamma_2^2(c_2\bar{x} + d_2)}{\alpha_2}e^{-\lambda\tau_1} - \gamma_2 - \lambda\right)\left(\frac{\gamma_3^2(c_3\bar{y} + d_3)}{\alpha_3}e^{-\lambda\tau_2} - \gamma_3 - \lambda\right) \\
&- \left(\frac{\bar{x}(\bar{x} + c_1)}{\alpha_1}\right)\left(\frac{\gamma_2^2\bar{y}(\bar{y} + c_2)}{\alpha_2}e^{-\lambda\tau_1}\right)\left(\frac{\gamma_3^2\bar{z}(\bar{z} + c_3)}{\alpha_3}e^{-\lambda\tau_2}\right) = 0
\end{aligned}$$

$$\begin{aligned}
\Leftrightarrow\ & \lambda^3 + \lambda^2(1 + \gamma_2 + \gamma_3 - \kappa_1 - \kappa_2 e^{-\lambda\tau_1} - \kappa_3 e^{-\lambda\tau_2}) + \lambda((\kappa_1 - \gamma_3 - 1)\kappa_2 e^{-\lambda\tau_1} \\
&+ (\kappa_1 - \gamma_2 - 1)\kappa_3 e^{-\lambda\tau_2} + \kappa_2\kappa_3 e^{-\lambda(\tau_1+\tau_2)} + \gamma_2 + \gamma_3 + \gamma_2\gamma_3 - \kappa_1(\gamma_2 + \gamma_3)) \\
&+ (\kappa_1 - 1)(\gamma_3\kappa_2 e^{-\lambda\tau_1} + \gamma_2\kappa_3 e^{-\lambda\tau_2} - \kappa_2\kappa_3 e^{-\lambda(\tau_1+\tau_2)} - \gamma_2\gamma_3) + \xi_1\xi_2\xi_3 e^{-\lambda(\tau_1+\tau_2)} = 0,
\end{aligned} \tag{3.12}$$

where

$$\kappa_1 = \frac{c_1\bar{z} + d_1}{\alpha_1},$$
$$\kappa_2 = \frac{\gamma_2^2(c_2\bar{x} + d_2)}{\alpha_2},$$
$$\kappa_3 = \frac{\gamma_3^2(c_3\bar{y} + d_3)}{\alpha_3},$$
$$\xi_1 = \frac{\bar{x}(\bar{x} + c_1)}{\alpha_1},$$
$$\xi_2 = \frac{\gamma_2^2\bar{y}(\bar{y} + c_2)}{\alpha_2},$$
$$\xi_3 = \frac{\gamma_3^2\bar{z}(\bar{z} + c_3)}{\alpha_3}.$$

In the limit $\tau_1 = \tau_2 = 0$, the characteristic equation (3.12) becomes

$$\lambda^3 + A\lambda^2 + B\lambda + C = 0,$$

where

$$A = 1 + \gamma_2 + \gamma_3 - \kappa_1 - \kappa_2 - \kappa_3,$$
$$B = (\kappa_1 - \gamma_3 - 1)\kappa_2 + (\kappa_1 - \gamma_2 - 1)\kappa_3 + \kappa_2\kappa_3 + \gamma_2 + \gamma_3 + \gamma_2\gamma_3 - \kappa_1(\gamma_2 + \gamma_3),$$
$$C = (\kappa_1 - 1)(\gamma_3\kappa_2 + \gamma_2\kappa_3 - \kappa_2\kappa_3 - \gamma_2\gamma_3) + \xi_1\xi_2\xi_3.$$

Lemma 3.3. *Let $\tau_1 = \tau_2 = 0$. By the Routh-Herwitz criterion, the steady state (x_8, y_8, z_8) or (x_9, y_9, z_9) of system (3.11) is stable provided that $A > 0$, $B > 0$, $C > 0$ and $AB > C$.*

Assuming that the conditions of Lemma 3.3 are satisfied, we analyse whether stability can be lost by the existence of a sufficiently large time delay. In the limit $\tau_2 = 0$ and $\tau_1 > 0$, the characteristic equation (3.12) becomes

$$\lambda^3 + \lambda^2(D - \kappa_3 e^{-\lambda\tau_1}) + \lambda(Ee^{-\lambda\tau_1} + F) + Ge^{-\lambda\tau_1} + H = 0, \tag{3.13}$$

where

$$
\begin{aligned}
D &= 1 + \gamma_2 + \gamma_3 - \kappa_1 - \kappa_3, \\
E &= \kappa_2(\kappa_1 + \kappa_3 - \gamma_3 - 1), \\
F &= \kappa_3(\kappa_1 - \gamma_2 - 1) + \gamma_2 + \gamma_3 + \gamma_2\gamma_3 - \kappa_1(\gamma_2 + \gamma_3), \\
G &= \kappa_2(\kappa_1 - 1)(\gamma_3 - \kappa_3) + \xi_1\xi_2\xi_3, \\
H &= \gamma_2(\kappa_1 - 1)(\kappa_3 - \gamma_3).
\end{aligned}
$$

We look for solutions of (3.13) of the form $\lambda = i\omega$ for some real $\omega > 0$. Substituting this into (3.13) and separating into real and imaginary parts we have

$$
\begin{aligned}
D\omega^2 - H &= (\kappa_3\omega^2 + G)\cos(\omega\tau_1) + E\omega\sin(\omega\tau_1), \\
\omega(F - \omega^2) &= (\kappa_3\omega^2 + G)\sin(\omega\tau_1) - E\omega\cos(\omega\tau_1).
\end{aligned}
\tag{3.14}
$$

Squaring and adding together gives a cubic equation of the form:

$$
g(z) = z^3 + pz^2 + qz + r = 0, \tag{3.15}
$$

where $z = \omega^2$ and

$$
\begin{aligned}
p &= D^2 - 2F - \kappa_3^2, \\
q &= F^2 - 2DH - 2G\kappa_3 - E^2, \\
r &= H^2 - G^2.
\end{aligned}
$$

Without loss of generality, suppose that (3.15) has 3 positive real roots, denoted by z_1, z_2, z_3, respectively, which would give 3 possible values of ω: $\omega_1 = \sqrt{z_1}$, $\omega_2 = \sqrt{z_2}$, $\omega_3 = \sqrt{z_3}$. Some algebraic manipulation of (3.14) gives

$$
\cos(\omega_k\tau_{1,k}) = \frac{(E + \kappa_3)\omega_k^4 + (DG - EF - H\kappa_3)\omega_k^2 - GH}{\kappa_3^2\omega_k^4 + (E^2 + 2G\kappa_3)\omega_k^2 + G^2}
$$

$$
\Rightarrow \quad \tau_{1,k,j} = \frac{1}{\omega_k}\left[\arccos\left(\frac{(E + \kappa_3)\omega_k^4 + (DG - EF - H\kappa_3)\omega_k^2 - GH}{\kappa_3^2\omega_k^4 + (E^2 + 2G\kappa_3)\omega_k^2 + G^2}\right) + 2j\pi\right],
$$

$$
k = 1, ..., 3, \quad j = 0, 1, 2, ...
$$

Define,

$$\tau_{1,0} = \min_{1\le k\le 3}\{\tau_{1,k,0}\}, \qquad \omega_0 = \omega_{k_0}, \qquad k_0 \in \{1,2,3\},$$

then $\tau_{1,0}$ is the first value of $\tau_1 > 0$ whereby the characteristic equation (3.13) has a pair of purely imaginary roots. We have the following result.

Theorem 3.1 *Suppose the conditions of Lemma 3.3 hold and that $g'(\omega^2) > 0$, where $g(z)$ is defined in* (3.15)*. In the limit $\tau_2 = 0$, the steady state (x_8, y_8, z_8) or (x_9, y_9, z_9) of system* (3.11) *is stable for $0 \le \tau_1 \le \tau_{1,0}$ and unstable for $\tau_1 > \tau_{1,0}$ and undergoes a Hopf bifurcation at $\tau_1 = \tau_{1,0}$.*

Proof. The conclusion of Lemma 3.3 ensures that the steady state (x_8, y_8, z_8) or (x_9, y_9, z_9) of system (3.11) is stable at $\tau_1 = 0$, and the fact that the roots of the characteristic equation (3.13) depend continuously on τ_1 implies that either steady state is also stable for sufficiently small positive values of τ_1. Since $\tau_{1,0}$ is the first positive τ_1, for which the eigenvalues lie on the imaginary axis, in order to verify whether or not the steady state actually loses stability at $\tau_1 = \tau_{1,0}$, one has to compute the sign of $d\mathrm{Re}(\lambda)/d\tau_1|_{\tau_1=\tau_{1,0}}$. Let $\lambda(\tau_1) = \mu(\tau_1) + i\omega(\tau_1)$ be the root of the characteristic equation (3.13) near $\tau_1 = \tau_{1,0}$, satisfying $\mu(\tau_{1,0}) = 0$ and $\omega(\tau_{1,0}) = \omega_0$. Substituting $\lambda = \lambda(\tau_1)$ into (3.13) and differentiating both sides with respect to τ_1 yields

$$\left(\frac{d\lambda}{d\tau_1}\right)^{-1} = \frac{(3\lambda^2 + 2D\lambda + F)e^{\lambda\tau_1}}{\lambda(-\kappa_3\lambda^2 + E\lambda + G)} + \frac{E - 2\kappa_3\lambda}{\lambda(-\kappa_3\lambda^2 + E\lambda + G)} - \frac{\tau_1}{\lambda}.$$

From this equation, one can find

$$\mathrm{sgn}\left\{\left[\frac{d(\mathrm{Re}\lambda)}{d\tau_1}\right]_{\tau_1=\tau_{1,0}}\right\} = \mathrm{sgn}\left\{\mathrm{Re}\left[\left(\frac{d\lambda}{d\tau_1}\right)^{-1}\right]_{\tau_1=\tau_{1,0}}\right\}$$

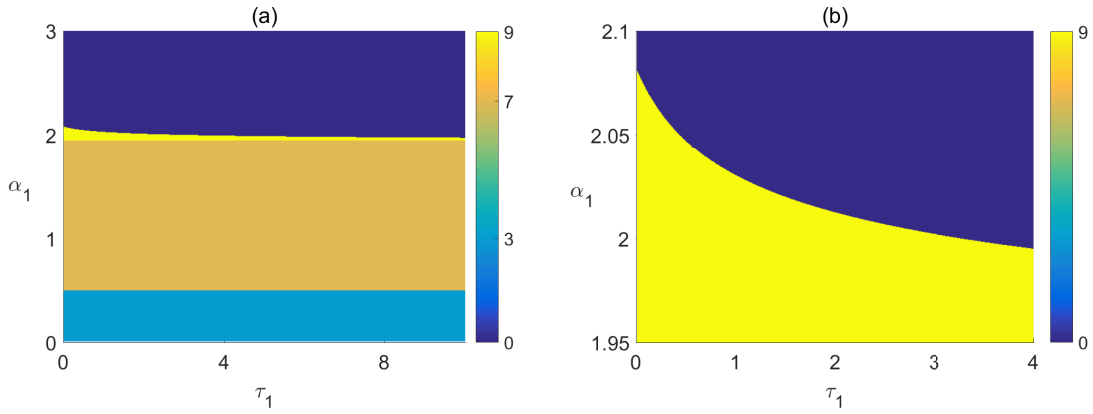

Figure 3.8: Parameter regions for stable and unstable steady states of SDRAM system (3.11). Each colour coded number is the indice of the corresponding steady state which is stable in that region, whilst all other steady states are unstable or infeasible. The blue region labelled 0 is where all steady states are unstable, leading to sustained oscillations. (b) is a magnified view of (a). Parameter values: $\tau_2 = 0$, $\alpha_2 = 5$, $\alpha_3 = 6$, $b_1 = 4$, $b_2 = 3$, $b_3 = 1$, $c_1 = 8$, $c_2 = 10$, $c_3 = 15$, $d_1 = 0.5$, $d_2 = 2$, $d_3 = 0.2$, $\gamma_2 = 0.8$, $\gamma_3 = 2$.

$$= \operatorname{sgn}\left\{\operatorname{Re}\left[\frac{(3\lambda^2+2D\lambda+F)e^{\lambda\tau_1}}{\lambda(-\kappa_3\lambda^2+E\lambda+G)}\right]_{\tau_1=\tau_{1,0}} + \operatorname{Re}\left[\frac{E-2\kappa_3\lambda}{\lambda(-\kappa_3\lambda^2+E\lambda+G)}\right]_{\tau_1=\tau_{1,0}}\right\}$$

$$\begin{aligned} = \operatorname{sgn}\Big\{ & \left(E^2\omega_0^4+(\kappa_3\omega_0^2+G)^2\omega_0^2\right)^{-1}\left[(F-3\omega_0^2)[\omega_0(\kappa_3\omega_0^2+G)\sin(\omega_0\tau_{1,0})\right. \\ & \left. -E\omega_0^2\cos(\omega_0\tau_{1,0})\right] + 2D\omega_0\left[\omega_0(\kappa_3\omega_0^2+G)\cos(\omega_0\tau_{1,0})+E\omega_0^2\sin(\omega_0\tau_{1,0})\right] \\ & -E^2\omega_0^2-2\kappa_3\omega_0^2(\kappa_3\omega_0^2+G)\Big\}. \end{aligned}$$

Substituting the expressions from system (3.14) gives

$$\begin{aligned} \operatorname{sgn}\left\{\left[\frac{d(\operatorname{Re}\lambda)}{d\tau_1}\right]_{\tau_1=\tau_{1,0}}\right\} &= \operatorname{sgn}\Big\{\Lambda^{-1}\big[(F-3\omega_0^2)(F-\omega_0^2)+2D(D\omega_0^2-H)-E^2 \\ &\qquad -2\kappa_3(\kappa_3\omega_0^2+G)\big]\Big\} \\ &= \operatorname{sgn}\Big\{\Lambda^{-1}\big[3\omega_0^4+(2D^2-4F-2\kappa_3^2)\omega_0^2+F^2-2DH \\ &\qquad -2\kappa_3 G-E^2\big]\Big\} \\ &= \operatorname{sgn}\left\{\frac{g'(\omega_0^2)}{\Lambda}\right\} > 0, \end{aligned}$$

where $\Lambda = E^2\omega_0^2 + (\kappa_3\omega_0^2+G)^2$. Hence, the eigenvalues of the characteristic equation (3.13) crosses the imaginary axis at $\tau_1 = \tau_{1,0}$ with a positive speed. This implies that the steady state (x_8, y_8, z_8) or (x_9, y_9, z_9) of system (3.11) does lose its stability at $\tau_1 = \tau_{1,0}$.□

Figure 3.8 demonstrates how increasing the time delay τ_1 results in a Hopf bifurcation of the steady state (x_9, y_9, z_9) and the emergence of a stable periodic orbit. For $0 < \alpha_1 < 0.5058$ and $0.5058 < \alpha_1 < 1.963$, steady state (x_3, y_3, z_3) and (x_7, y_7, z_7), respectively, are stable for any time delay. However for $1.963 < \alpha_1 < 2.083$, there exists a critical time delay which leads to sustained oscillations when τ_1 passes this value. In accordance with Theorem 3.1, once the stability of the steady state (x_9, y_9, z_9) is lost, it can never be regained for higher values of τ, so the system will be exhibiting oscillatory behaviour. Beyond $\alpha_1 = 2.083$ the steady states are unstable for all τ_1.

In the limit $\tau_1 = 0$ with $\tau_2 > 0$, the story is identical to the limit $\tau_2 = 0$ with $\tau_1 > 0$, so this analysis has not been included here. Next we look at the case where $\tau_1 = \tau_2 = \tau > 0$. The characteristic equation is given by

$$\lambda^3 + \lambda^2(I - Je^{-\lambda\tau}) + \lambda(Ke^{-\lambda\tau} + Le^{-2\lambda\tau} + M) + Ne^{-\lambda\tau} + Pe^{-2\lambda\tau} + Q = 0, \qquad (3.16)$$

where

$$\begin{aligned}
I &= 1 + \gamma_2 + \gamma_3 - \kappa_1, \\
J &= \kappa_2 + \kappa_3, \\
K &= \kappa_2(\kappa_1 - \gamma_3 - 1) + \kappa_3(\kappa_1 - \gamma_2 - 1), \\
L &= \kappa_2\kappa_3, \\
M &= \gamma_2 + \gamma_3 + \gamma_2\gamma_3 - \kappa_1(\gamma_2 + \gamma_3), \\
N &= (\kappa_1 - 1)(\gamma_3\kappa_2 + \gamma_2\kappa_3), \\
P &= \kappa_2\kappa_3(1 - \kappa_1) + \xi_1\xi_2\xi_3, \\
Q &= \gamma_2\gamma_3(1 - \kappa_1).
\end{aligned}$$

Here we use an iterative procedure adopted from B. Rahman et al. [130] to find a new function $F(\omega)$, the roots of which give the Hopf frequency associated with the purely imaginary roots of the characteristic equation (3.16). The procedure we employ for finding the function $F(\omega)$ works as follows. Consider a general transcendental characteristic

equation [131–133],

$$\Delta(\tau,\lambda)=\sum_{k=0}^{n}p_k(\lambda)e^{-k\lambda\tau}, \tag{3.17}$$

where $\tau\geq 0$; $p_k(\lambda)$, $k=0,1,2,...,$ are polynomials in λ; and $|p_k(\lambda)/p_0(\lambda)|<1$, $k=1,2,...,n$, for $|\lambda|\to\infty$ and $\mathrm{Re}(\lambda)\geq 0$. Substituting $\lambda=i\omega$ into (3.17) and conjugating $\Delta(\tau,i\omega)$ gives

$$\Delta(\tau,i\omega)=\sum_{k=0}^{n}p_k(i\omega)e^{-ki\omega\tau},\qquad \overline{\Delta(\tau,i\omega)}=\sum_{k=0}^{n}\overline{p_k(i\omega)}e^{ki\omega\tau}.$$

Clearly, $\Delta(\tau,i\omega)=0$ if and only if $\overline{\Delta(\tau,i\omega)}=0$. Define $\Delta^{(j)}(\tau,i\omega)$ recursively as

$$\begin{aligned}
\Delta^{(1)}(\tau,i\omega)&=\overline{p_0(i\omega)}\Delta(\tau,i\omega)-p_n(i\omega)e^{-ni\omega\tau}\overline{\Delta(\tau,i\omega)}=\sum_{k=0}^{n-1}p_k^{(1)}(i\omega)e^{-ki\omega\tau},\\
&\vdots\\
\Delta^{(j)}(\tau,i\omega)&=\overline{p_0^{(j-1)}(i\omega)}\Delta^{(j-1)}(\tau,i\omega)-p_{n-j+1}^{(j-1)}(i\omega)e^{-(n-j+1)i\omega\tau}\overline{\Delta^{(j-1)}(\tau,i\omega)}\\
&=\sum_{k=0}^{n-j}p_k^{(j)}(i\omega)e^{-ki\omega\tau},\\
&\vdots\\
\Delta^{(n-1)}(\tau,i\omega)&=p_0^{(n-1)}(i\omega)+p_1^{(n-1)}(i\omega)e^{-i\omega\tau}.
\end{aligned}$$

From $p_0^{(j+1)}(i\omega)$ we obtain

$$p_0^{(j+1)}(i\omega)=|p_0^{(j)}(i\omega)|^2-|p_{n-j}^{(j)}(i\omega)|^2,\quad j=0,1,2,...,n-2.$$

Moreover, from $\Delta^{(n-1)}(\tau,i\omega)$, let

$$F(\omega)=|p_0^{(n-1)}(i\omega)|^2-|p_1^{(n-1)}(i\omega)|^2.$$

If $\Delta(\tau,i\omega)=0$, then ω is a root of $F(\omega)=0$.

Now returning to (3.16) one can use the same argument as above with $n=2$ to find the function $F(\omega)$:

$$F(\omega)=|p_0^1(i\omega)|^2-|p_1^1(i\omega)|^2,$$

where

$$p_0^1(i\omega) = \omega^6 + (I^2 - 2M)\omega^4 + (M^2 - L^2 - 2IQ)\omega^2 + Q^2 - P^2, \tag{3.18}$$

$$\begin{aligned} p_1^1(i\omega) = &- (IJ + K)\omega^4 + (J(Q - P) + K(M - L) - IN)\omega^2 + N(Q - P) \\ &+ i[J\omega^5 + (N - J(L + M) - IK)\omega^3 + (K(P + Q) - N(L + M))\omega]. \end{aligned}$$

The function $F(\omega)$ is then calculated to give

$$F(\omega) = \omega^{12} + A_1\omega^{10} + A_2\omega^8 + A_3\omega^6 + A_4\omega^4 + A_5\omega^2 + A_6, \tag{3.19}$$

where,

$$\begin{aligned} A_1 &= 2I^2 - J^2 - 4M, \\ A_2 &= I^4 - (J^2 + 4M)I^2 + 2[J(J(L + M) - N) + 3M^2 - 2IQ - L^2] - K^2, \\ A_3 &= - 4I^3Q + [2(M^2 - JN - L^2) - K^2]I^2 + 2[J(J(Q - P) - 2KL) + 4MQ]I \\ &\quad - 4M^3 - J^2M^2 + 2[J(2N - JL) + K^2 + 2L^2]M + J[4(LN - KP) - JL^2] \\ &\quad - 2(K^2L + P^2) - N^2 + 2Q^2, \\ A_4 &= M^4 - [2(2IQ + JN + L^2) + K^2]M^2 + 2[K^2L + N^2 - 2Q^2 + 2(J(KP - LN) \\ &\quad + P^2)]M + (6Q^2 - N^2 - 2P^2)I^2 + 2[K^2(P + Q) + 2L^2Q + 2N(J(Q - P) - KL)]I \\ &\quad + L^4 - (2JN + K^2)L^2 + 2(2JKQ + N^2)L + J^2[P(2Q - P) - Q^2] - 4KNP, \\ A_5 &= [2(I(Q - P) - LM) - L^2 - M^2]N^2 + 2[2(Q(JP + KL) + KMP) - J(P^2 + Q^2)]N \\ &\quad + 2P^2(2IQ + L^2 - M^2) - K^2(P + Q)^2 + 2Q^2(M^2 - L^2 - 2IQ), \\ A_6 &= (P^2 - Q^2)^2 - N^2(P - Q)^2. \end{aligned}$$

If $A_6 < 0$ in (3.19), then the function $F(\omega)$ has at least one positive root, ω, satisfying $F(\omega) = 0$. We can prove this as follows. Assuming $A_6 < 0$ implies that $F(0) = A_6 < 0$. Since $F(\omega)$ is a continuous function of ω, and also $\lim_{\omega\to\infty} F(\omega) = \infty$, this means there exists a positive root $\omega > 0$ such that $F(\omega) = 0$.

We now consider the case where $A_6 \geq 0$. Let $z = \omega^2$, then the equation $F(\omega) = 0$ can

be written as

$$h(z) = z^6 + A_1 z^5 + A_2 z^4 + A_3 z^3 + A_4 z^2 + A_5 z + A_6 = 0. \tag{3.20}$$

Without loss of generality, suppose that (3.20) has six positive real roots denoted by z_1, z_2, z_3, z_4, z_5, z_6, respectively, which would give six possible values of ω:

$$\omega_1 = \sqrt{z_1}, \quad \omega_2 = \sqrt{z_2}, \quad \omega_3 = \sqrt{z_3}, \quad \omega_4 = \sqrt{z_4}, \quad \omega_5 = \sqrt{z_5}, \quad \omega_6 = \sqrt{z_6}.$$

Now looking for solutions of (3.16) of the form $\lambda = i\omega$ for some real $\omega > 0$, and separating into real and imaginary parts we have

$$\begin{aligned}
(J\omega^2 + N)\cos(\omega\tau) + K\omega\sin(\omega\tau) &= I\omega^2 - Q - [P\cos(2\omega\tau) + L\omega\sin(2\omega\tau)], \\
-(J\omega^2 + N)\sin(\omega\tau) + K\omega\cos(\omega\tau) &= \omega(\omega^2 - M) + P\sin(2\omega\tau) - L\omega\cos(2\omega\tau).
\end{aligned}$$

Squaring and adding together gives

$$\beta\cos(u) + \delta\sin(u) = \epsilon,$$

where

$$\begin{aligned}
u &= 2\omega\tau, \\
\beta &= 2[P(I\omega^2 - Q) + L\omega^2(\omega^2 - M)], \\
\delta &= 2\omega[P(M - \omega^2) + L(I\omega^2 - Q)], \\
\epsilon &= (I\omega^2 - Q)^2 + \omega^2(\omega^2 - M)^2 + \omega^2(L^2 - K^2) + P^2 - (J\omega^2 + N)^2.
\end{aligned}$$

Dividing by $\sqrt{\beta^2 + \delta^2}$ we obtain

$$\frac{\beta\cos(u)}{\sqrt{\beta^2 + \delta^2}} + \frac{\delta\sin(u)}{\sqrt{\beta^2 + \delta^2}} = \frac{\epsilon}{\sqrt{\beta^2 + \delta^2}}. \tag{3.21}$$

Note that,

$$\left(\frac{\beta}{\sqrt{\beta^2 + \delta^2}}\right)^2 + \left(\frac{\delta}{\sqrt{\beta^2 + \delta^2}}\right)^2 = 1.$$

Hence, there must exist a value θ such that

$$\cos(\theta) = \frac{\beta}{\sqrt{\beta^2+\delta^2}}, \quad \sin(\theta) = \frac{\delta}{\sqrt{\beta^2+\delta^2}}, \quad \text{and} \quad \theta = \arctan\left(\frac{\delta}{\beta}\right).$$

Thus we can rewrite (3.21) as follows:

$$\begin{aligned} \cos(u)\cos(\theta) + \sin(u)\sin(\theta) &= \frac{\epsilon}{\sqrt{\beta^2+\delta^2}} \\ \Leftrightarrow \quad \cos(u-\theta) &= \frac{\epsilon}{\sqrt{\beta^2+\delta^2}}. \end{aligned}$$

Through some algebraic manipulation we are able to find the critical time delays given by

$$\begin{aligned} \tau_{k,j} =& \frac{1}{2\omega_k}\left[\arctan\left(\frac{\delta_k}{\beta_k}\right) + \arccos\left(\frac{\epsilon_k}{\sqrt{\beta_k^2+\delta_k^2}}\right) + j\pi\right], \\ & k = 1, 2, \ldots, 6, \quad j = 0, 1, 2, \ldots. \end{aligned}$$

Define,

$$\tau_0 = \min_{1\le k\le 6} \tau_{k,0}, \qquad \omega_0 = \omega_{k_0}, \qquad k_0 \in \{1,2,3,4,5,6\},$$

then τ_0 is the first value of $\tau > 0$ such that the characteristic equation (3.16) has a pair of purely imaginary roots. We can state some implicit conditions on whether a Hopf bifurcation arises at the critical time delay by looking to prove the transversality condition. Let $\lambda(\tau) = \mu(\tau) + i\omega(\tau)$ be the root of the characteristic equation (3.16) near $\tau = \tau_0$, satisfying $\mu(\tau_0) = 0$ and $\omega(\tau_0)$. Substituting $\lambda = \lambda(\tau)$ into (3.16) and differentiating both sides with respect to τ yields

$$\left(\frac{d\lambda}{d\tau}\right)^{-1} = \frac{3\lambda^2 + 2I\lambda + M + (K - 2J\lambda)e^{-\lambda\tau} + Le^{-2\lambda\tau}}{\lambda[(-J\lambda^2 + K\lambda + N)e^{-\lambda\tau} + (2L\lambda + 2P)e^{-2\lambda\tau}]} - \frac{\tau}{\lambda}.$$

From this equation we have

$$\begin{aligned}
\operatorname{sgn}\left\{\left[\frac{d(\mathrm{Re}\lambda)}{d\tau}\right]_{\tau=\tau_0}\right\} &= \operatorname{sgn}\left\{\mathrm{Re}\left[\left(\frac{d\lambda}{d\tau}\right)^{-1}\right]_{\tau=\tau_0}\right\} \\
&= \operatorname{sgn}\left\{\mathrm{Re}\left[\frac{3\lambda^2+2I\lambda+M+(K-2J\lambda)e^{-\lambda\tau}+Le^{-2\lambda\tau}}{\lambda[(-J\lambda^2+K\lambda+N)e^{-\lambda\tau}+(2L\lambda+2P)e^{-2\lambda\tau}]}\right]_{\tau=\tau_0}\right\} \\
&= \operatorname{sgn}\Big\{(\omega^2(R^2+S^2))^{-1}\big[(2KP-LN-5JL\omega^2)\sin(\omega\tau) \\
&\qquad -\omega(4JP+3KL)\cos(\omega\tau)+\omega(2(JN+L^2)+K^2-2J^2\omega^3 \\
&\qquad +R(M-3\omega^2)+2SI\omega)\big]\Big\},
\end{aligned}$$

where

$$\begin{aligned}
R &= -K\omega\cos(\omega\tau)+(J\omega^2+N)\sin(\omega\tau)-2L\omega\cos(2\omega\tau)+2P\sin(2\omega\tau), \\
S &= (J\omega^2+N)\cos(\omega\tau)+K\omega\sin(\omega\tau)+2P\cos(2\omega\tau)+2L\omega\sin(2\omega\tau).
\end{aligned}$$

If $\operatorname{sgn}\{[d(\mathrm{Re}\lambda)/d\tau]_{\tau=\tau_0}\} > 0$ then the steady state undergoes a Hopf bifurcation at the critical time delay τ_0. Alternatively, we can state the following result.

Theorem 3.2. *Suppose the conditions of Lemma 3.3 hold. If* $h'(z_0)p_0^1(i\omega_0) > 0$, *where* $h(z)$ *and* $p_0^1(i\omega)$ *are defined in* (3.20) *and* (3.18), *respectively, and* $z_0 = \omega_0^2$, *then the steady state* (x_8, y_8, z_8) *or* (x_9, y_9, z_9) *of system* (3.11) *is stable for* $0 \le \tau \le \tau_0$ *and unstable for* $\tau > \tau_0$ *and undergoes a Hopf bifurcation at* $\tau = \tau_0$.

Proof. Firstly, by Lemma 3.3, the steady state (x_8, y_8, z_8) or (x_9, y_9, z_9) of system (3.11) is stable at $\tau = 0$. We have shown that τ_0 is the first value of τ whereby the characteristic equation (3.16) has a pair of purely imaginary eigenvalues $\lambda = \pm i\omega_0$. We cannot obtain an explicit proof of the existence of a Hopf bifurcation through direct computation. Thus we follow the methodology of Li et al. [132] and Rahman et al. [130] instead by introducing a function

$$S_1(\omega) = \operatorname{sgn}[\omega F'(\omega)p_0^1(i\omega)],$$

which determines possible changes in the number of roots with positive real part of (3.16).

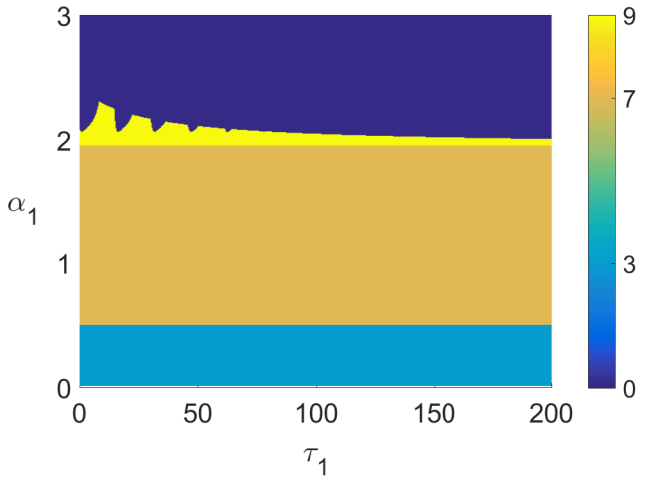

Figure 3.9: Parameter regions for stable and unstable steady states of SDRAM system (3.11). Each colour coded number is the indice of the corresponding steady state which is stable in that region, whilst all other steady states are unstable or infeasible. The blue region labelled 0 is where all steady states are unstable, leading to sustained oscillations. Parameter values: $\tau_2 = 15$, $\alpha_2 = 5$, $\alpha_3 = 6$, $b_1 = 4$, $b_2 = 3$, $b_3 = 1$, $c_1 = 8$, $c_2 = 10$, $c_3 = 15$, $d_1 = 0.5$, $d_2 = 2$, $d_3 = 0.2$, $\gamma_2 = 0.8$, $\gamma_3 = 2$.

From the definition of the function $h(z)$, we have

$$F(\omega) = h(\omega^2) \quad \Rightarrow \quad F'(\omega) = 2\omega h'(\omega^2) = 2\omega h'(z),$$

which, under the assumption that $h'(z_0)p_0^1(i\omega_0) > 0$, implies

$$S_1(\omega_0) = \text{sgn}[\omega_0 F'(\omega_0)p_0^1(i\omega_0)] = \text{sgn}[2\omega_0^2 h'(z_0)p_0^1(i\omega_0)] = \text{sgn}[h'(z_0)p_0^1(i\omega_0)] > 0.$$

From Theorem 2 in [132] we have

$$\text{sgn}\left\{\left[\frac{d\text{Re}[\lambda(\tau)]}{d\tau}\right]_{\tau=\tau_0}\right\} > 0,$$

hence the steady state (x_8, y_8, z_8) or (x_9, y_9, z_9) undergoes a Hopf bifurcation at $\tau = \tau_0$.□

Finally we would like to investigate, analytically, the case where $\tau_1 \neq \tau_2$. The corresponding characteristic equation is given by

$$\lambda^3 + \lambda^2(U - \kappa_2 e^{-\lambda\tau_1} - \kappa_3 e^{-\lambda\tau_2}) + \lambda(Ve^{-\lambda\tau_1} + We^{-\lambda\tau_2} + Le^{-\lambda(\tau_1+\tau_2)} + M) + Xe^{-\lambda\tau_1} + Ye^{-\lambda\tau_2} + Pe^{-\lambda(\tau_1+\tau_2)} + Q = 0, \tag{3.22}$$

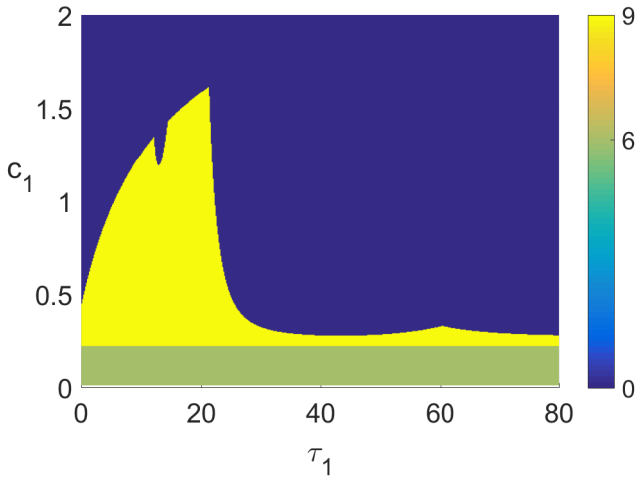

Figure 3.10: Parameter regions for stable and unstable steady states of SDRAM system (3.11). Each colour coded number is the indice of the corresponding steady state which is stable in that region, whilst all other steady states are unstable or infeasible. The blue region labelled 0 is where all steady states are unstable, leading to sustained oscillations. Parameter values: $\tau_2 = 15$, $\alpha_1 = 4$, $\alpha_2 = 5$, $\alpha_3 = 6$, $b_1 = 4$, $b_2 = 3$, $b_3 = 1$, $c_2 = 10$, $c_3 = 15$, $d_1 = 0.5$, $d_2 = 2$, $d_3 = 0.2$, $\gamma_2 = 0.8$, $\gamma_3 = 2$.

where

$$U = 1 + \gamma_2 + \gamma_3 - \kappa_1,$$

$$V = (\kappa_1 - \gamma_3 - 1)\kappa_2,$$

$$W = (\kappa_1 - \gamma_2 - 1)\kappa_3,$$

$$X = (\kappa_1 - 1)\gamma_3\kappa_2,$$

$$Y = (\kappa_1 - 1)\gamma_2\kappa_3,$$

and L, M, P, Q are the same as defined for (3.16). However the number of free parameters, time delays and exponential terms in the coefficients of the characteristic polynomial on the left hand side of (3.22) makes it infeasible to perform any meaningful mathematical analysis on the characteristic equation (3.22). We leave this case to be analysed numerically.

In Figure 3.9 the parameters are the same as in Figure 3.8, however, now τ_2 is not chosen in the limit $\tau_2 = 0$ but instead, $\tau_2 = 15$. In this scenario, notice how in the parameter region $1.963 < \alpha_1 < 2.309$, for small τ_1 all steady states are unstable but then as τ_1 is increased, steady state (x_9, y_9, z_9) experiences a diminishing switch-like behaviour between stable and unstable. Unlike Figure 3.8, when stability is lost at a critical time delay,

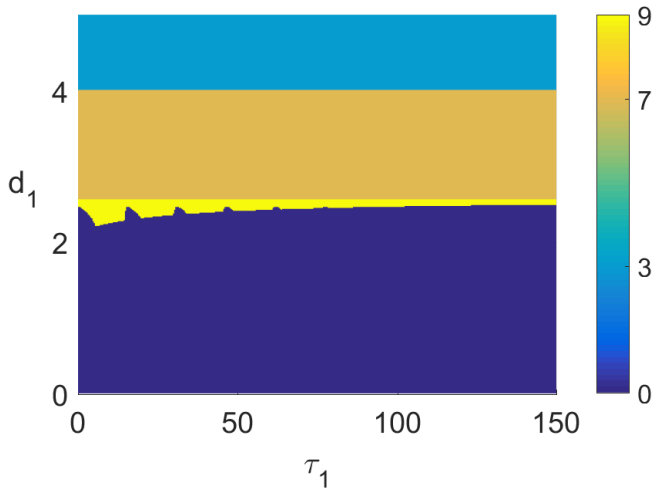

Figure 3.11: Parameter regions for stable and unstable steady states of SDRAM system (3.11). Each colour coded number is the indice of the corresponding steady state which is stable in that region, whilst all other steady states are unstable or infeasible. The blue region labelled 0 is where all steady states are unstable, leading to sustained oscillations. Parameter values: $\tau_2 = 15$, $\alpha_1 = 4$, $\alpha_2 = 5$, $\alpha_3 = 6$, $b_1 = 4$, $b_2 = 3$, $b_3 = 1$, $c_1 = 8$, $c_2 = 10$, $c_3 = 15$, $d_2 = 2$, $d_3 = 0.2$, $\gamma_2 = 0.8$, $\gamma_3 = 2$.

the steady state (x_9, y_9, z_9) does not remain unstable for larger values of τ_1. This result highlights the importance of correct mathematical representation of the transcription and translation processes, since inclusion of multiple transcriptional and translational delays can lead to regions in the parameter space where, depending on the careful choice of time delay values, either sustained periodic oscillations occur or the solution tends towards a stable steady state.

Figure 3.10 looks at the stability relationship between c_1 and τ_1. We see that there are only two attainable stable steady states through varying the parameter c_1. In the region of parameter space where (x_6, y_6, z_6) is stable, it remains so for any time delay. There is again a region in the parameter space where switching occurs between stable and unstable steady state (x_9, y_9, z_9) as τ_1 is increased. Notice the spiking behaviour of the unstable region for $1.195 < c_1 < 1.348$.

We see that Figure 3.11 appears almost as a flipped image of Figure 3.9. In the regions of the parameter space where steady state (x_3, y_3, z_3) or (x_7, y_7, z_7) are stable, they remain so for any time delay τ_1. Similar to parameter α_1, there exists a region $2.215 < d_1 < 2.563$ where if the steady state (x_9, y_9, z_9) loses stability due to an increase in τ_1, it experiences switching behaviour between stable and unstable for larger τ_1.

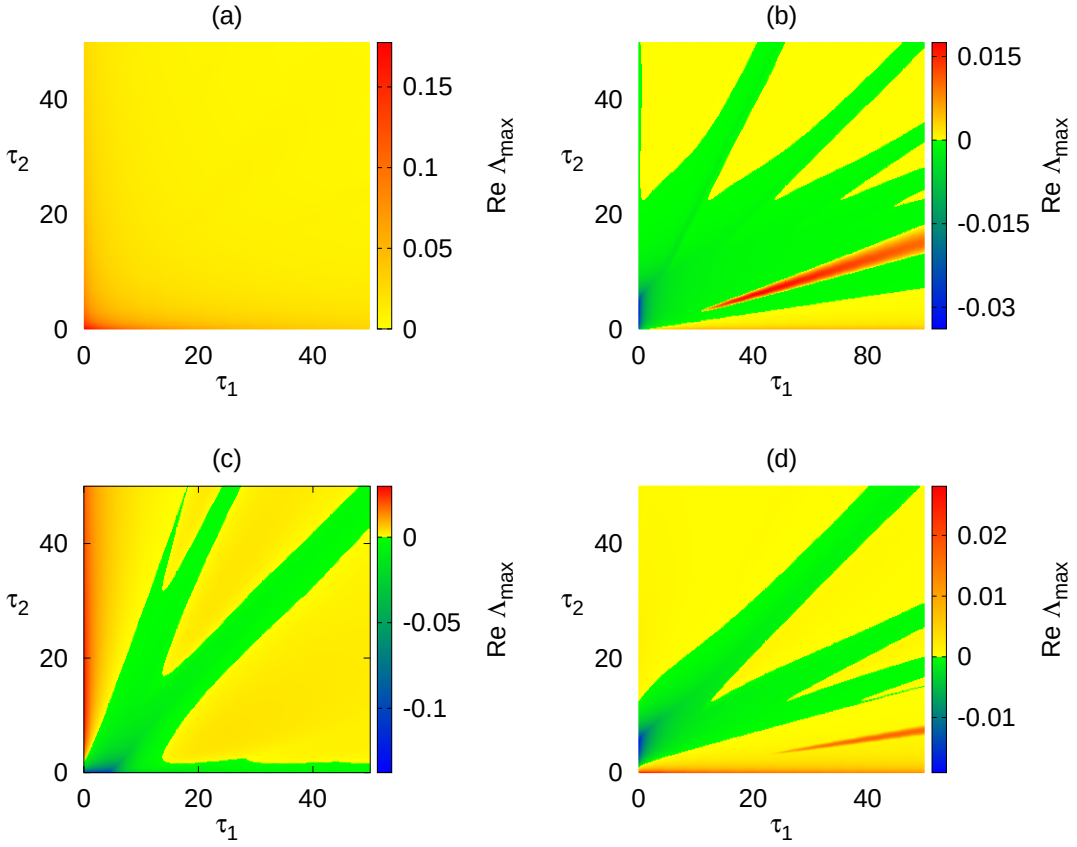

Figure 3.12: The values of Max(Re(λ)) in the (τ_1, τ_2) parameter space for steady state (x_9, y_9, z_9) of SDRAM system. All other steady states are either unstable or infeasible for these parameter schemes. (a) Parameter values: $\alpha_1 = 4$, $\alpha_2 = 5$, $\alpha_3 = 6$, $b_1 = 4$, $b_2 = 3$, $b_3 = 1$, $c_1 = 8$, $c_2 = 10$, $c_3 = 15$, $d_1 = 0.5$, $d_2 = 2$, $d_3 = 0.2$, $\gamma_2 = 0.8$, $\gamma_3 = 2$. (b) $\alpha_1 = 2$. (c) $c_1 = 1$. (d) $d_1 = 2.4$. All other parameters remain the same as (a) in (b)-(d).

Figure 3.12 shows stability regions in the (τ_1, τ_2) parameter space. The parameters fixed in Figure 3.12(a) are the same as those used throughout Figures 3.8-3.11. However, notice how the value of $\alpha_1 = 4$ places the parameter choice beyond the range of the y axis in Figure 3.9, and thus it sits in the region where all steady states are unstable for any τ_1. This is also illustrated in Figure 3.12(a), the steady states are unstable for any choices of either time delay. In Figure 3.12(b), the parameter $\alpha_1 = 2$ is fixed. Notice that this parameter choice lies in the region of Figure 3.8 where steady state (x_9, y_9, z_9) is stable and subsequently loses stability as τ_1 is increased. We see that Figure 3.12(b) produces rich dynamics of switching between regions where steady state (x_9, y_9, z_9) is stable (Max(Re(λ)) < 0) and regions where all steady states are unstable (Max(Re(λ)) > 0). In Figures 3.12(c) and 3.12(d) parameters c_1 and d_1 are fixed so that they lie in the regions of Figures 3.10 and 3.11, respectively, where steady state (x_9, y_9, z_9) is stable. All other

parameters remain the same. Again we see spiking regions that spread across the entire parameter space.

In all Figures it can be seen that the losses and gains in stability all occur around (x_9, y_9, z_9), showing that the stability of this steady state is not robust against parameter variations. This result is highlighted further by Figure 3.12 as it shows the sensitivity of steady state (x_9, y_9, z_9) to losing stability through changes in the transcriptional and translational time delays.

3.4 Discussion

In this chapter we have discussed a mathematical model for the analysis of a GRN and focussed on the role played by the transcriptional and translational time delays in the dynamics of a three-gene *Repressilator* model with auto-activation. We have established conditions for stability of seven equilibria and found that none of these can undergo a switch in stability due to the existence of time delays. By reducing the model to the one with two time delays, we could investigate the last two steady states by considering a scenario where protein x is expressed under a smaller time scale to y and z, such that the time delays associated with protein x are negligible. We found, analytically, the boundary of the Hopf bifurcation depending on the two time delays and other system parameters, and illustrated different types of behaviour by direct simulation. Mathematical analysis has shown that only the steady states with non-zero x, y, and z components (labelled (x_8, y_8, z_8) and (x_9, y_9, z_9)) have the potential to undergo a Hopf bifurcation depending on the time delays. However numerical simulations show us that it is in fact only steady state (x_9, y_9, z_9) that can undergo a Hopf bifurcation as a result of increasing time delays. Our results also suggest that under certain parameter choices, steady state (x_9, y_9, z_9) can alternate between stable and unstable as a time delay is increased. The numerical simulations reveal switching between different stable steady states through variations in the system parameters. This is in agreement with the biology, as the changes in stable steady states can account for different cell fates of GRNs in the immune system.

Chapter 4

Time-Delayed Model of a Genetic Network with Switches and Oscillations

The two types of systems that are of particular interest in this chapter are the *Repressilator* [74] and the *Toggle switch* [80]. As mentioned in the previous chapter, the *Repressilator* is a model comprised of three genes which are connected in such a way that the protein coded by each gene inhibits the expression of the next gene in the cycle, thus acting as a repressor. The *Toggle switch* is made up of two genes with mutually repressing proteins, which leads to bistability. Bistability is a type of switch which permits the coexistence of two stable steady states, and is known to be a key component in biological systems such as cell fates of GRNs during the immune response to an antigen.

The *Repressilator* and *Toggle switch* have been studied in a variety of ways [134–138], however all of these models looked at the two systems independently of each other. A paper by Gonze [139] looked to combine the two and unravel the compositional rules that govern its dynamics. This type of model was warranted since biological systems are composed of interconnected positive and negative circuits [140]. They investigated the dynamical properties that arise through the coupling of the *Repressilator* and *Toggle switch*. Two forms of coupling were investigated. In the first case, one protein of the *Repressilator* activates the expression of one gene in the *Toggle switch*. In the second case, a protein in the *Toggle switch* activates the expression of one gene in the *Repressilator*. Both types

are what's known as master/slave systems, since one subsystem is under the control of the other through unidirectional coupling. In the study, Gonze accounted for the coupling through a linear function and it was addressed that using a more elaborate coupling term leads to qualitatively similar results. Gonze first investigated the system where a protein in the *Repressilator* activates the *Toggle switch*. It was shown through numerical simulation, and using the coupling term as a bifurcation parameter, that the amplitude of the oscillatory coupling may lead to four different dynamical behaviour scenarios. When the amplitude of the coupling is sufficiently large, oscillations of the *Repressilator* are able to induce a periodic switch in the *Toggle switch*. However, when the amplitude of coupling is insufficient, a periodic switch cannot be induced. Instead, the trajectory of the coupled protein, X, in the *Toggle switch* oscillates with low-amplitude around the lower steady state. When the amplitude of coupling is very low there are two possible scenarios. Under certain conditions it is possible for X to oscillate with low-amplitude around the upper steady state, or a phenomenon of birythmicity occurs. Birythmicity is where, under particular initial conditions, low-amplitude oscillations around the upper steady state are induced, whilst under a different set of initial conditions there are low-amplitude oscillations around the lower steady state. Gonze also investigated the effect of the period of oscillations on the dynamical behaviour of the Toggle switch. No periodic switch is observed given a sufficiently small period.

Investigating the second type of coupling, where the *Toggle switch* activates the *Repressilator*, a transient perturbation was also considered. It was shown that an external signal acting on the *Toggle switch* has the potential to induce oscillations in the *Repressilator* or in fact stop any existing oscillations. This paper by Gonze highlights how one can obtain control, through parameter tuning and network structure, over the dynamical behaviour of an oscillatory system coupled with a bistable switch. This is important as unidirectional coupling is likely to be present at multiple stages of gene regulatory networks which were shown to be hierarchical [139]. It should be noted that bidirectional (mutual) coupling between biological switches and oscillators also exist in many biological networks, such as bidirectional coupling between the ATM switch and the p53-Mdm2 oscillator in the p53 signaling network [141], and this form of coupling between the *Toggle switch* and *Repressilator* has also been studied [142].

This chapter explores the impact of transcriptional and translational delays on a five-

gene system with unidirectional coupling, where the expression of a gene in the *Toggle switch* is under the control of a protein in the *Repressilator*. Although the literature studied the effects of coupling amplitude on the oscillatory dynamics of the system, in this chapter stability analysis is also performed to establish the conditions for a Hopf bifurcation where solutions exhibit such oscillations. We then make a comparative analysis between the delayed model, described using delay differential equations, and the existing ODE model in the literature. This is done by studying the dynamical behaviours observed in numerical simulations of the DDE system, and comparing the results to those found by Gonze. The existence of new dynamical behaviours are shown which were impossible in the model system without the time delays.

4.1 The Delayed Model

The *Repressilator* is a model composed of three genes which are cyclically connected in such a way that the protein coded by each gene in the system acts as a repressor for the transcription of the next gene in the cycle [139]. The dynamics of this model can be described by the following set of ordinary differential equations:

$$\begin{aligned}
\frac{dM_i}{dt} &= T\left(-M_i + \frac{\alpha_i}{1 + P^m_{\mathrm{mod}(i+1,3)}}\right), \quad \text{with} \quad i = 1, 2, 3, \\
\frac{dP_i}{dt} &= T(\beta_i M_i - \gamma_i P_i), \quad \text{with} \quad i = 1, 2, 3.
\end{aligned}$$

Here, M_i and P_i represent the concentrations of mRNA and protein, respectively, of the corresponding ith gene in the system. The Hill function $\alpha_i/(1 + P^m_{\mathrm{mod}(i+1,3)})$ accounts for the inhibition where "mod" is the modulo function. The parameter α_i represents the maximum rate of mRNA synthesis of gene i. Parameter T has been introduced to allow us to easily control time scale of the dynamics. Variables and time have been rescaled and adimensionalised.

The dynamics of the *Toggle switch* system, which consists of two genes that mutually inhibit each other, are described by the following ODEs:

$$\begin{aligned}
\frac{dX}{dt} &= \frac{a_1}{1 + Y^n} - d_1 X + b_1, \\
\frac{dY}{dt} &= \frac{a_2}{1 + X^n} - d_2 Y + b_2.
\end{aligned}$$

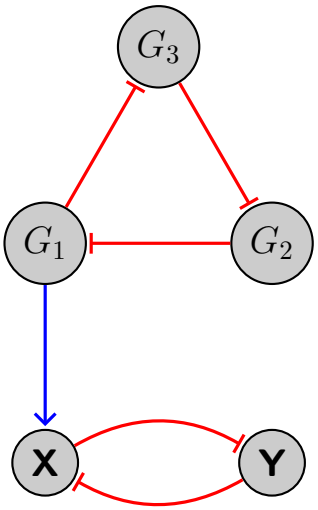

Figure 4.1: Network motif of the *Repressilator* coupled with a *Toggle switch*. The nodes are genes G_1, G_2, and G_3 of the *Repressilator*, which are connected by edges, in red, representing regulation of each gene by inhibition from the preceding gene in the cycle. The genes X and Y of the *Toggle switch* are connected by edges, in red, representing regulation of each gene by mutual repression. The *Repressilator* and *Toggle switch* are coupled through an edge, in blue, connecting gene G_1 with X which represents regulation of gene X by activation from G_1.

There is no distinction made between the gene and the protein, unlike in the *Repressilator* model. Qualitatively, the results will be the same if we were to include equations which account for the evolution of mRNAs for X and Y. In this model, the inhibition is described by the Hill functions $a_1/(1+Y^n)$ and $a_2/(1+X^n)$ where a_1 and a_2 denote the maximum rate of X and Y mRNA synthesis, respectively, and n is the cooperativity. Parameters b_1 and b_2 describe an independent synthesis source of X and Y, resulting from another promoter perhaps, which is unaffected by the inhibition of X and Y, but can be controlled by external factors. Again, variables and time have been rescaled and adimensionalised.

We are interested in the type of coupling where the *Repressilator* is in control of the *Toggle switch*, see Figure 4.1. This model, studied by Gonze [139], is given by the following ODEs:

$$\begin{aligned}
\frac{dM_i}{dt} &= T\left(-M_i + \frac{\alpha_i}{1+P^m_{\mathrm{mod}(i+1,3)}}\right), \quad \text{with} \quad i=1,2,3,\\
\frac{dP_i}{dt} &= T(\beta_i M_i - \gamma_i P_i), \quad \text{with} \quad i=1,2,3,\\
\frac{dX}{dt} &= \frac{a_1}{1+Y^n} - d_1 X + b_1,\\
\frac{dY}{dt} &= \frac{a_2}{1+X^n} - d_2 Y + b_2,
\end{aligned} \tag{4.1}$$

where $a_1 = AP_1 + B$ is the linear coupling parameter, which depends on the variable P_1. In this system, it is assumed that one protein of the *Repressilator*, P_1, promotes the expression of gene X of the *Toggle switch*.

In Figure 4.2, the numerical simulation results of model (4.1) from [139] have been reproduced. We see that a periodic switch can be observed when amplitude of the forcing is sufficient, which is shown in Figure 4.2(a) and (b). Figure 4.2(c) and (d) then shows that when the amplitude of forcing is not high enough, a switch cannot be induced, instead X remains close to the bottom steady state branch. When the forcing amplitude is further reduced, it is possible to induce birythmicity. Whereby, depending on the initial conditions, X can undergo small amplitude oscillations around the upper or lower steady state branch, shown in Figure 4.2(e) and (f). As stated in [139], there are conditions on the values of the coupling parameters A and B to obtain oscillation-induced switches. Figure 4.3(a) summarizes these results for the types of behaviours that can be observed as a function of the values of A and B. When B is sufficiently small and A is sufficiently large, a periodic switch can be observed. This is denoted by the dark blue region in Figure 4.3(a). When both A and B are small, the system cannot jump from the bottom branch to the top branch so low-amplitude oscillations occur around the lower branch (light blue region). When B is large, the system cannot jump from the top branch to the bottom branch. When this is the case, either A is large (green region) or A is small enough where the system is unable to jump from the bottom branch to the top branch and, depending on the initial conditions, the system will be stuck around the bottom or top branch, and thus birythmicity is present (yellow region). Also, although it is not shown, when B is very large ($B > 6.8$) only low-amplitude oscillations around the upper branch occurs.

In the rest of this chapter, we look at the effect of transcriptional and translational delays on the dynamical behaviour of system (4.1). We will see how the necessary conditions for phenomena such as birythmicity and periodic switching can change due to time delays. To account for these delays we can rewrite system (4.1) as the following set of

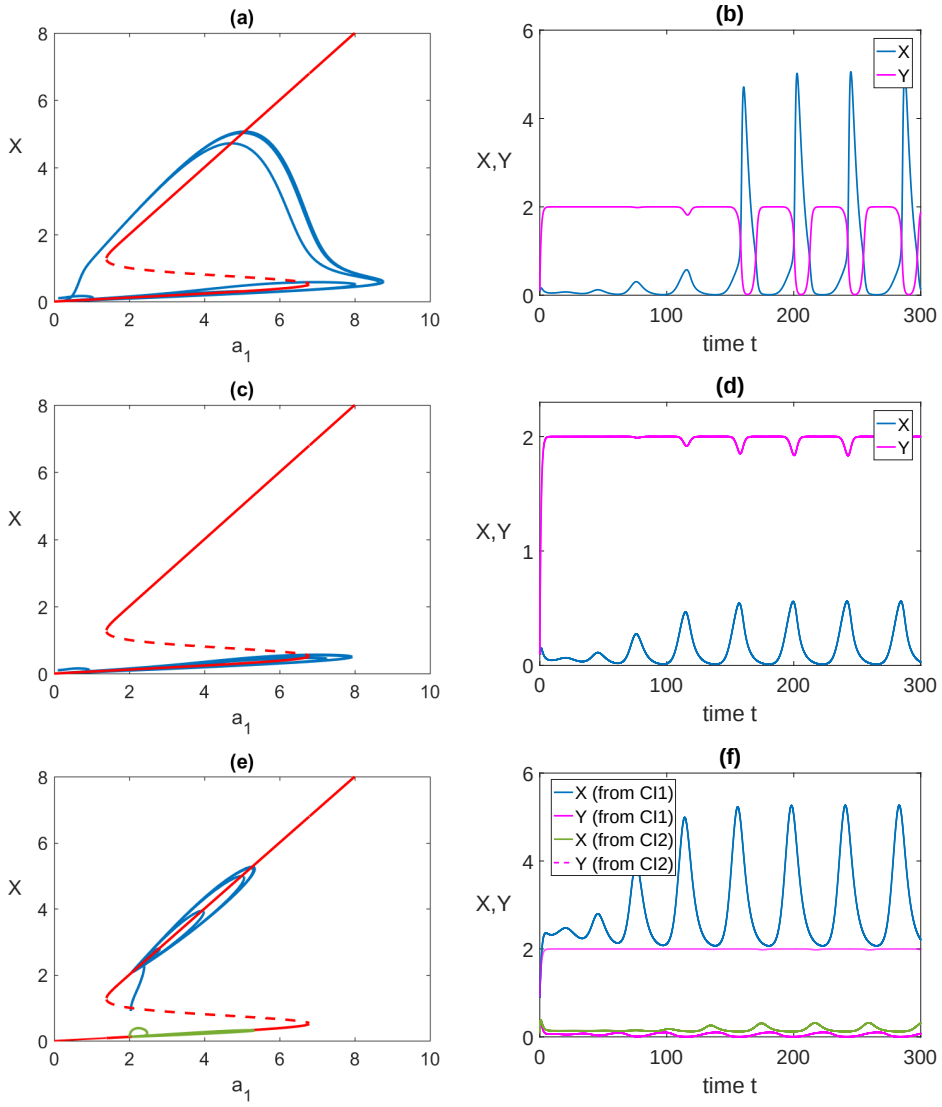

Figure 4.2: Periodic switch induced by oscillations. Red curve is the X steady state as a function of the coupling parameter a_1. (a) Bifurcation diagram of variable X as a function of parameter a_1. This parameter is a function of P_1 of the Repressilator and therefore oscillates. The blue curve corresponds to the trajectory of X and shows that this variable switches between the lower and upper steady states. (b) Time evolutions of X and Y. (c) When the amplitude of the coupling is insufficient, a periodic switch cannot be induced. instead it oscillates around the lower steady state. (d) Time evolutions of X and Y. (e) When amplitude of coupling is very low, oscillations of the Repressilator can induce phenomenon of birythmicity: depending on initial conditions, variable X can undergo small-amplitude oscillations around upper or lower steady states. (f) Corresponding evolutions of X and Y. Parameters: $T = 0.2$, $\alpha_1 = \alpha_2 = \alpha_3 = 100$, $\beta_1 = \beta_2 = \beta_3 = 5$, $\gamma_1 = \gamma_2 = \gamma_3 = 5$, $d_1 = d_2 = 1$, $b_1 = b_2 = 0$, $a_2 = 2$, $m = 2$, $n = 4$. Coupling parameters: $A = 0.21$, $B = 0$ ((a) and (b)), $A = 0.19$, $B = 0$ ((c) and (d)), $A = 0.08$, $B = 2$ ((e) and (f)). For the latter case, initial conditions are $X(0) = 0.1$ and $Y(0) = 0.9$ (denoted by CI1), leading to the lower limit cycle or $X(0) = 0.9$ and $Y(0) = 0.1$ (denoted by CI2), leading to the upper limit cycle.

delay differential equations:

$$\begin{aligned}
\frac{dM_i}{dt} &= T\left(-M_i + \frac{\alpha_i}{1 + P_{\mathrm{mod}(i+1,3)}(t-\tau_{m_i})^m}\right), \quad \text{with} \quad i = 1,2,3,\\
\frac{dP_i}{dt} &= T(\beta_i M_i(t-\tau_{p_i}) - \gamma_i P_i), \quad \text{with} \quad i = 1,2,3,\\
\frac{dX}{dt} &= \frac{a_1}{1 + Y(t-\tau_X)^n} - d_1 X + b_1,\\
\frac{dY}{dt} &= \frac{a_2}{1 + X(t-\tau_Y)^n} - d_2 Y + b_2,
\end{aligned} \tag{4.2}$$

where $a_1 = AP_1 + B$ is the linear coupling parameter, τ_{m_i} are the delays associated with the transcription of mRNA from gene i in the *Repressilator*, τ_{p_i} are the delays accounting for those present in translation processes of gene i, τ_X and τ_Y are the transcriptional delays associated with the mutual inhibition processes of gene X and Y in the *Toggle switch*.

4.2 Time Delayed Model: Positivity and Steady States

Before continuing with analysis of the model, first we must define initial conditions where appropriate and address whether all solutions to the model give positive values for all time to guarantee it's biological feasibility. The initial conditions for model (4.2) are

$$\begin{aligned}
M_1(s) &= \phi_1(s), \quad s \in [-\tau_{\max}, 0],\\
P_1(s) &= \phi_2(s), \quad s \in [-\tau_{\max}, 0],\\
M_2(s) &= \phi_3(s), \quad s \in [-\tau_{\max}, 0],\\
P_2(s) &= \phi_4(s), \quad s \in [-\tau_{\max}, 0],\\
M_3(s) &= \phi_5(s), \quad s \in [-\tau_{\max}, 0],\\
P_3(s) &= \phi_6(s), \quad s \in [-\tau_{\max}, 0],\\
X(s) &= \phi_7(s), \quad s \in [-\tau_{\max}, 0],\\
Y(s) &= \phi_8(s), \quad s \in [-\tau_{\max}, 0],
\end{aligned} \tag{4.3}$$

where $\tau_{\max} = \max(\tau_{m_1}, \tau_{p_1}, \tau_{m_2}, \tau_{p_2}, \tau_{m_3}, \tau_{p_3}, \tau_X, \tau_Y)$ and $\phi_j(s) \in C([-\tau_{\max}, 0], \mathbb{R})$ with $\phi_j(s) \geq 0$ $(-\tau_{\max} \leq s \leq 0,\ j = 1,2,...,8)$. $C([-\tau_{\max}, 0], \mathbb{R})$ is the Banach space of continuous mappings of interval $[-\tau_{\max}, 0]$ into $\mathbb{R}$. It is also assumed that $M_1(0) > 0$, $P_1(0) > 0$, $M_2(0) > 0$, $P_2(0) > 0$, $M_3(0) > 0$, $P_3(0) > 0$, $X(0) > 0$, and $Y(0) > 0$ to be sure that some proteins are produced.

Now we prove that the solution $(M_1(t), P_1(t), M_2(t), P_2(t), M_3(t), P_3(t), X(t), Y(t))$ of model (4.2) with initial condition (4.3) is positive for all $t > 0$. Again, the proof for this makes use of the methodology applied in [93]. First, we show $M_1(t) > 0$ for all $t > 0$ by contradiction. Let $t_1 > 0$ be the first time that $M_1(t_1)P_2(t_1) = 0$; assuming that $M_1(t_1) = 0$ implies $P_2(t_1) \geq 0$ for all $t \in [0; t_1]$ and since t_1 is the first time when $M_1(t_1) = 0$, this also means that $dM_1(t_1)/dt \leq 0$; meaning the function $M_1(t)$ is decreasing at $t = t_1$. However, evaluating the first equation of system (4.2) at $t = t_1$ gives

$$\frac{dM_1(t_1)}{dt} = T\left(\frac{\alpha_1}{1 + P_2(t_1 - \tau_{m_1})^m}\right) > 0,$$

which yields a contradiction. This implies that $M_1(t) \geq 0$ for all $t > 0$. Similarly, let $t_2 > 0$ be the first time that $M_1(t_2)P_1(t_2) = 0$. As we know that $M_1(t) > 0$ for all $t > 0$, the only way this can happen is if $P_1(t_2) = 0$. This means that $dP_1(t_2)/dt \leq 0$. However, evaluating the second equation of system (4.2) at $t = t_2$ gives

$$\frac{dP_1(t_2)}{dt} = T\beta_1 M_1(t_2 - \tau_{p_1}) > 0,$$

which gives a contradiction, implying that $P_1(t) \geq 0$ for all $t > 0$. In an analogous way to this we can prove the positivity of $M_2(t)$, $P_2(t)$, $M_3(t)$, $P_3(t)$, $X(t)$, and $Y(t)$. We then have that all solutions of model (4.2) are greater than or equal to zero for all $t > 0$, that is, the model is well posed.

The steady states $(\bar{M_1}, \bar{P_1}, \bar{M_2}, \bar{P_2}, \bar{M_3}, \bar{P_3}, \bar{X}, \bar{Y})$ of model (4.2) can be found as roots

of the following system of algebraic equations:

$$
\begin{aligned}
T\left(\frac{\alpha_1}{1+\bar{P}_2^m}-\bar{M}_1\right)&=0,\\
T(\beta_1\bar{M}_1-\gamma_1\bar{P}_1)&=0,\\
T\left(\frac{\alpha_2}{1+\bar{P}_3^m}-\bar{M}_2\right)&=0,\\
T(\beta_2\bar{M}_2-\gamma_2\bar{P}_2)&=0,\\
T\left(\frac{\alpha_3}{1+\bar{P}_1^m}-\bar{M}_3\right)&=0,\\
T(\beta_3\bar{M}_3-\gamma_3\bar{P}_3)&=0,\\
\frac{a_1}{1+\bar{Y}^n}-d_1\bar{X}+b_1&=0,\\
\frac{a_2}{1+\bar{X}^n}-d_2\bar{Y}+b_2&=0.
\end{aligned}
$$

The $\bar{P}_1$ component can then be found by solving the algebraic formula

$$
\bar{P}_1=\alpha_1\beta_1/\gamma_1\left[1+\left(\frac{\alpha_2\beta_2}{\gamma_2\left(1+\left(\frac{\alpha_3\beta_3}{\gamma_3(1+\bar{P}_1^m)}\right)^m\right)}\right)^m\right].
$$

Hence we can find steady state values for $\bar{X}$ and $\bar{Y}$ as

$$
\bar{X}=\frac{1}{d_1}\left(\frac{A\bar{P}_1+B}{1+\left(\frac{1}{d_2^n}\left(\frac{a_2}{1+\bar{X}^n}+b_2\right)^n\right)}+b_1\right),\qquad \bar{Y}=\frac{1}{d_2}\left(\frac{a_2}{1+\bar{X}^n}+b_2\right).
$$

The steady state values for the remaining variables can then be found as follows:

$$
\bar{M}_3=\frac{\alpha_3}{1+\bar{P}_1^m},\quad \bar{P}_3=\frac{\beta_3}{\gamma_3}\bar{M}_3,\quad \bar{M}_2=\frac{\alpha_2}{1+\bar{P}_3^m},\quad \bar{P}_2=\frac{\beta_2}{\gamma_2}\bar{M}_2,\quad \bar{M}_1=\frac{\alpha_1}{1+\bar{P}_2^m}.
$$

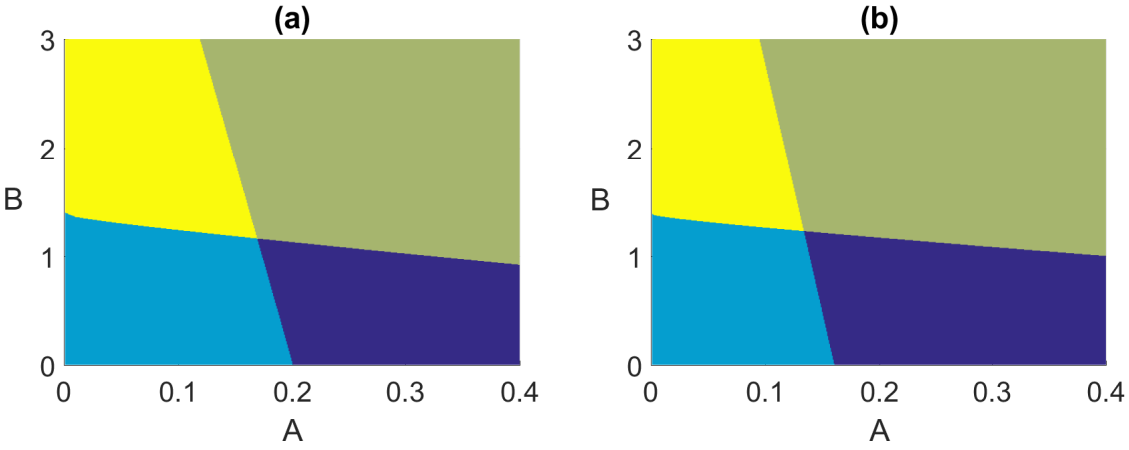

Figure 4.3: Effect of the coupling parameters A and B on the oscillation-induced periodic switch in the ODE and DDE systems, (4.1) and (4.2), respectively. (a) Oscillatory behaviour of X in the ODE model (4.1). (b) Behaviour of X in the DDE model (4.2) with delays only in the *Repressilator*. Dark blue region: When B is sufficiently small and A sufficiently large, a periodic switch is observed. Light blue region: When A and B are small, low amplitude oscillations around the lower steady state branch are observed. Green region: When both A and B are large enough, we see low amplitude oscillations around the upper steady state branch. Yellow region: When A is sufficiently small and B large, birythmicity is observed. Parameter values: $\tau_R = 1$ and $\tau_S = 0$ ((b) only). $T = 0.2$, $\alpha_1 = \alpha_2 = \alpha_3 = 100$, $\beta_1 = \beta_2 = \beta_3 = 5$, $\gamma_1 = \gamma_2 = \gamma_3 = 5$, $d_1 = d_2 = 1$, $b_1 = b_2 = 0$, $a_2 = 2$, $m = 2$, $n = 4$.

4.3 Analysis of the Delayed Repressilator Coupled with Toggle Switch Model

The equation for eigenvalues λ of the linearisation near a steady state of system (4.2) has the form

$$\left[(\lambda+T)^3(\lambda+\gamma_1 T)(\lambda+\gamma_2 T)(\lambda+\gamma_3 T)+T^6\rho e^{-\lambda\tau_R}\right]\left[(\lambda+d_1)(\lambda+d_2)+\sigma e^{-\lambda\tau_S}\right]=0, \tag{4.4}$$

where $\tau_R = \tau_{m_1} + \tau_{p_1} + \tau_{m_2} + \tau_{p_2} + \tau_{m_3} + \tau_{p_3}$ and $\tau_S = \tau_X + \tau_Y$, and

$$\rho = \frac{\alpha_1\alpha_2\alpha_3\beta_1\beta_2\beta_3 m^3 \bar{P}_1^{m-1}\bar{P}_2^{m-1}\bar{P}_3^{m-1}}{(1+\bar{P}_1)^2(1+\bar{P}_2)^2(1+\bar{P}_3)^2}, \qquad \sigma = \frac{-n^2 a_2(A\bar{P}_1+B)\bar{X}^{n-1}\bar{Y}^{n-1}}{(1+\bar{X}^n)^2(1+\bar{Y}^n)^2}.$$

In the limit $\tau_R = 0$, $\tau_S = 0$, the characteristic equation reduces to

$$\left[(\lambda+T)^3(\lambda+\gamma_1 T)(\lambda+\gamma_2 T)(\lambda+\gamma_3 T)+T^6\rho\right]\left[(\lambda+d_1)(\lambda+d_2)+\sigma\right]=0, \tag{4.5}$$

For the steady state $(\bar{P}_1, \bar{M}_1, \bar{P}_2, \bar{M}_2, \bar{P}_3, \bar{M}_3, \bar{X}, \bar{Y})$ to be stable we require that the roots of equation (4.5) have negative real part. We can therefore look at the polynomials in the square brackets independently. Looking at the second bracket and expanding we have

$$\lambda^2 + (d_1 + d_2)\lambda + d_1 d_2 + \sigma = 0.$$

The eigenvalues have negative real part provided that $d_1 d_2 + \sigma > 0$ and $d_1 + d_2 > 0$. The latter relation is satisfied since $d_1 > 0$ and $d_2 > 0$.

Now looking at the first square bracket on the left hand side of equation (4.5), we have the equation

$$\lambda^6 + \tilde{a}_1\lambda^5 + \tilde{a}_2\lambda^4 + \tilde{a}_3\lambda^3 + \tilde{a}_4\lambda^2 + \tilde{a}_5\lambda + \tilde{a}_6 = 0, \tag{4.6}$$

where

$$\begin{aligned}
\tilde{a}_1 &= T(\gamma_1 + \gamma_2 + \gamma_3 + 3) > 0,\\
\tilde{a}_2 &= T^2[\gamma_1(\gamma_2 + \gamma_3 + 3) + \gamma_2(\gamma_3 + 3) + 3\gamma_3 + 3] > 0,\\
\tilde{a}_3 &= T^3[\gamma_1(\gamma_2(\gamma_3 + 3) + 3\gamma_3 + 3) + \gamma_2(3\gamma_3 + 3) + 3\gamma_3 + 1] > 0,\\
\tilde{a}_4 &= 3T^4[\gamma_1(\gamma_2(\gamma_3 + 1) + \gamma_3 + 1/3) + \gamma_2(\gamma_3 + 1/3) + (\gamma_3/3)] > 0,\\
\tilde{a}_5 &= 3T^5[\gamma_3(\gamma_2(\gamma_1 + 1/3) + (\gamma_1/3)) + (\gamma_1\gamma_2/3)] > 0,\\
\tilde{a}_6 &= T^6(\gamma_1\gamma_2\gamma_3 + \rho) > 0.
\end{aligned}$$

Then using the Routh-Hurwitz criterion, the remaining non-zero elements of the Routh array are as follows:

$$\begin{aligned}
\tilde{b}_1 &= \frac{\tilde{a}_1\tilde{a}_2 - \tilde{a}_0\tilde{a}_3}{\tilde{a}_1}, \quad \tilde{b}_2 = \frac{\tilde{a}_1\tilde{a}_4 - \tilde{a}_0\tilde{a}_5}{\tilde{a}_1}, \quad \tilde{b}_3 = \tilde{a}_6,\\
\tilde{c}_1 &= \frac{\tilde{b}_1\tilde{a}_3 - \tilde{a}_1\tilde{b}_2}{\tilde{b}_1}, \quad \tilde{c}_2 = \frac{\tilde{b}_1\tilde{a}_5 - \tilde{a}_1\tilde{b}_3}{\tilde{b}_1},\\
\tilde{d}_1 &= \frac{\tilde{c}_1\tilde{b}_2 - \tilde{b}_1\tilde{c}_2}{\tilde{c}_1}, \quad \tilde{d}_2 = \tilde{b}_3,\\
\tilde{e}_1 &= \frac{\tilde{d}_1\tilde{c}_2 - \tilde{c}_1\tilde{d}_2}{\tilde{d}_1},\\
\tilde{f}_1 &= \tilde{d}_2.
\end{aligned}$$

Then by the Routh-Hurwitz criterion, all roots of (4.6) have negative real part provided

that $\tilde{b}_1$, $\tilde{c}_1$, $\tilde{d}_1$, $\tilde{e}_1$, $\tilde{f}_1 > 0$. This leads to the following result.

Lemma 4.1. *Let $\tau_R = \tau_S = 0$. The steady state $(\bar{P}_1, \bar{M}_1, \bar{P}_2, \bar{M}_2, \bar{P}_3, \bar{M}_3, \bar{X}, \bar{Y})$ of the system (4.2) is stable whenever the conditions $\tilde{b}_1$, $\tilde{c}_1$, $\tilde{d}_1$, $\tilde{e}_1$, $\tilde{f}_1 > 0$ and $d_1 d_2 + \sigma > 0$ hold.*

As in previous chapters, we assume the conditions of Lemma 4.1 hold for the remainder of the analysis. The only way the steady state $(\bar{P}_1, \bar{M}_1, \bar{P}_2, \bar{M}_2, \bar{P}_3, \bar{M}_3, \bar{X}, \bar{Y})$ of system (4.2) can lose stability is if a pair of complex conjugate eigenvalues cross the imaginary axis.

4.3.1 The Effect of Delays in the Toggle Switch

We wish to investigate whether there exists a critical time delay of τ_S or τ_R that can induce a Hopf bifurcation resulting in sustained oscillations. Since τ_R and τ_S appear exclusively in the first and second square brackets of (4.4), respectively, we can look at each case independently of one another. First, we look at the case where $\tau_S > 0$ and $\tau_R = 0$, that is, there are no delays in the Repressilator sub-network.

Substituting $\lambda = i\nu$, for real ν, into the equation

$$(\lambda + d_1)(\lambda + d_2) + \sigma e^{-\lambda \tau_S} = 0, \tag{4.7}$$

and separating into real and imaginary parts gives

$$\begin{aligned} \cos(\nu \tau_S) &= \frac{\nu^2 - d_1 d_2}{\sigma}, \\ \sin(\nu \tau_S) &= \frac{(d_1 + d_2)\nu}{\sigma}. \end{aligned} \tag{4.8}$$

Squaring and adding together we have

$$\nu^4 + (d_1^2 + d_2^2)\nu^2 + d_1^2 d_2^2 - \sigma^2 = 0.$$

Let $z = \nu^2$ then we define

$$h(z) = z^2 + (d_1^2 + d_2^2)z + d_1^2 d_2^2 - \sigma^2 = 0,$$

which can be solved to give the critical frequency as

$$\nu_0^2 = \frac{1}{2}\left[-(d_1^2+d_2^2) + \sqrt{(d_1^2+d_2^2)^2 - 4(d_1^2 d_2^2 - \sigma^2)}\right]. \tag{4.9}$$

One should note that ν_0^2 will only admit positive real values, provided $d_1^2 d_2^2 < \sigma^2$, which implies that, for $d_1^2 d_2^2 \geq \sigma^2$, the roots of (4.7) have negative real parts for all values of the time delay τ_S. Note that

$$\frac{dh(z)}{dz} = 2z + d_1^2 + d_2^2 > 0 \text{ for any } z \geq 0.$$

The critical value of the time delay τ_S can be found from (4.8), which gives

$$\tau_{S_0,j} = \frac{1}{\nu_0}\left[\arctan\left(\frac{(d_1+d_2)\nu_0}{\nu_0^2 - d_1 d_2}\right) + j\pi\right], \quad j = 0, 1, 2, ...,$$

where ν_0 is determined by (4.9). When $\tau_S = \tau_{S_0,j}$, the equation (4.7) has a pair of purely imaginary roots. In order to verify whether or not the steady state actually loses stability at $\tau_{S_0,j}$ one has to compute the sign of $d\mathrm{Re}(\lambda)/d\tau_S|_{\tau_S=\tau_{S_0,j}}$. Let $\lambda(\tau_S) = \mu(\tau_S) + i\nu(\tau_S)$ be the root of (4.7) near $\tau_S = \tau_{S_0,j}$ satisfying $\mu(\tau_{S_0,j}) = 0$ and $\nu(\tau_{S_0,j}) = \nu_0$. Substituting $\lambda = \lambda(\tau_S)$ into (4.7) and differentiating both sides with respect to τ_S yields

$$\left(\frac{d\lambda}{d\tau_S}\right)^{-1} = \frac{(2\lambda + d_1 + d_2)e^{\lambda\tau_S}}{\sigma\lambda} - \frac{\tau_S}{\lambda}.$$

From this equation, we can find

$$\begin{aligned}
\mathrm{sgn}\left\{\left[\frac{d(\mathrm{Re}\lambda)}{d\tau_S}\right]_{\tau_S=\tau_{S_0,j}}\right\} &= \mathrm{sgn}\left\{\mathrm{Re}\left[\left(\frac{d\lambda}{d\tau_S}\right)^{-1}\right]_{\tau_S=\tau_{S_0,j}}\right\} \\
&= \mathrm{sgn}\left\{\mathrm{Re}\left[\frac{(2\lambda+d_1+d_2)e^{\lambda\tau_S}}{\sigma\lambda}\right]_{\tau_S=\tau_{S_0,j}}\right\} \\
&= \mathrm{sgn}\left\{\frac{2\sigma\nu_1^2\cos(\nu_1\tau_{S_0}) + \sigma\nu_1(d_1+d_2)\sin(\nu_1\tau_{S_0})}{\sigma^2\nu_1^2}\right\}.
\end{aligned}$$

Substituting expressions from system (4.8) gives

$$\mathrm{sgn}\left\{\left[\frac{d(\mathrm{Re}\lambda)}{d\tau_S}\right]_{\tau_S=\tau_{S_0,j}}\right\} = \frac{2\nu_1^2 + d_1^2 + d_2^2}{\sigma^2} = \frac{h'(\nu_1^2)}{\sigma^2} > 0.$$

Hence, the roots of the equation (4.7) cross the imaginary axis at $\tau_S = \tau_{S_0}$, and never

cross back for higher values of τ_S. Here, τ_{S_0} is the first value of time delay $\tau_S \geq 0$ where the roots lie on the imaginary axis. Thus, we can state the following result.

Theorem 4.1 *Suppose the conditions of Lemma 4.1 hold and that* $\tau_R = 0$. *If* $d_1^2 d_2^2 \geq \sigma^2$, *the steady state* $(\bar{P}_1, \bar{M}_1, \bar{P}_2, \bar{M}_2, \bar{P}_3, \bar{M}_3, \bar{X}, \bar{Y})$ *of system* (4.2) *is stable for all values of the time delay* $\tau_S \geq 0$. *If* $d_1^2 d_2^2 < \sigma^2$, *this steady state is stable for* $0 \leq \tau_S < \tau_{S_0}$ *and unstable for* $\tau_S > \tau_{S_0}$ *and undergoes a Hopf bifurcation at* $\tau_S = \tau_{S_0}$.

4.3.2 The Effect of Delays in the Repressilator

Next we investigate whether there exists a critical value of the time delay τ_R which can induce sustained oscillations through a Hopf bifurcation. Here it is assumed that $\tau_S = 0$ and $\tau_R > 0$. Substituting $\lambda = i\omega$, with real $\omega > 0$, into the equation

$$(\lambda + T)^3(\lambda + \gamma_1 T)(\lambda + \gamma_2 T)(\lambda + \gamma_3 T) + T^6 \rho e^{-\lambda \tau_R} = 0 \tag{4.10}$$

and separating into real and imaginary parts gives

$$\begin{aligned} \cos(\omega \tau_R) &= \frac{\omega^6 - \tilde{a}_2 \omega^4 + \tilde{a}_4 \omega^2 - T^6 \gamma_1 \gamma_2 \gamma_3}{T^6 \rho}, \\ \sin(\omega \tau_R) &= \frac{\tilde{a}_1 \omega^5 - \tilde{a}_3 \omega^3 + \tilde{a}_5 \omega}{T^6 \rho}. \end{aligned} \tag{4.11}$$

Squaring and adding together we have

$$\begin{aligned} &\omega^{12} + (\tilde{a}_1^2 - 2\tilde{a}_2)\omega^{10} + (2(\tilde{a}_4 - \tilde{a}_1\tilde{a}_3) + \tilde{a}_2^2)\omega^8 + (2(\tilde{a}_1\tilde{a}_5 - \tilde{a}_2\tilde{a}_4 - \gamma_1\gamma_2\gamma_3 T^6) + \tilde{a}_3^2)\omega^6 \\ &\quad + (2(\tilde{a}_2\gamma_1\gamma_2\gamma_3 T^6 - \tilde{a}_3\tilde{a}_5) + \tilde{a}_4^2)\omega^4 + (\tilde{a}_5^2 - 2\tilde{a}_4\gamma_1\gamma_2\gamma_3 T^6)\omega^2 + T^{12}(\gamma_1^2\gamma_2^2\gamma_3^2 - \rho^2) = 0. \end{aligned}$$

Let $z = \omega^2$ then we have

$$\begin{aligned} g(z) = z^6 &+ (\tilde{a}_1^2 - 2\tilde{a}_2)z^5 + (2(\tilde{a}_4 - \tilde{a}_1\tilde{a}_3) + \tilde{a}_2^2)z^4 + (2(\tilde{a}_1\tilde{a}_5 - \tilde{a}_2\tilde{a}_4 - \gamma_1\gamma_2\gamma_3 T^6) + \tilde{a}_3^2)z^3 \\ &+ (2(\tilde{a}_2\gamma_1\gamma_2\gamma_3 T^6 - \tilde{a}_3\tilde{a}_5) + \tilde{a}_4^2)z^2 + (\tilde{a}_5^2 - 2\tilde{a}_4\gamma_1\gamma_2\gamma_3 T^6)z \\ &+ T^{12}(\gamma_1^2\gamma_2^2\gamma_3^2 - \rho^2) = 0. \end{aligned} \tag{4.12}$$

Without loss of generality, suppose that this equation has 6 positive real roots, denoted by z_1, z_2, z_3, z_4, z_5, z_6 respectively, which would give 6 possible values of ω: $\omega_1 = \sqrt{z_1}$, $\omega_2 = \sqrt{z_2}$, $\omega_3 = \sqrt{z_3}$, $\omega_4 = \sqrt{z_4}$, $\omega_5 = \sqrt{z_5}$, and $\omega_6 = \sqrt{z_6}$. With some algebraic manipulation we obtain

$$\tau_{R_{k,j}} = \frac{1}{\omega_k}\left[\arctan\left(\frac{\tilde{a}_1\omega_k^5 - \tilde{a}_3\omega_k^3 + \tilde{a}_5\omega_k}{\omega_k^6 - \tilde{a}_2\omega_k^4 + \tilde{a}_4\omega_k^2 - T^6\gamma_1\gamma_2\gamma_3}\right) + j\pi\right], \quad j = 0, 1, 2, ..., \quad k = 1, 2, ..., 6.$$

Define

$$\tau_{R_0} = \min_{1\leq k\leq 6}\{\tau_{R_{k,0}}\}, \quad \omega_0 = \omega_{k_0}, \quad k_0 \in \{1, 2, 3, 4, 5, 6\}.$$

τ_{R_0} is the first value of the time delay $\tau_R > 0$ where (4.10) has purely imaginary roots. We can state the following result.

Theorem 4.2 *Let $\tau_S = 0$. Suppose the conditions of Lemma 4.1 hold and $g'(z_0) > 0$, where $g(z)$ is defined in* (4.12)*. Then the steady state $(\bar{M}_1, \bar{P}_1, \bar{M}_2, \bar{P}_2, \bar{M}_3, \bar{P}_3, \bar{X}, \bar{Y})$ of system* (4.2) *is stable for $0 \leq \tau_R < \tau_{R_0}$ and unstable for $\tau_R > \tau_{R_0}$ and undergoes a Hopf bifurcation at $\tau_R = \tau_{R_0}$.*

Proof. The conclusion of Lemma 4.1 ensures the steady state $(\bar{M}_1, \bar{P}_1, \bar{M}_2, \bar{P}_2, \bar{M}_3, \bar{P}_3, \bar{X}, \bar{Y})$ of system (4.2) is stable at $\tau_R = \tau_S = 0$ and guarantees that the roots of (4.7) have negative real part when $\tau_S = 0$. Now to prove that the steady state $(\bar{M}_1, \bar{P}_1, \bar{M}_2, \bar{P}_2, \bar{M}_3, \bar{P}_3, \bar{X}, \bar{Y})$ loses stability at the critical time delay τ_{R_0}, let $\lambda(\tau_R) = \mu(\tau_R) + i\omega(\tau_R)$ be the root of (4.10) near $\tau_R = \tau_{R_0}$ satisfying $\mu(\tau_{R_0}) = 0$ and $\omega(\tau_{R_0}) = \omega_0$. Substituting $\lambda = \lambda(\tau_R)$ into (4.10) and differentiating with respect to τ_R yields

$$\left(\frac{d\lambda}{d\tau_R}\right)^{-1} = \frac{(6\lambda^5 + 5\tilde{a}_1\lambda^4 + 4\tilde{a}_2\lambda^3 + 3\tilde{a}_3\lambda^2 + 2\tilde{a}_4\lambda + \tilde{a}_5)e^{\lambda\tau_R}}{T^6\rho\lambda} - \frac{\tau_R}{\lambda}.$$

From this we find

$$\begin{aligned}
&\operatorname{sgn}\left\{\operatorname{Re}\left[\left(\frac{d\lambda}{d\tau_R}\right)^{-1}\right]_{\tau_R=\tau_{R_0}}\right\} \\
&\quad=\operatorname{sgn}\left\{\operatorname{Re}\left[\frac{(6\lambda^5+5\tilde{a}_1\lambda^4+4\tilde{a}_2\lambda^3+3\tilde{a}_3\lambda^2+2\tilde{a}_4\lambda+\tilde{a}_5)e^{\lambda\tau_R}}{T^6\rho\lambda}\right]_{\tau_R=\tau_{R_0}}\right\} \\
&\quad=\operatorname{sgn}\left\{\frac{T^6\rho[(6\omega_0^5-4\tilde{a}_2\omega_0^3+2\tilde{a}_4\omega_0)\cos(\omega_0\tau_{R_0})+(5\tilde{a}_1\omega_0^4-3\tilde{a}_3\omega_0^2+\tilde{a}_5)\sin(\omega_0\tau_{R_0})]}{T^{12}\rho^2\omega_0}\right\}.
\end{aligned}$$

Then substituting expressions from (4.11) it follows that

$$\operatorname{sgn}\left\{\operatorname{Re}\left[\left(\frac{d\lambda}{d\tau_R}\right)^{-1}\right]_{\tau_R=\tau_{R_0}}\right\}=\operatorname{sgn}\left\{\frac{g'(\omega_0^2)}{T^{12}\rho^2}\right\}>0.$$

Hence, the eigenvalues of the characteristic equation cross the imaginary axis at $\tau_R=\tau_{R_0}$, thus the steady state $(\bar{M}_1,\bar{P}_1,\bar{M}_2,\bar{P}_2,\bar{M}_3,\bar{P}_3,\bar{X},\bar{Y})$ of system (4.2) does lose stability at $\tau_R=\tau_{R_0}$. □

Using the results of Theorem 4.1 and Theorem 4.2 we obtain the following result for the case where $\tau_R>0$ and $\tau_S>0$.

Theorem 4.3. *Suppose the conditions of Lemma 4.1 hold and* $\sigma^2>d_1^2d_2^2$ *and* $g'(z_0)>0$, *where* $g(z)$ *is defined in* (4.12). *Then the steady state* $(\bar{M}_1,\bar{P}_1,\bar{M}_2,\bar{P}_2,\bar{M}_3,\bar{P}_3,\bar{X},\bar{Y})$ *of system* (4.2) *is stable for* $0\leq\tau_S<\tau_{S_0}$ *and* $0\leq\tau_R<\tau_{R_0}$, *and unstable for* $\tau_S>\tau_{S_0}$ *or* $\tau_R>\tau_{R_0}$, *and undergoes a Hopf bifurcation at* $\tau_S=\tau_{S_0}$ *or* $\tau_R=\tau_{R_0}$.

4.4 Oscillatory Behaviour of the DDE System

In previous chapters, time delays have been shown to have a significant impact on the dynamical behaviour of GRNs when modelled using DDEs. However in past research the effect of time delays on steady state stability has been investigated, here we wish to study the effect of time delays on the oscillatory behaviour of a protein from the *Toggle switch* sub-network in (4.2) with regards to switching and birythmicity. For the purpose of making a comparative analysis between the ODE and DDE models, we adopt the methodology in [139] to display our findings.

We now investigate the effects of time delays in the DDE model (4.2) on the parameter-

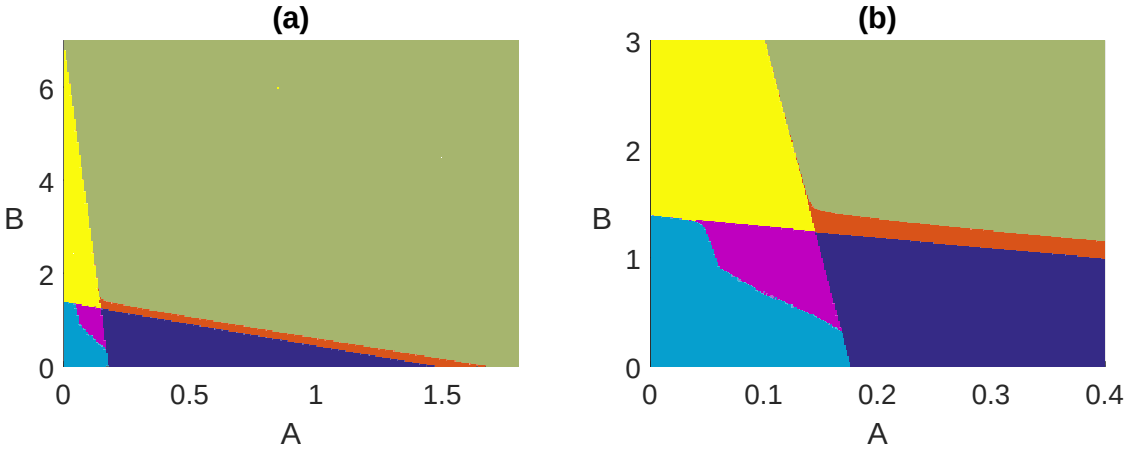

Figure 4.4: Effect of the coupling parameters A and B on the oscillation-induced periodic switch in the DDE system (4.2) with delays only in the *Toggle switch*. (b) is a magnification of (a). Dark blue: When B is sufficiently small and A sufficiently large, a periodic switch is observed. Light blue: When A and B are small, low amplitude oscillations around the lower steady state branch are observed. Green: When both A and B are large enough, we see low amplitude oscillations around the upper steady state branch. Yellow: When A is sufficiently small and B large, birythmicity is observed. Orange: For small B there is a range of possible choices of A where, depending on initial conditions, low amplitude oscillations around the upper steady state branch or periodic switch is observed. Pink: For small B if A is sufficiently small and within a certain range, depending on initial conditions, low amplitude oscillations around the lower steady state branch or periodic switch is observed. Parameter values: $\tau_R = 0$, $\tau_S = 40$, $T = 0.2$, $\alpha_1 = \alpha_2 = \alpha_3 = 100$, $\beta_1 = \beta_2 = \beta_3 = 5$, $\gamma_1 = \gamma_2 = \gamma_3 = 5$, $d_1 = d_2 = 1$, $b_1 = b_2 = 0$, $a_2 = 2$, $m = 2$, $n = 4$.

dependent periodic switch and general system behaviour. Firstly it should be noted that with regards to stability of steady states, the individual time delays were not important. What's important, is the combined time delay of the *Toggle switch* and likewise the combined time delay of the *Repressilator*, i.e. the sum of the individual time delays present in each respective sub-network. This is also the case with regards to the effect of time delays on the system behaviour after oscillations are induced. Therefore, we denote the combined time delay in the *Repressilator* as $\tau_R = \tau_{m_1} + \tau_{p_1} + \tau_{m_2} + \tau_{p_2} + \tau_{m_3} + \tau_{p_3}$, and the combined delay in the *Toggle switch* as $\tau_S = \tau_X + \tau_Y$.

In Figure 4.3(b) the combined time delay in the *Repressilator* is increased to $\tau_R = 1$, whilst the time delay in the *Toggle switch* is kept as $\tau_S = 0$. The presence of delays in the *Repressilator* simply makes the upright boundary line shift slightly to the left, whilst the point of intersection of this line and the vertical axis remains at $B = 6.8$. It therefore requires a smaller coupling amplitude to induce birythmicity. Overall, the time delays from the *Repressilator* have little effect on the oscillatory dynamics of X in the *Toggle*

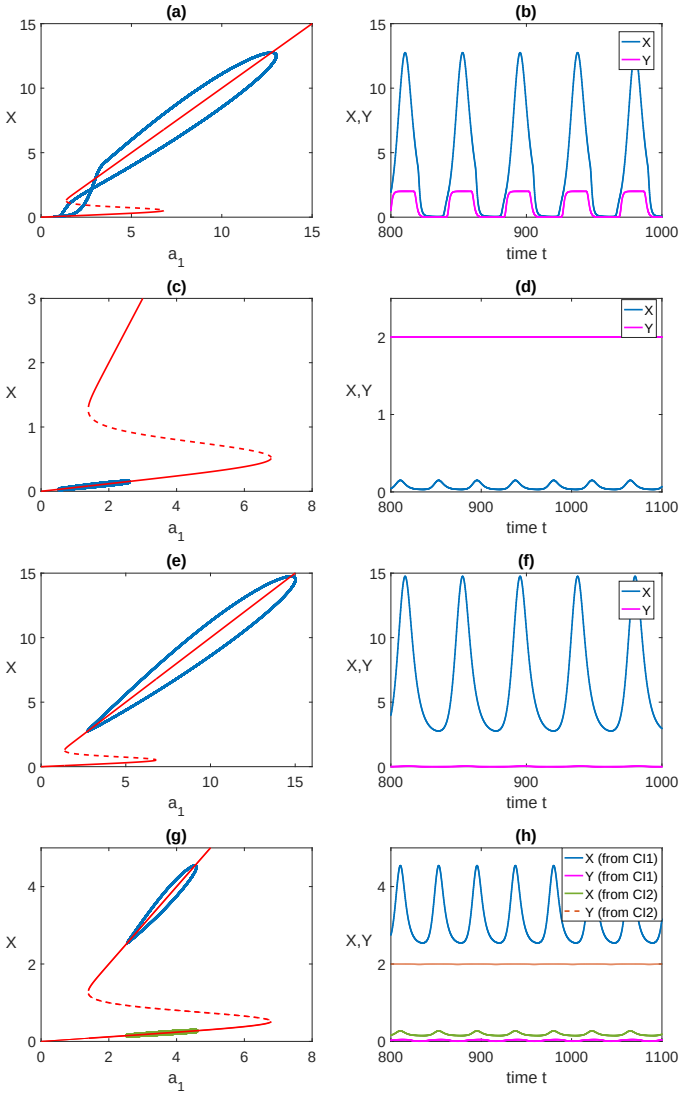

Figure 4.5: Oscillatory behaviour in the DDE model (4.2). (a) Bifurcation diagram of variable X as a function of parameter a_1. The blue curve shows that this variable switches between the lower and upper steady states, with different dynamics than seen in the ODE model (4.1). (b) Time evolutions of X and Y. (c) When amplitude of coupling is insufficient, a periodic switch cannot be induced and variable X oscillates around the lower steady state. (d) Corresponding time evolution of X and Y. (e) When amplitude of coupling is high, oscillations around the upper steady state can occur. (f) Corresponding time evolution of X and Y. (g) When amplitude of coupling is very low, oscillations of the Repressilator can induce birythmicity. (h) Corresponding evolutions of X and Y. Parameter values: $\tau_R = 0$, $\tau_S = 40$, $T = 0.2$, $\alpha_1 = \alpha_2 = \alpha_3 = 100$, $\beta_1 = \beta_2 = \beta_3 = 5$, $\gamma_1 = \gamma_2 = \gamma_3 = 5$, $d_1 = d_2 = 1$, $b_1 = b_2 = 0$, $a_2 = 2$, $m = 2$, $n = 4$. Coupling parameters: $A = 0.3$, $B = 0.5$ ((a) and (b)), $A = 0.05$, $B = 0.5$ ((c) and (d)), $A = 0.3$, $B = 2.5$ ((e) and (f)), $A = 0.05$, $B = 2.5$ ((g) and (h)). For the latter case, initial conditions are $X(0) = 0.1$ and $Y(0) = 10$ (denoted by CI1), leading to the lower limit cycle or $X(0) = 10$ and $Y(0) = 0.1$ (denoted by CI2), leading to the upper limit cycle.

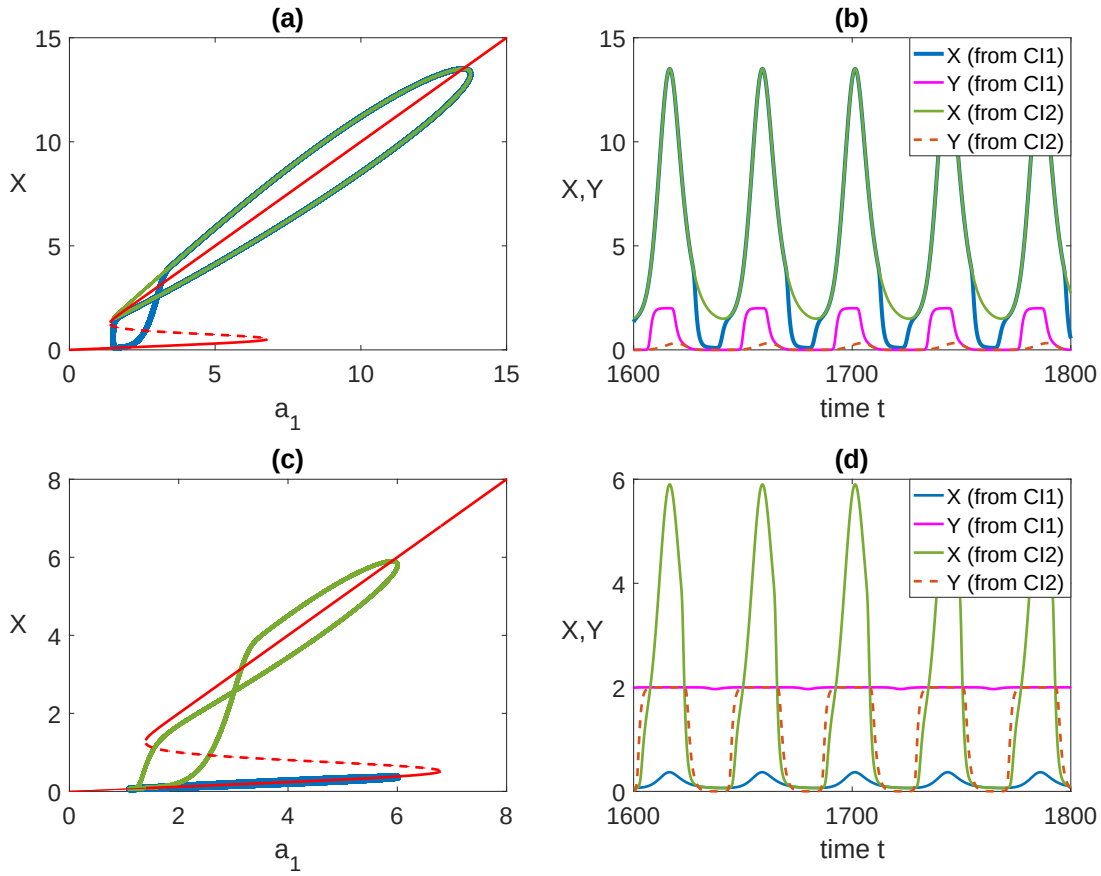

Figure 4.6: New Oscillatory behaviour found in the DDE model (4.2). (a) For sufficiently large amplitude of coupling, it is possible to induce a phenomenon where, depending on initial conditions, variable X can undergo small-amplitude oscillations around the upper steady state or undergo a periodic switch. (b) Time evolution of corresponding X and Y. (c) For a sufficiently small amplitude of coupling, a type of behaviour is possible where, depending on initial conditions, variable X can undergo a periodic switch or undergo small-amplitude oscillations around the lower steady state. (d) Corresponding time evolution of X and Y. Parameter values: $\tau_R = 0$, $\tau_S = 40$, $T = 0.2$, $\alpha_1 = \alpha_2 = \alpha_3 = 100$, $\beta_1 = \beta_2 = \beta_3 = 5$, $\gamma_1 = \gamma_2 = \gamma_3 = 5$, $d_1 = d_2 = 1$, $b_1 = b_2 = 0$, $a_2 = 2$, $m = 2$, $n = 4$. Coupling parameters: $A = 0.3$, $B = 1.25$ ((a) and (b)), $A = 0.12$, $B = 1$ ((c) and (d)). Initial conditions are $X(0) = 0.1$ and $Y(0) = 10$ (denoted by CI1), or $X(0) = 10$ and $Y(0) = 0.1$ (denoted by CI2).

switch. With this in mind we now ignore the presence of time delays in the *Repressilator* and investigate the effects of time delays in the *Toggle switch*.

The types of oscillatory behaviour that can occur as a result of delays in the *Toggle switch* is summarized in Figure 4.4. The same four behaviours of periodic switching, lower oscillations, upper oscillations, and birythmicity are still present in the DDE system as appeared in the ODE model. Interestingly, the inclusion of these time delays in the *Toggle switch* has given rise to new behaviours as well, unseen in the ODE model. The dynamics

of X remain the same for choices of A and B which lie in the light blue region (lower oscillations), green region (upper oscillations), and yellow region (birythmicity). However, in the dark blue region a periodic switch is still induced in X although the dynamical behaviour is drastically different, shown in Figure 4.5(a) and (b). The solution for X begins to oscillate around the upper steady state branch but as a_1 becomes very small X switches for a short time to the lower branch before switching back to the upper branch. More importantly, the new behaviour that occurs due to the inclusion of time delays in the *Toggle switch* is seen in the orange and pink regions of Figure 4.4. When the coupling parameter B is small and amplitude of coupling A is sufficiently large such that it lies in the orange region, a phenomenon is induced whereby, depending on the initial conditions, X will either oscillate around the upper steady state branch or undergo a periodic switch. These dynamics are depicted in Figure 4.6(a) and (b). Similarly, another new type of behaviour is observed in the pink region of Figure 4.4 where, depending on the initial conditions, X will either oscillate around the lower steady state branch or undergo a periodic switch. These dynamics are illustrated in Figure 4.6(c) and (d).

The bifurcation and solution diagrams shown here reveal new types of behaviour that could not be possible in the network described by the ODE model (4.1). If we look at the periodic switch observed in Figure 4.2(a) and (b) we see that in the model without delays the solution of X stays near the lower steady state branch for a long time before passing the second saddle node, where it then goes to the upper branch. X only stays along the upper branch for a short time before switching to the lower branch again. Conversely, if we look at the periodic switch observed in the DDE model, in Figure 4.5(a) and (b), we see that X does not move far along the lower steady state branch. The dynamics also contrast in that more time is spent along the upper branch, shown in Figure 4.5(b), than in the ODE model.

We see that the time delays associated with the two parts of the network, namely, the *Repressilator* and *Toggle switch* need to be treated separately. Compared to the behaviours seen in Figure 4.3(a), the plot in Figure 4.3(b) reveals very little change. Overall, the inclusion of delays in the *Repressilator* doesn't produce a dramatic difference in dynamics of X.

The final comparison that can be made between the results of the DDE model and those found by Gonze [139] is the appearance of two new oscillatory dynamics. Figure 4.4

gives rise to parameter regions where X is capable of undergoing a periodic switch and either upper or lower oscillations depending on initial conditions. The new behaviours that appear as a result of the delays in the *Toggle switch* are not limited to this, other forms of spiking dynamics in the oscillations of X can also be observed (not shown here). It is evident that in modelling systems where non-negligible time delays exist, such as in GRNs, careful consideration of these delays can help unravel new information that may have otherwise been lost.

4.5 Discussion

In this chapter we have discussed a mathematical model for the analysis of a GRN comprised of the *Repressilator* [74] coupled with the *Toggle switch* [80] where one protein in the *Toggle switch* is under the control of one protein in the *Repressilator* in a master/slave setup. We have focussed on the role of transcriptional and translational time delays on the dynamics of the coupled GRN. Our analysis extends an ealier result of Gonze [139] by introducing time delays into the system, where we were able to find new dynamical behaviours that were not possible in the absence of the time delays. Numerical simulations have allowed us to observe these new behaviours and make direct comparisons with the earlier results.

The results in this chapter show that although it may be difficult to control values of coupling parameters in practice, other parameters in the oscillator itself could be altered to produce the desired amplitude of oscillations. Likewise, time delays would also be difficult to alter however understanding the potential effects that time delays can have on the system dynamics could indeed help to provide greater control over parameter tuning in an artificial and experimental environment.

Chapter 5

Discussion and Future Work

5.1 Summary and Conclusions

Research into mathematical models of genetic regulatory networks has provided great insight into the behaviour and development of key life processes in an organism, in a quantitative as well as qualitative way. Correct mathematical representation of real biological systems is vital to achieve a more complete picture of the mechanisms at work in the biological environment. Inclusion of time delays into these models can help unravel the causes of certain phenomena such as Hopf bifurcations and help understand their biological implications.

This thesis examined the effects of time delays in systems describing the dynamics of genetic regulatory networks. In a real biological setting, these delays are associated with the transcription and translation processes during gene expression and, due to the relative time scales of the intrinsic processes, are non-negligible and therefore need to be properly accounted for. We have considered three different GRN network motifs, each with its own forms of regulation between genes. Delay differential equations have been used to describe each model and comparisons have been made with the equivalent ODE description.

The first model focused on the role of transcriptional and translational time delays in an activation-inhibition GRN, and discussed the relevance of behaviour in such models to the onset and development of certain types of cancer. The analysis provided analytical expressions of steady states and showed conditions for the occurrence of periodic oscillations due to the time delays. The results from numerical simulations illustrated the presence

of new oscillatory behaviour in the simplified delayed model, with fast mRNA dynamics, which could not be seen in the existing ODE model in the literature. It also showed the relationships between various system parameters and the time delays, and their effect on steady state stability.

The second model focused on the role of transcriptional and translational time delays in a three-gene network where each gene inhibits the expression of the next gene in the cycle, whilst promoting the expression of itself. It was shown that although the literature suggests that oscillations cannot exist in a *Repressilator* model with a small Hill coefficient, the inclusion of auto-activation and asymmetry could in fact give rise to oscillations. The results of the analysis showed that only one of the steady states has the potential to lose stability through parameter variations, and that the presence of multiple delays can lead to periodic switching of stability for this steady state. The switching between stability of the other steady states was representative of cell fate decisions in the immune system, which showed the importance of parameter tuning on the long term system behaviour.

The third model focused on the effect of transcriptional and translational time delays on the *Repressilator* model coupled with a *Toggle switch*. This was done by making a comparative analysis between the DDE model and an ODE model from earlier literature. Steady state stability analysis was performed to provide analytical conditions for the occurrence of oscillations due to time delays, and numerical simulations were used to study the effect of the delays on the different types of oscillations that can be exhibited by one of the system proteins. The results suggest that with regards to both stability and behaviour of oscillations, it is the combined delays of each respective sub-network that has an impact on the system dynamics, rather than the individual delays. It was found that the delays in the *Repressilator* have little effect on the dynamics of the observed protein in the *Toggle switch*, however the delays in the *Toggle switch* lead to new types of oscillatory behaviour, which were impossible in the ODE system. These results stress the importance of transcriptional and translational time delays in not only steady state stability, but also the system behaviour once oscillations have been induced.

The outcomes of this thesis stress the significance of time delays within GRNs. Without careful consideration of delays, it may be likely that one could miss vital information surrounding the genetic model; whether it be oscillations induced by delay dependent Hopf bifurcations, or rich dynamical patterns which exist only in a delayed model setting.

Indeed direct mathematical analysis of such systems can become troublesome and in some cases impossible using known mathematical methods, especially for larger systems. However, advances in computational power and computational methods may lead to greater possibilities and permit further understanding of delayed genetic systems.

5.2 Future Research

The work presented in the thesis can be extended in several interesting and important research directions. One possibility would be to account for the fact that in most experiments the transcriptional and translational time delay are not fixed but rather obey some form of a delay distribution. Recent work on the effects of delay distribution on system dynamics [143–145] has shown that, even for the same mean delay, details of the distribution can also play an important role. He and Cao [59] have used Lyapunov functional approach to derive conditions for global stability of equilibria in some types of GRNs with distributed delays, and it would be insightful to investigate the possibility of extending this methodology to other types of GRNs and various types of delay kernels. Alternatively, one could use the framework of a master stability function for systems with distributed delays [146] to study possible synchronization dynamics in GRNs with a large number of proteins involved.

Since GRNs are known to be made up of multiple feedback networks, further investigation into other network motifs of coupled switches and oscillators could be explored. Gonze [139] looked at another type of connection between the *Toggle switch* and *Repressilator* where, instead, a protein in the *Repressilator* is under the control of a protein in the *Toggle switch*. It is then shown that an external signal acting on the *Toggle switch* can induce oscillations in the *Repressilator* or in fact stop the existing oscillations. It would most certainly be worth incorporating time delays into systems such as these which include external signals, as these signals are known to play an important role in GRNs in the immune system, such as T cell development. Other forms of coupling within delayed systems of the *Repressilator* and *Toggle switch* could also be studied, such as bidirectional coupling [142].

As it has already been mentioned, in some cases gene expression behaviour is characterised by a switch-like behaviour that can be better modelled using piecewise-linear rather

than continuous transcription functions [38, 41]. Whilst some preliminary work has been done recently on the analysis of piecewise-linear systems with discrete time delays, primarily in engineering applications [147–149], the dynamics of GRNs with piecewise-linear transcription functions and transcriptional/translational delays have remained completely unexplored. Further inclusion of distributed delays would make such models mathematically very challenging, but it could provide a new level of understanding of GRN dynamics.

Bibliography

[1] U. Alon, *An Introduction to Systems Biology*, Champan & Hall, Boca Raton, USA, 2007.

[2] H. de Jong, "Modeling and simulation of genetic regulatory systems: a literature review," *Journal of Computational Biology*, vol. 9, no. 1, pp. 67-103, 2002.

[3] G. Bernot, J.-P. Comet, A. Richard, M. Chaves, J.-L. Gouzé, and R. Dayan, "Modeling and analysis of gene regulatory networks," in *Modeling in Computational Biology and Biomedicine*, F. Cazals and P. Kornprobst, Eds., pp. 47-80, Springer, Berlin, Germany, 2013.

[4] D. Endy and R. Brent, "Modelling cellular behaviour," *Nature*, vol. 409, no. 6818, pp. 391-395, 2001.

[5] J. Hasty, D. McMillen, F. Isaacs, and J.J. Collins, "Computational studies of gene regulatory networks: in numero molecular biology," *Nature Reviews Genetics*, vol. 2, no. 4, pp. 268-279, 2001.

[6] A. Tušek and Ž. Kurtanjek, "Mathematical modelling of gene regulatory networks," in *Applied Biological Engineering—Principles and Practice*, chapter 5, InTech, Rijeka, Croatia, 2012.

[7] M. Hecker, S. Lambeck, S. Toepfer, E. van Someren, and R. Guthke, "Gene regulatory network inference: data integration in dynamic models—a review," *BioSystems*, vol. 69, no. 1, pp. 86-103, 2009.

[8] S. A. Kauffman, "Metabolic stability and epigenesis in randomly constructed genetic nets," *Journal of Theoretical Biology*, vol. 22, no. 3, pp. 437-467, 1969.

[9] R. Thomas, "Boolean formalization of genetic control circuits," *Journal of Theoretical Biology*, vol. 42, no. 3, pp. 563-585, 1973.

[10] R. Somogyi and C. A. Sniegoski, "Modeling the complexity of genetic networks: understanding multigenic and pleiotropic regulation," *Complexity*, vol. 1, no. 6, pp. 45-63, 1996.

[11] R. Albert, "Boolean modelling of genetic regulatory networks," in *Complex Networks*, vol. 650 of *Lecture Notes in Physics*, pp. 459-481, Springer, Berlin, Germany, 2004.

[12] P. Smolen, D. A. Baxter, and J. H. Byrne, "Modeling transcriptional control in gene networks—methods, recent results, and future directions," *Bulletin of Mathematical Biology*, vol. 62, no. 2, pp. 247-292, 2000.

[13] I. Shmulevich, E. R. Dougherty, and W. Zhang, "From Boolean to probabilistic Boolean networks as models of genetic regulatory networks," *Proceedings of the IEEE*, vol. 90, no. 11, pp. 1778-1792, 2002.

[14] A. Silvescu and V. Honavar, "Temporal Boolean network models of genetic networks and their inference from gene expression time series," *Complex Systems*, vol. 13, no. 1, pp. 61-78, 2001.

[15] M. Davidich and S. Bornholdt, "The transition from differential equations to Boolean networks: a case study in simplifying a regulatory network model," *Journal of Theoretical Biology*, vol. 255, no. 3, pp. 269-277, 2008.

[16] R. Xu, G.K. Venayagamoorthy, and D.C. Wunsch II, "Modeling of gene regulatory networks with hybrid differential evolution and particle swarm optimization," *Neural Networks*, vol. 20, no. 8, pp. 917-927, 2007.

[17] F. Karlsson and M. Hörnquist, "Order or chaos in Boolean gene networks depends on the mean fraction of canalizing functions," *Physica A*, vol. 384, no. 2, pp. 747-757, 2007.

[18] G. N. Brock, V. Pihur, and L. Kubatko, "Detecting gene regulatory networks from microarray data using fuzzy logic," in *Fuzzy Systems in Bioinformatics and Computational Biology*, Y. Jin and L. Wang, Eds., vol. 242 of *Studies in Fuzziness and Soft Computing*, pp. 141-163, Springer, Berlin, Germany, 2009.

[19] P. J. Woolf and Y. Wang, "A fuzzy logic approach to analyzing gene expression data," *Physiological Genomics*, vol. 3, no. 1, pp. 9-15, 2000.

[20] L. G. Volkert and N. Malhis, "An efficient method for fuzzy identification of regulatory events in gene expression time series data," in *Proceedings of the IEEE Symposium on Computational Intelligence in Bioinformatics and Computational Biology (CIBCB '04)*, pp. 17-24, IEEE, La Jolla, Claif, USA, October 2004.

[21] P. Das, P. Rakshit, A. Konar, M. Nasipuri, and A. K. Nagar, "Fuzzy relational system for identification of gene regulatory network," in *Proceedings of the World Congress in Computer Science, Computer Engineering, and Applied Computing (WORLDCOMP '09)*, Las Vegas, Nev, USA, July 2009.

[22] T. A. Al Qazlan, A. Hamdi-Cherif, and C. Kara-Mohamed, "State of the art of fuzzy methods for gene regulatory networks inference," *The Scientific World Journal*, vol. 2015, Article ID 148010, 11 pages, 2015.

[23] B. C. Goodwin, *Temporal Organization in Cells*, Academic Press, New York, NY, USA, 1963.

[24] B. C. Goodwin, "Oscillatory behavior in enzymatic control processes," in *Advances in Enzyme Regulation*, G. Weber, Ed., pp. 425-438, Pergamon Press, Oxford, UK, 1965.

[25] J.-L. Gouzé, "Positive and negative circuits in dynamical systems," *Journal of Biological Systems*, vol. 6, no. 1, pp. 11-15, 1998.

[26] E.H. Snoussi, "Necessary conditions for multistationarity and stable periodicity," *Journal of Biological Systems*, vol. 6, no. 1, pp. 3-9, 1998.

[27] J. J. Tyson and H.G. Othmer, "The dynamics of feedback control circuits in biochemical pathways," *Progress in Theoretical Biology*, vol. 5, pp. 1-62, 1978.

[28] A. D. Keller, "Specifying epigenetic states with autoregulatory transcription factors," *Journal of Theoretical Biology*, vol. 170, no. 2, pp. 175-181, 1994.

[29] R. Heinrich and S. Schuster, *The Regulation of Cellular Systems*, Chapman & Hall, New York, NY, USA, 1996.

[30] J. L. Cherry and F. R. Adler, "How to make a biological switch," *Journal of Theoretical Biology*, vol. 203, no. 2, pp. 117-133, 2000.

[31] G. Yagil, "Quantitative aspects of protein induction," *Current Topics in Cellular Regulation*, vol. 9, pp. 183-235, 1975.

[32] A. Polynikis, S. J. Hogan, and M. di Bernado, "Comparing different ODE modelling approaches for gene regulatory networks," *Journal of Theoretical Biology*, vol. 261, no. 4, pp. 511-530, 2009.

[33] S. Widder, J. Schicho, and P. Schuster, "Dynamic patterns of gene regulation. I. Simple two-gene systems," *Journal of Theoretical Biology*, vol. 246, no. 3, pp. 395-419, 2007.

[34] S. Goutelle, M. Maurin, F. Rougier et al., "The Hill equation: a review of its capabilities in pharmacological modelling," *Fundamental and Clinical Pharmacology*, vol. 22, no. 6, pp. 633-648, 2008.

[35] J. N. Weiss, "The Hill equation revisited: uses and misuses," *The FASEB Journal*, vol. 11, no. 11, pp. 835-841, 1997.

[36] M. Santillán, "On the use of the Hill functions in mathematical models of gene regulatory networks," *Mathematical Modelling of Natural Phenomena*, vol. 3, no. 2, pp. 85-97, 2008.

[37] L. Glass and S. A. Kauffman, "The logical analysis of continuous, non-linear biochemical control networks," *Journal of Theoretical Biology*, vol. 39, no. 1, pp. 103-129, 1973.

[38] L. Glass, "Classification of biological networks by their qualitative dynamics," *Journal of Theoretical Biology*, vol. 54, no. 1, pp. 85-107, 1975.

[39] E. Plahte, T. Mestl, and S. W. Omholt, "A methodological basis for description and analysis of systems with complex switch-like interactions," *Journal of Mathematical Biology*, vol. 36, no. 4, pp. 321-348, 1998.

[40] E. Plahte and S. Kjøglum, "Analysis and generic properties of gene regulatory networks with graded response functions," *Physica D*, vol. 201, no. 1-2, pp. 150-176, 2005.

[41] R. Casey, H. de Jong, and J.-L. Gouzé, "Piecewise-linear models of genetic regulatory networks: equilibria and their stability," *Journal of Mathematical Biology*, vol. 52, no. 1, pp. 27-56, 2006.

[42] J. Gebert, N. Radde, and G.-W. Weber, "Modeling gene regulatory networks with piecewise linear differential equations," *European Journal of Operational Research*, vol. 181, no. 3, pp. 1148-1165, 2007.

[43] E. Plahte, T. Mestl, and S. W. Omholt, "Global analysis of steady points for systems of differential equations with sigmoid interactions," *Dynamics and Stability of Systems*, vol. 9, no. 4, pp. 275-291, 1994.

[44] H. El Snoussi and R. Thomas, "Logical identification of all steady states: the concept of feedback loop characteristic states," *Bulletin of Mathematical Biology*, vol. 55, no. 5, pp. 973-991, 1993.

[45] A. Hoffmann, A. Levchenko, M. L. Scott, and D. Baltimore, "The IκB-NF-κB signaling module: temporal control and selective gene activation," *Science*, vol. 298, no. 5596, pp. 1241-1245, 2002.

[46] S. L. Werner, D. Barken, and A. Hoffmann, "Stimulus specificity of gene expression programs determined by temporal control of IKK activity," *Science*, vol. 309, no. 5742, pp. 1857-1861, 2005.

[47] N. Geva-Zatorsky, N. Rosenfeld, S. Itzkovitz et al., "Oscillations and variability in the p53 system," *Molecular Systems Biology*, vol. 2, no. 1, Article ID 2006.0033, 2006.

[48] L. Ma, J. Wagner, J. J. Rice, W. Hu, A. J. Levine, and G. A. Stolovitzky, "A plausible model for the digital response of p53 to DNA damage," *Proceedings of the National Academy of Sciences of the United States of America*, vol. 102, no. 40, pp. 14266-14271, 2005.

[49] B. T. Hennessy, D. L. Smith, P. T. Ram, Y. Lu, and G. B. Mills, "Exploiting the PI3K/AKT pathway for cancer drug discovery," *Nature Reviews Drug Discovery*, vol. 4, no. 12, pp. 988-1004, 2005.

[50] T. M. K. Cheng, S. Gulati, R. Agius, and P. A. Bates, "Understanding cancer mechanisms through network dynamics," *Briefings in Functional Genomics*, vol. 11, no. 6, Article ID els025, pp. 543-560, 2012.

[51] L. B. Edelman, J. A. Eddy, and N. D. Price, "*In silico* models of cancer," *Wiley Interdisciplinary Reviews: Systems Biology and Medicine*, vol. 2, no.4, pp. 438-459, 2010.

[52] N. A. M. Monk, "Oscillatory expression of Hes1, p53, and NF-κB driven by transcriptional time delays," *Current Biology*, vol. 13, no. 16, pp. 1409-1413, 2003.

[53] A. Wan and X. Zou, "Hopf bifurcation analysis for a model of genetic regulatory system with delay," *Journal of Mathematical Analysis and Applications*, vol. 356, no. 2, pp. 464-476, 2009.

[54] K. Wang, L. Wang, Z. Teng, and H. Jiang, "Stability and bifurcation of genetic regulatory networks with delays," *Neurocomputing*, vol. 73, no. 16-18, pp. 2882-2892, 2010.

[55] M. Bodnar, U. Foryś, and J. Poleszczuk, "Analysis of biochemical reactions models with delays," *Journal of Mathematical Analysis and Applications*, vol. 376, no. 1, pp. 74-83, 2011.

[56] Z. Wang, Z. Liu, and R. Yuan, "Stability and bifurcation in a gene regulatory network model with delay," *Zeitschrift für Angewandte Mathematik und Mechanik*, vol. 92, no. 4, pp. 290-303, 2012.

[57] M. Xiao, W. X. Zheng, and J. Cao, "Stability and bifurcation of genetic regulatory networks with small RNAs and multiple delays," *International Journal of Computer Mathematics*, vol. 91, no. 5, pp. 907-927, 2014.

[58] M. Xiao and J. Cao, "Genetic oscillation deduced from Hopf bifurcation in a genetic regulatory network with delays," *Mathematical Biosciences*, vol. 215, no. 1, pp. 55-63, 2008.

[59] W. He and J. Cao, "Robust stability of genetic regulatory networks with distributed delay," *Cognitive Neurodynamics*, vol. 2, no. 4, pp. 355-361, 2008.

[60] B. D. Aguda, Y. Kim, M. G. Piper-Hunter, A. Friedman, and C. B. Marsh, "MicroRNA regulation of a cancer network: consequences of the feedback loops involving miR-17-92, E2F, and Myc," *Proceedings of the National Academy of Sciences of the United States of America*, vol. 105, no. 50, pp. 19678-19683, 2008.

[61] B. D. Aguda, "Modeling microRNA-transcription factor networks in cancer," in *MicroRNA Cancer Regulation: Advanced Concepts, Bioinformatics and Systems Biology Tools*, U. Schmitz, O. Wolkenhauer, and J. Vera, Eds., vol. 774 of *Advances in Experimental Medicine and Biology*, pp. 149-167, Springer, Dordrecht, The Netherlands, 2013.

[62] A. S. Ribeiro, J. J. Grefenstette, and S. A. Kauffman, "Modeling gene regulatory networks with delayed stochastic dynamics," in *Handbook of Research on Computational Methodologies in Gene Regulatory Networks*, S. Das, D. Caragea, S. M. Welch, and W. H. Hsu, Eds., pp 198-218, Medical Information Science Reference, New York, NY, USA, 2010.

[63] N. MacDonald, "Time lag in a model of a biochemical reaction sequence with end product inhibition," *Journal of Theoretical Biology*, vol. 67, no. 3, pp. 549-556, 1977.

[64] I. R. Epstein and Y. Luo, "Differential delay equations in chemical kinetics. Nonlinear models: the cross-shaped phase diagram and the Oregonator," *The Journal of Chemical Physics*, vol. 95, no. 1, pp. 244-254, 1991.

[65] J. Paulsson, "Models of stochastic gene expression," *Physics of Life Reviews*, vol. 2, no. 2, pp. 157-175, 2005.

[66] S. Rosenfeld, "Stochastic cooperativity in non-linear dynamics of gene regulatory networks," *Mathematical Biosciences*, vol. 210, no. 1, pp. 121-142, 2007.

[67] A. Raj and A. van Oudenaarden, "Nature, nurture, or chance: stochastic gene expression and its consequences," *Cell*, vol. 135, no. 2, pp. 216-226, 2008.

[68] P. S. Swain, M. B. Elowitz, and E. D. Siggia, "Intrinsic and extrinsic contributions to stochasticity in gene expression," *Proceedings of the National Academy of Sciences of the United States of America*, vol. 99, no. 20, pp. 12795-12800, 2002.

[69] K. M. Herbert, A. La Porta, B. J. Wong et al., "Sequence resolved detection of pausing by single RNA polymerase molecules," *Cell*, vol. 125, no. 6, pp. 1083-1094, 2006.

[70] A. S. Ribeiro, O.-P. Smolander, T. Rajala, A. Häkkinen, and O. Yli-Harja, "Delayed stochastic model of transcription at the single nucleotide level," *Journal of Computational Biology*, vol. 16, no. 4, pp. 539-553, 2009.

[71] M. Voliotis, N. Cohen, C. Molina-París, and T. B. Liverpool, "Fluctuations, pauses and backtracking in DNA transcription," *Biophysical Journal*, vol. 94, no. 2, pp. 334-348, 2008.

[72] A. S. Ribeiro, "Stochastic and delayed stochastic models of gene expression and regulation," *Mathematical Biosciences*, vol. 223, no. 1, pp. 1-11, 2010.

[73] M. J. Dunlop, R. S. Cox III, J. H. Levine, R. M. Murray, and M. B. Elowitz, "Regulatory activity revealed by dynamic correlations in gene expression noise," *Nature Genetics*, vol. 40, no. 12, pp. 1493-1498, 2008.

[74] M. B. Elowitz and S. Leibler, "A synthetic oscillatory network of transcriptional regulators," *Nature*, vol. 403, no. 6767, pp. 335-338, 2000.

[75] M. B. Elowitz, A. J. Levine, E. D. Siggia, and P. S. Swain, "Stochastic gene expression in a single cell," *Science*, vol. 297, no. 5584, pp. 1183-1186, 2002.

[76] S. Rosenfeld, "Stochastic oscillations in genetic regulatory networks: application to microarray experiments," *Eurasip Journal on Bioinformatics and Systems Biology*, vol. 2006, Article ID 59526, 2006.

[77] M. Kærn, T. C. Elston, W. J. Blake, and J. J. Collins, "Stochasticity in gene expression: from theories to phenotypes," *Nature Reviews Genetics*, vol. 6, no. 6, pp. 451-464, 2005.

[78] D. Bratsun, D. Volfson, L. S. Tsimring, and J. Hasty, "Delay-induced stochastic oscillations in gene regulations," *Proceedings of the National Academy of Sciences of the United States of America*, vol. 102, no. 41, pp. 14593-14598, 2005.

[79] E. Zavala and T. T. Marquez-Lago, "Delays induce novel stochastic effects in negative feedback gene circuits," *Biophysical Journal*, vol. 106, no. 2, pp. 467-478, 2014.

[80] T. S. Gardner, C. R. Cantor, and J. J. Collins, "Construction of a genetic toggle switch in *Escherichia coli*," *Nature*, vol. 403, no. 6767, pp. 339-342, 2000.

[81] H. El Samad, M. Khammash, L. Petzold, and D. Gillespie, "Stochastic modelling of gene regulatory networks," *International Journal of Robust and Nonlinear Control*, vol. 15, no. 15, pp. 691-711, 2005.

[82] M. Barrio, K. Burrage, A. Leier, and T. Tian, "Oscillatory regulation of Hes1: discrete stochastic delay modelling and simulation," *PLoS Computational Biology*, vol. 2, no. 9, article e117, 2006.

[83] X. Cai, "Exact stochastic simulation of coupled chemical reactions with delays," *Journal of Chemical Physics*, vol. 126, Article ID 124108, 2007.

[84] M. Jansen and P. Pfaffelhuber, "Stochastic gene expression with delay," *Journal of Theoretical Biology*, vol. 364, pp. 355-363, 2015.

[85] N. Friedman, M. Linial, I. Nachman, and D. Péer, "Using Bayesian networks to analyze expression data," *Journal of Computational Biology*, vol. 7, no. 3-4, pp. 601-620, 2000.

[86] D. Heckerman, "A tutorial on learning with Bayesian networks," Microsoft Research Technical Report MSR-TR-95-06, 1996.

[87] A. V. Werhli and D. Husmeier, "Reconstructing gene regulatory networks with Bayesian networks by combining expression data with multiple sources of prior knowledge," *Statistical Applications in Genetics and Molecular Biology*, vol. 6, article 15, 2007.

[88] P. T. Spellman, G. Sherlock, M. Q. Zhang et al., "Comprehensive identification of cell cycle-regulated genes of the yeast *Saccharomyces cerevisiae* by microarray hybridization," *Molecular Biology of the Cell*, vol. 9, no. 12, pp. 3273-3297, 1998.

[89] J. M. Heffernan and R. M. Corless, "Solving some delay differential equations with computer algebra," *Applied Probability Trust*, 2005.

[90] W. Michiels and S. Niculescu, *Stability, control, and computation for time-delay systems: An eigenvalue-based approach*, SIAM, Philadelphia, 2014.

[91] T. Erneaux, *Applied Delay Differential Equations*, Springer, New York, NY, USA, 2009.

[92] J. Lewis, "Autoinhibition with transcriptional delay: a simple mechanism for the zebrafish somitogenesis oscillator," *Current Biology*, vol. 13, pp. 1398-1408, 2003.

[93] Y. N. Kyrychko and K. B. Blyuss, "Global properties of a delayed SIR model with temporary immunity and nonlinear incidence rate," *Nonlinear Analysis Real World Applications*, vol. 6, no. 3, pp. 495-507, 2005.

[94] G. Danaei, S. Vander Hoorn, A.D Lopez, C.J.L. Murray, and M. Ezzati, "Causes of cancer in the world: comparative risk assessment of nine behavioural and environmental risk factors," *The Lancet*, vol. 366, no. 9499, pp. 1784-1793, 2005.

[95] M. Boshart, L. Gissmann, H. Ikenberg, A. Kleinheinz, W. Scheurlen, and H. zur Hausen, "A new type of papillomavirus DNA, its presence in genital cancer biopsies and in cell lines derived from cervical cancer," *The EMBO Journal*, vol. 3, no. 5, pp. 1151-1157, 1984.

[96] D.F. Easton, "How many more breast cancer predisposition genes are there?" *Breast Cancer Research*, vol. 1, no. 1, pp. 14-17, 1999.

[97] G. Thomas, K.B. Jacobs, M. Yeager et al., "Multiple loci identified in a genome-wide association study of prostate cancer," *Nature Genetics*, vol. 40, no. 3, pp. 310-315, 2008.

[98] B.M. Wolpin, C. Rizzato, P. Kraft et al., "Genome-wide association study identifies multiple susceptibility loci for pancreatic cancer," *Nature Genetics*, vol. 46, no. 9, pp. 994-1000, 2014.

[99] H.-Y. Yeh, S.-W. Cheng, Y.-C. Lin, C.-Y. Yeh, S.-F. Lin, and V.-W. Soo, "Identifying significant genetic regulatory networks in the prostate cancer from microarray data based on transcription factor analysis and conditional independency," *BMC Medical Genomics*, vol. 2, article 70, 2009.

[100] E. Bonnet, T. Michoel, and Y. Van de Peer, "Prediction of a gene regulatory network linked to prostate cancer from gene expression, microRNA and clinical data," *Bioinformatics*, vol. 26, no. 18, Article ID btq395, pp. i638-i644, 2010.

[101] X. Wang and O. Gotoh, "Inference of cancer-specific gene regulatory networks using soft computing rules," *Gene Regulation and Systems Biology*, vol. 2010, no. 4, pp. 19-34, 2010.

[102] S. Vineetha, C. Chandra Shekara Bhat, and S.M. Idicula, "Gene regulatory network from microarray data of colon cancer patients using TSK-type recurrent neural fuzzy network," *Gene*, vol. 506, no. 2, pp. 408-416, 2012.

[103] P.B. Madhamshettiwar, S.R. Maetschke, M.J. Davis, A. Reverter, and M.A. Ragan, "Gene regulatory network inference: evaluation and application to ovarian cancer allows the prioritization of drug targets," *Genome Medicine*, vol. 4, no. 5, article 41, 2012.

[104] F. K. Ahmad, S. Deris, and N.H. Othman, "The inference of breast cancer metastasis through gene regulatory networks," *Journal of Biomedical Informatics*, vol. 45, no. 2, pp. 350-362, 2012.

[105] F. Emmert-Streib, R. D. M. Simoes, P. Mullan, B. Haibe-Kains, and M. Dehmer, "The gene regulatory network for breast cancer: integrated regulatory landscape of cancer hallmarks," *Frontiers in Genetics*, vol. 5, article 15, 2014.

[106] R. J. Prill, P. A. Iglesias, and A. Levchenko, "Dynamic properties of network motifs contribute to biological network organization," *PLoS Biology*, vol. 3, no. 11, article e343, 2005.

[107] K. Parmar, K. B. Blyuss, Y. N. Kyrychko, and S. J. Hogan, "Time-delayed models of gene regulatory networks," *Computational and Mathematical Methods in Medicine*, vol. 2015, Article ID 347273, 16 pages, 2015.

[108] H. B. Tiedemann, E. Schneltzer, S. Zeiser et al., "From dynamic expression patterns to boundary formation in the presomitic mesoderm," *PLoS Computational Biology*, vol. 8, no. 6, Article ID e1002586, 2012.

[109] C. Li and J. Wang, "Quantifying cell fate decisions for differentiation and reprogramming of a human stem cell network: landscape and biological paths," *PLoS Computational Biology*, vol. 9, no. 8, Article ID e1003165, 2013.

[110] J. D. Murray, *Mathematical biology: I. An Introduction*, Springer, New York, NY, USA, 2002.

[111] Z. Li, P. Li, A. Krishnan, and J. Liu, "Large-scale dynamic gene regulatory network inference combining differential equation models with local dynamic Bayesian network analysis," *Bioinformatics*, vol. 27, no. 19, Article ID btr454. pp. 2686-2691, 2011.

[112] O. Folger, L. Jerby, C. Frezza, E. Gottlieb, E. Ruppin, and T. Shlomi, "Predicting selective drug targets in cancer through metabolic networks," *Molecular Systems Biology*, vol. 7, article 501, 2011.

[113] K. Raza and R. Jaiswal, "Reconstruction and analysis of cancer-specific gene regulatory networks from gene expression profiles," *International Journal on Bioinformatics and Biosciences*, vol. 3, no. 2, pp. 25-34, 2013.

[114] T.-T. Zhou, "Network systems biology for targeted cancer therapies," *Chinese Journal of Cancer*, vol. 31, no. 3, pp. 134-141, 2012.

[115] G. A. Banks, R. J. Roselli, R. Chen, and T. D. Giorgio, "A model for the analysis of nonviral gene therapy," *Gene Therapy*, vol. 10, no. 20, pp. 1766-1775, 2003.

[116] A. Tsygvintsev, S. Marino, and D. E. Kirschner, "A mathematical model of gene therapy for the treatment of cancer," in *Mathematical Methods and Models in Biomedicine*, U. Ledzewicz, H. Schattler, A. Friedman, and E. Kashdan, Eds., Lecture Notes on Mathematical Modelling in the Life Sciences, pp. 367-385, Springer, New York, NY, USA, 2013.

[117] H. Singh, A. A. Khan, and A. R. Dinner, "Gene regulatory networks in the immune system," *Trends in Immunology*, vol. 35, no. 5, pp. 211-218, 2014.

[118] A. S. Perelson, "Immunology for physicists," *Reviews of Modern Physics*, vol. 69, no. 4, pp. 1219-1267, 1997.

[119] R. Sciammas, Y. Li, A. Warmflash, Y. Song, A. R. Dinner, and H. Singh, "An incoherent regulatory network architecture that orchestrates B cell diversification in response to antigen signaling," *Molecular Systems Biology*, vol. 7, no. 495, 2011.

[120] L. Mariani, M. Löhning, A. Radbruch, and T. Höfer, "Transcriptional control networks of cell differentiation: insights from helper T lymphocytes," *Progress in Biophysics & Molecular Biology*, vol. 86, no. 1, pp. 45-76, 2004.

[121] A. Yates, R. Callard, and J. Stark, "Combining cytokine signalling with T-bet and GATA-3 regulation in Th1 and Th2 differentiation: a model for cellular decision-making," *Journal of Theoretical Biology*, vol. 231, no. 2, pp. 181-196, 2004.

[122] H. J. van den Ham and R. J. de Boer, "From the two-dimensional Th1 and Th2 phenotypes to high-dimensional models for gene regulation," *International Immunology*, vol. 20, no. 10, pp. 1269-1277, 2008.

[123] W. C. Lo, R. I. Arsenescu, and A. Friedman, "Mathematical model of the roles of T cells in inflammatory bowel disease," *Bulletin of Mathematical Biology*, vol. 75, no. 9, pp. 1417-1433, 2013.

[124] O. Purcell, N. J. Savery, C. S. Grierson, and M. di Bernado, "A comparative analysis of synthetic genetic oscillators," *Journal of the Royal Society Interface*, vol. 7, no. 52, pp. 1503-1524, 2010.

[125] N. Suzuki, C. Furusawa, and K. Kaneko, "Oscillatory protein expression dynamics endows stem cells with robust differentiation potential," *PLoS ONE* 6(11): e27232, 2011.

[126] T. Hong, J. Xing, L. Li, and J. J. Tyson, "A simple theoretical framework for understanding heterogeneous differentiation of $CD4^+$ T cells," *BMC Systems Biology*, vol. 6, no. 66, 2012.

[127] T. Hong, C. Oguz, and J. J. Tyson, "A mathematical framework for understanding four-dimensional heterogeneous differentiation of $CD4^+$ T cells," *Bulletin of Mathematical Biology*, vol. 77, no. 6, pp. 1046-1064, 2015.

[128] M. Andrecut, J. D. Halley, D. A. Winkler, and S. Huang, "A general model for binary cell fate decision gene circuits with degeneracy: indeterminacy and switch behaviour in the absence of cooperativity," *PLoS ONE* 6(5): e19358, 2011.

[129] H. El Samad, D. Del Vecchio, and M. Khammash, "Repressilators and promotilators: Loop dynamics in synthetic gene networks," *American Control Conference - ACC*, pp. 4405-4410, 2005.

[130] B. Rahman, K. B. Blyuss and Y. Kyrychko, "Dynamics of neural systems with discrete and distributed time delays," *SIAM Journal on Applied Dynamical Systems*, vol. 14, no. 4, pp. 2069-2095, 2015.

[131] K. Gu, L. Kharitonov, and L. Chen, *Stability of Time-Delay Systems*, Birkhäauser Boston, 2003.

[132] J. Li, L. Zhang, and Z. Wang, "Two effective stability criteria for linear time-delay systems with complex coefficients," *Journal of Systems Science and Complexity*, vol. 24, pp. 835-849, 2011.

[133] Y. Kuang, *Delay Differential Equations: With Applications in Population Dynamics*, Academic Press, 1993.

[134] T. Tian and K. Burrage, "Stochastic models for regulatory networks of the genetic toggle switch," *Proceedings of the National Academy of Sciences of the United States of America*, vol. 103, no. 22, pp. 8372-8377, 2006.

[135] J. Wang, J. Zhang, Z. Yuan, and T. Zhou, "Noise-induced switches in network systems of the genetic toggle switch," *BMC Systems Biology*, vol. 1, no. 50, 2007.

[136] A. Loinger and O. Biham, "Stochastic simulations of the repressilator circuit," *Physical Review E*, vol. 76, no. 5, 051917, 2007.

[137] J. Garcia-Ojalvo, M. B. Elowitz, and S. H. Strogatz, "Modelling a synthetic multicellular clock: repressilators coupled by quorum sensing," *Proceedings of the National Academy of Sciences of the United States of America*, vol. 101, no. 30, pp. 10955-10960, 2004.

[138] R. Wang, L. Chen, and K. Aihara, "Synchronising a multicellular system by external input: an artificial control strategy," *Bioinformatics*, vol. 22, no. 14, pp. 1775-1781, 2006.

[139] D. Gonze, "Coupling oscillations and switches in genetic networks," *BioSystems*, vol. 99, no. 1, pp. 60-69, 2010.

[140] T. Y. Tsai, Y. S. Choi, W. Ma, J. R. Pomerening, C. Tang, and J. E. Jr. Ferrell, "Robust, tunable biological oscillations from interlinked positive and negative feedback loops," *Science*, vol. 321, pp. 126-129, 2008.

[141] X. P. Zhang, F. Liu, Z. Cheng, and W. Wang, "Cell fate decision mediated by p53 pulses," *Proceedings of the National Academy of Sciences of the United States of America*, vol. 106, no. 30, pp. 12245-12250, 2009.

[142] P. Zhou, C. Shuiming, Z. Liu, C. Luonan, and R. Wang, "Coupling switches and oscillators as a means to shape cellular signals in biomolecular systems," *Chaos, Solitons & Fractals*, vol. 50, pp. 115-126, 2013.

[143] K. B. Blyuss and Y. N. Kyrychko, "Stability and bifurcations in an epidemic model with varying immunity period," *Bulletin of Mathematical Biology*, vol. 72, no. 2, pp. 490-505, 2010.

[144] Y. N. Kyrychko, K. B. Blyuss, and E. Schöll, "Amplitude death in systems of coupled oscillators with distributed-delay coupling," *European Physical Journal B*, vol. 84, no. 2, pp. 307-315, 2011.

[145] Y. N. Kyrychko, K. B. Blyuss, and E. Schöll, "Amplitude and phase dynamics in oscillators with distributed-delay coupling," *Philosophical Transactions of the Royal Society of London A. Mathematical, Physical and Engineering Sciences*, vol. 371, no. 1999, Article ID 20120466, 2013.

[146] Y. N. Kyrychko, K. B. Blyuss, and E. Schöll, "Synchronization of networks of oscillators with distributed delay coupling," *Chaos*, vol. 24, no. 4, Article ID 043117, 2014.

[147] M. Lakshmanan and D. V. Senthilkumar, *Dynamics of Nonlinear Time-Delay Systems*, Springer Series in Synergetics, Springer, Berlin, Germany, 2010.

[148] R. Suresh, D. V. Senthilkumar, M. Lakshmanan, and J. Kurths, "Transition to complete synchronization and global intermittent synchronization in an array of time-delay systems," *Physical Review E*, vol. 86, no. 1, Article ID 016212, 2012.

[149] J. Sieber, P. Kowalczyk, S. J. Hogan, and M. Di Bernardo, "Dynamics of symmetric dynamical systems with delayed switching," *Journal of Vibration and Control*, vol. 16, no. 7-8, pp. 1111-1140, 2010.